ROLE OF α -AMINO-3-HYDROXY-5-METHYL-4-ISOXAZOLEPROPIONIC ACID (AMPA) RECEPTOR ON METHYLMERCURY-INDUCED CALCIUM DYSREGULATION ON MOTOR NEURONS

By

Alexandra Colón-Rodríguez

A DISSERTATION

Submitted to
Michigan State University
in partial fulfillment of the requirements
for the degree of

Comparative Medicine and Integrative Biology – Environmental Toxicology – Doctor of Philosophy

2017

ABSTRACT

ROLE OF α-AMINO-3-HYDROXY-5-METHYL-4-ISOXAZOLEPROPIONIC ACID (AMPA) RECEPTOR ON METHYLMERCURY-INDUCED CALCIUM DYSREGULATION ON MOTOR NEURONS

By

Alexandra Colón-Rodríguez

Methylmercury (MeHg) is a persistent environmental neurotoxicant to which humans are exposed mainly through the consumption of fish. MeHg leads to neuronal cell death in acute or chronic exposure and its mechanism of toxicity is not yet understood. Due to its high prevalence in the environment and its mechanism of toxicity MeHg has been considered a possible contributor to the development of Amyotrophic Lateral Sclerosis (ALS). Alterations in glutamate reuptake and Ca^{2+} regulation in ALS and after MeHg exposures have been well documented. Most importantly, MeHg-induced alterations in intracellular Ca^{2+} ($[Ca^{2+}]_i$) in motor neurons lead to early onset ALS-like phenotype in the superoxide dismutase 1 (SOD1-G93A) mouse, a mouse model genetically susceptible to ALS. One of the ion channels that contribute to the alterations in $[Ca^{2+}]_i$ observed in ALS and after MeHg exposure is the ionotropic glutamate receptor α-amino-3-hydroxy-5-methyl-4-isoxazolepropionate (AMPA).

My research has focused on characterizing the effects of MeHg on motor neurons *in vitro.* I used two cell lines: a mouse motor neuron hybrid cell line NSC34 and an induced pluripotent stem cell derived-motor neuron (hiPSC-MN) cell line of human origin. I investigated MeHg toxicity in these cell types and on AMPA receptors in order to understand the role these ion channels play in the observed alterations in $[Ca^{2+}]_i$. Results from the studies in this dissertation demonstrate that MeHg exposure *in vivo* or *in vitro* lead to alterations in the AMPA receptor and the RNA editing enzyme ADAR2 gene expression. Also, that hiPSC-MNs are more

susceptible than NSC34 cells to MeHg toxicity observed as an earlier concentration dependent cell death. I also identified that MeHg induces a bi-phasic increase in $[Ca^{2+}]_i$ in hiPSC-MNs and Ca^{2+} permeable AMPA receptors are mediating those increases. Taken together these results suggest a potential role of the AMPA receptors in MeHg-induced toxicity in MNs. These findings contribute to the understanding of MeHg-induced toxicity in motor neurons and provide a platform for ongoing studies in our lab which are focused on identifying the underlying mechanisms by which MeHg is contributing to the accelerated onset of ALS-like phenotype.

To mom, dad, and my family who taught me the importance of perseverance and hard work.

ACKNOWLEDGEMENTS

Dr. William Atchison, thank you for your support, guidance and advice for all these years. Your work with underrepresented minorities and other Puerto Rican students like myself is exemplary and has been an inspiration for many mentees including myself. I hope to one day be as good as you are. Thank you and Mary Jo for making me feel as if I was part of the family and for making my time in Michigan a great one.

To my committee members, Dr. John Fyfe, Dr. Patricia Ganey, and Dr. Cindy Jordan, and the CMIB program director Dr. Vilma Yuzbasiyan-Gurkan, Thank you!!! Your guidance, support and advice have contributed immensely to my growth and success as a scientist. I admire your work and hope to count with your mentorship as I continue this journey. To my mentor, Dr. Ravindra K. Hajela, thank you for teaching me almost all the techniques that I know. Your honesty, advice and challenges shaped me into the scientist that I have become and I will be forever grateful for that. Thank you for always telling me to reach for the stars and to be strong, that has allowed me to challenge myself and pursue things that I thought I never could before. I respect you as the amazing scientist you are and admire your discipline and hard work. I strive to one day be a little bit more like you are.

My time at the Atchison lab would not have been the same without the awesome people I got to work with and share so many good memories with. Dr. Elizabeth Molina Campos, Dr. Brenda Marrero-Rosado, Dr. Sara Ciotti and Dr. Aaron Bradford thank you for all your advice and all the fun times. Dr. Heidi Hannon, thank you for all your help with the cell viability and the calcium fluorimetry experiments. Also, your encouragement and advice were incredibly important in helping me to keep pushing the last few weeks. Alberto Perez, thank you for all the help with the confocal microscopy and the immunocytochemistry. Nicole Colón, I would not

have been able to finish all the experiments I had planned to complete this dissertation without your help. You are an exceptional scientist and I am looking forward to the day that I can call you my colleague.

To my family who I owe everything that I am, Thank You!

Mom you are the hardest working woman I have ever known and it is because of you that I strive to be the best version of myself that I can be. Dad although you are not with us anymore it is important that I let you know that to see you struggle inspired me to pursue a career in neurotoxicology. I thought that by doing this I would be able to help you and understand you better. I hope you are smiling down at me. Ginny, you inspire me to not quit and to keep pushing to give the best of me, always. Thank you for being the best big sister, for your support, and for always taking care of me. Christopher and Ashley, I love you and I am very proud of you. Thanks for always supporting me. To my amazing friends, including Emmanuel Vázquez-Rivera and Dr. Madiha Khalid, thank you for all the fun times, for everything you have done for me and for your unconditional support. Finally, to my husband, Phillip, this journey would have been very difficult without all your advice and encouragement. Thanks for everything you have done for me, for us and for the causes that I support.

¡Familia y amigos gracias por todo su apoyo, los amo y los llevo en mi corazón siempre!

¡Gracias por existir!

PREFACE

Several parts of this dissertation have been published or submitted for publication. That includes portions of chapter one, which has been published in the Journal of Neurotoxicology; portions of the discussion which have been published in Current Environmental Health Reports and the appendix which has been submitted for publication. Portions of chapter two were presented at the Society of Toxicology Annual Meeting on 2014. Portions of chapter three were presented at the Society of Toxicology Annual Meeting on 2016 and 2017. All the content that is in this dissertation is one that I have authored.

Abstracts from posters published

1. The Toxicologist, Supplement to Toxicological Sciences, 138 (1), Abstract #1384, 2014, Brain region dependent effects of methylmercury on expression of ligand and voltage-gated calcium channels in rat. **Colón-Rodríguez A**., Hajela R.K., Atchison W.D.

2. The Toxicologist, Supplement to Toxicological Sciences, 150 (1), Abstract #1575, 2016, Contribution of AMPA receptors in methylmercury-induced cell death in the motor neuron NSC34 cell line. **Colón-Rodríguez A.,** Hajela R.K., Atchison W.D.

3. The Toxicologist, Supplement to Toxicological Sciences, 150 (1), Abstract #1143, 2017, Methylmercury alters intracellular calcium concentrations in human-induced pluripotent stem cell motor neurons in a concentration dependent manner. **Colón-Rodríguez A.**, Colón-Carrión N., Atchison W.D.

Scientific articles published

1. **Colón-Rodríguez A.** Hannon H.E., and Atchison W.D. (2016). Effects of methylmercury on spinal cord afferents and efferents—a review. Neurotoxicology.

2. Bailey J.M., **Colón-Rodríguez A.**, and Atchison W.D. (2017). Evaluating a Gene-Environment interaction in amyotrophic lateral sclerosis: methylmercury exposure and mutated SOD1. Current Environmental Health Reports.

TABLE OF CONTENTS

LIST OF TABLES

LIST OF FIGURES

KEY TO ABBREVIATIONS

ADAR	adenosine deaminase acting on RNA
ALS	amyotrophic lateral sclerosis
AMPA	α-amino-3-hydroxy-5-methyl-4-isoxazolepropionic acid
ANOVA	analysis of variance
Ca^{2+}	calcium ion
Ca^{2+}_e	extracellular calcium
Ca^{2+}_i	intracellular calcium
$[Ca^{2+}]_i$	intracellular calcium concentrations
CGC	cerebellar granule cells
CNS	central nervous system
CNQX	6-cyano-7-nitroquinoxaline-2,3-dione
d	days
DIV	days in vitro
EGTA	ethylene glycol-bis(2-aminoethylether)-N,N,N',N'-tetraacetic acid
Fura-2-AM	Fura-2-acetoxymethylester
GABA	gamma-amino butyric acid
$GABA_A$	gamma-amino butyric acid receptor A, ionotropic receptor
hr	hour
HBS	HEPES-buffered saline
HEPES	(4-(2-hydroxyethyl)-1-piperazineethanesulfonic acid)
hiPSC	human induced pluripotent stem cell
Hg	mercury

$HgCl_2$	mercuric chloride
K	potassium
KA	kainic acid
KCL	potassium chloride
µ	micro
M	molar
MD	Minamata disease
mEPP	miniature end plate potential
MeHg	methylmercury
min	minute
MK-801	dizocilpine
MN	motor neuron
NF-200	heavy-chain neurofilament of 200 kilodaltons
Na	sodium
NAS	1-Naphthyl acetyl spermine trihydrochloride
nM	nano molar
NMDA	N-methyl-D-aspartate
NMJ	neuromuscular junction
PND	post-natal day
qPCR	quantitative real-time PCR
RTPCR	reverse transcription PCR
s	second
SEM	standard error of the mean

TPEN	N,N,N',N'-tetrakis (2-pyridylmethyl) ethane-1,2-diamine
VGCC	voltage gated calcium channel
v/v	volume per volume
w/v	weight per volume
Zn^{2+}	zinc ion

CHAPTER ONE: INTRODUCTION

A) Background

a. Methylmercury (MeHg) neurotoxicity

Mercury is an environmental toxicant derived from both natural and anthropogenic sources. In the environment, elemental mercury (Hg^0) originates from the Earth's crust and volcanic emissions. Anthropogenic sources include burning of coal, waste incineration and gold mining. Hg^0 enters the atmosphere as a vapor, where it then becomes part of the water cycle. Once in the atmosphere, Hg^0 can remain in its vaporous state and move throughout the atmosphere, or become oxidized to Hg^{2+} and recycle to the Earth in rain (Clarkson and Magos, 2006, Horowitz et al. , 2014). Accumulated Hg^{2+} can be methylated by sulfate-reducing bacteria in bodies of water, generating MeHg. Given its lipophilic properties, MeHg then enters the aquatic food chain through the process of bioaccumulation. Humans are exposed to MeHg primarily through the consumption of contaminated seafood (Clarkson, 1995).

MeHg is the most prevalent form of organic Hg normally encountered, and it is of environmental and public health concern due to its prevalence and persistence in the environment. Two major MeHg poisoning events initiated the many studies and discoveries about MeHg toxicity: the long-term exposures in Minamata, Japan (1953- 1956) and the acute exposures in Iraq (1970s) (Bakir et al. , 1973, Clarkson and Magos, 2006, Eto, 1997). Studies from both of these poisoning events led to the following findings: there is a latent period between the exposure to MeHg and the onset of symptoms; severity of symptoms is dose-dependent; the first and most prevalent symptom is paresthesia, the second is ataxia, followed by muscle weakness, tremor, dysarthria, hearing and visual impairment (Bakir, Damluji, 1973, Eto, 1997). Patients presenting with these clinical signs as a result of environmental exposure to MeHg were

diagnosed with the neurologic syndrome of Minamata disease (MD) (McAlpine and Araki, 1958).

MeHg causes both adult and developmental neurotoxicity. Developmental toxicity was observed in the two major poisoning episodes of Minamata and Iraq (Bakir, Damluji, 1973, Eto, 1997). However, MeHg exposure occurs over the life span and adult onset exposures are an unexplored area. This is especially relevant for the population in the Amazon region of Madre de Dios, Peru (Ashe, 2012, Fraser, 2016, Gardner, 2012). The increase use of Hg for artisanal gold mining in this region has made it the current largest known source of Hg pollution in the world (Wade, 2013). Hg vapors are released to the environment while it is burned off the gold and is also disposed into water sources, where it is bio converted into MeHg. It has been reported that gold miners are exposed to Hg dermally and through vapors, but also to MeHg because of their common dietary practices of fish consumption (Ashe, 2012, Fraser, 2016, Gardner, 2012, Wade, 2013). This is one of the largest known adult Hg and MeHg exposures and the neurological effects have not yet been studied. However, it is believed that 48,000 people have been affected so far (Fraser, 2016). In 2012, it was reported that only 11% of the population at Madre de Dios mining zones had levels of Hg above 16 mg/gram of dry hair, a concentration considered as symptomatic by the World Health Organization (Ashe, 2012). However, recent reports indicating if and how these levels have changed are lacking. Based on previous reports discussed here, if exposure to MeHg continues in Madre de Dios, Peru in a similar manner as it has been reported since 2012, it is expected for this population to present neurological signs similar to those observed in MD.

Neurologic signs of MD correlate with degeneration of susceptible neuronal populations, including cerebellar granule cells and somatosensory neurons (Al-saleem, 1976, Bakir, Damluji,

1973, Eto, 1997, Eto et al. , 2002, Takeuchi et al. , 1962). The discrete mechanisms leading to MeHg-induced neurodegeneration remain elusive and multiple mechanisms may ultimately contribute to degeneration. The dysregulation of intracellular Ca^{2+} appears to be a critical component. MeHg exposure *in vitro* and *in vivo* leads to a time-and-concentration-dependent increase in intracellular Ca^{2+} concentrations ($[Ca^{2+}]_i$) in multiple primary neurons and immortalized cells (Hare et al. , 1993, Johnson et al. , 2011, Marty and Atchison, 1997, Ramanathan and Atchison, 2011). This effect manifests as at least two kinetically distinct phases *in vitro*. MeHg-induced alterations in $[Ca^{2+}]_i$ can be measured using a technique called single-cell Ca^{2+} microfluorimetry. Cells in culture can be loaded with the fluorophore Fura-2-acetoxymethyl ester (Fura-2AM) which readily crosses the cell membrane and bind to free Ca^{2+}. Once in the cells, esterases cleave the ester moiety and release the active, ionic compound to bind to free Ca^{2+}. Changes in $[Ca^{2+}]_i$ are then measured at 505 nm by calculating the ratio obtained using alternating excitation at 340 nm and 380 nm, corresponding to bound and unbound $Ca^{2+}{}_i$, respectively (Grynkiewicz et al. , 1985, Limke and Atchison, 2009). Using this technique and fluorophore it was identified that MeHg causes alterations in $[Ca^{2+}]_i$ in two distinct phases: phase 1 results from release of Ca^{2+} from intracellular stores whereas phase 2 corresponds with the influx of extracellular Ca^{2+} ($Ca^{2+}{}_e$) (Limke et al. , 2004, Marty and Atchison, 1997).

MeHg accumulates in different neuronal cells types; however, that does not necessarily contribute to their degeneration. In comparative studies, MeHg toxicity in cerebellar granule cells was was not dependent on MeHg accumulation, as it accumulates in greater amounts and is less cytotoxic in the cerebellar Purkinje cells, a larger cell type (Edwards et al. , 2005). However, Purkinje cells have high levels of the Ca^{2+} binding protein calbindin that cerebellar granule cells

do not. This apparently confers relative protection against the damage triggered by Ca^{2+} dysregulation. The absence of Ca^{2+} binding proteins and the presence of certain ligand- and voltage-gated ion channels have been considered as important contributing factors to MeHg toxicity (Limke et al. , 2004).

b. Motor system

i. Organization of the motor system

Motor information is transmitted from the primary motor cortex (via upper motor neurons (MNs)) to the muscles via lower MNs, permitting essential functions such as respiration, digestion, and voluntary movement. Classification of MNs is based on the type and contractile properties of innervated muscle fibers. The three main MN classifications are: α, β and γ. α MNs are responsible for skeletal muscle contraction and innervate extrafusal skeletal muscle, β MNs are involved in muscle contraction as well and innervate the intra- and extrafusal fibers, and the γ MNs are responsible for the muscle spindle and thus innervate intrafusal muscle fibers (Burke, 1980, Burke et al. , 1973). β MNs are not as well characterized as α and γ MNs. Thus, a comparison of β MNs with the other two types is not yet possible. However, several studies have identified unique characteristics in α and γ MNs that can make them uniquely susceptible to neuronal degeneration as a result of exposure to environmental toxicants or neurodegenerative diseases (Kanning et al. , 2010). α MNs are larger in size than γ MNs, resulting in a greater volume of axoplasm and membrane to be maintained, having a higher threshold for activation. α MNs also have more dendrites as opposed to the γ MNs which have fewer synaptic inputs. This contributes to the difference in synaptic communication of these two cell types. Because α MNs are the most abundant MNs, they are further subdivided as: α fast- twitch fatigable (FF), fast-twitch fatigue resistant (FR) and slow twitch fatigue resistant (S) (Burke, Levine, 1973). These

three classifications of α MNs vary in size, arborization and the response of the muscle fiber they innervate (Kanning, Kaplan, 2010).

Sensory and MNs work cooperatively to enable environmental perception and movement. Sensory neurons receive information through receptors from the skin and send the signal through the dorsal column to the thalamus where it is then relayed to the primary somatosensory cortex. There the sensory signal is sent to three different association areas: 1) the unimodal and 2) multimodal sensory association area, and 3) the multimodal motor association area. Within the sensory association regions, specific sensory signals are sorted and integrated into a single sensory response, which is then interpreted and converted into a motor response by the multimodal motor association area. The motor response is then sent to the premotor and primary motor cortices. MNs that originate in the primary motor cortex descend through two major pathways, the lateral pathway, which controls voluntary movement, or the ventromedial pathway, which controls posture and locomotion. The ventromedial pathway is controlled by the brainstem. This pathway comes from the primary motor cortex, makes a connection with the lower MNs in the brainstem superior colliculus or reticular nuclei and their axons make a connection with the α MNs in the spinal cord (Bear et al. , 2006). Subclasses of dorsal root ganglia also form synapses with interneurons and the α MNs from the spinal cord to modulate reflexive motor movement without central integration (Boron and Boulpaep, 2009).

Interactions between sensory afferents and motor efferents are essential for their mutual function in the nervous system. Dysfunction or degeneration of one could lead to a similar effect in the other. Also, sensory and MN diversity in morphology, electrical properties and receptor expression could be an important factor in the susceptibility of these cell populations to MeHg toxicity.

c. Effects of MeHg on motor efferents

Effects of MeHg on motor efferents have not been extensively studied. However, the onset of motor dysfunction can occur in adults at hair mercury concentrations of 200 ppm (Bakir, Damluji, 1973, Clarkson and Magos, 2006) and motor degeneration occurred after both acute and chronic exposure to MeHg in Minamata (Eto, 1997). Motor dysfunction in MeHg-poisoned humans includes ataxia, muscle weakness, and inability to walk; these observations are consistent with clinical signs of neuromuscular-like disorders, suggesting MeHg impacts MN function to some extent (Dietrich et al. , 2005, Eto, 1997, Eto, Tokunaga, 2002, Rustam et al. , 1975).

i. Morphological changes and degeneration

In an effort to understand the mechanism of MeHg induced-toxicity and degeneration of MNs, early studies focused on determining the correlation between the pathways of MeHg exposure and its presence in the central nervous system. Adult Wistar rats exposed to 100 or 200 μg MeHg via intraperitoneal injection daily for 2 – 50 days presented MeHg accumulation in the spinal cord (upper cervical cord) and cerebellum after 10 days of exposure. The concentration found at these sites was ~ 2,000 μg. Interestingly, presence of MeHg in the spinal cord was mostly in the anterior horn where effector MNs are present. Thus, as expected, rats exposed to the highest MeHg concentration (200 μg/day) developed progressive motor coordination disorders such as hind leg weakness (Møller-Madsen, 1990). As previously observed in human exposures, a latent period was observed between the times the rats were exposed to MeHg and the onset of the observed motor dysfunction (Bakir, Damluji, 1973, Eto, 1997, Møller-Madsen, 1990). Oral MeHg exposure *ad libitum* in water to 20 mg/L for 6 to 84 days caused the same results and MeHg deposits were visible in the spinal cord at day 16 for neurons and day 20 for

glia (Møller-Madsen, 1991). Although there has been no correlation between MeHg accumulation and neuronal degeneration, when the spinal cord tissue was saturated at day 28, the majority of MeHg was deposited in the anterior horn and ataxia was observed (Møller-Madsen, 1991). This could correlate to the degeneration of MNs present in the anterior horns; however, that was not the focus of previous studies and therefore not assessed.

In order to identify if MeHg was indeed causing the degeneration of MNs in the spinal cord, another group exposed adult Wistar rats to 10 mg/kg/day MeHg with equimolar amounts of L-cysteine orally for 10 days. As was demonstrated previously by Møller-Madsen, 1990, 1991, MeHg accumulated preferentially in the anterior horn at around 14 days (4 days after the final dose). Lumbar spinal cord sections as well as spinal anterior roots demonstrated neurophagia, atrophy and degeneration of large MNs (20 – 50 μm diameter) and myelinated fibers at days 14 – 18 (Su et al. , 1998). Small and medium size MNs did not present damage or MeHg accumulation. Although these observations directly support previous findings of MeHg toxicity in α MNs, it is important to note that the concentrations used in this study are nearing the MeHg LD_{50}, lethal dose to fifty percent of the population, and the co-administration of L-cysteine was performed which enhances MeHg uptake (Aschner et al. , 1990).

MN degeneration after MeHg exposure also occurs *in vitro* in a MN-like cell line, NSC34. NSC34 cells are a hybrid between mouse embryonic spinal cord MNs and neuroblastoma cells (Cashman et al. , 1992) and have been extensively used for studying MN diseases (Muyderman et al. , 2009). When exposed *in vitro* to MeHg (0.25 – 16 μM) for 48 hr, NSC34 cells undergo a concentration-dependent cell death (Chapman and Chan, 1999). Exposure to $HgCl_2$ (15 – 200 μM) for 48 hr also resulted in a concentration-dependent cell death

of NSC34 cells. However, the calculated LD_{50} of MeHg (1.74 μM) and $HgCl_2$ (7.95 μM) suggests that MeHg is more toxic than $HgCl_2$ in NSC34 cells (Chapman and Chan, 1999).

Only one study has focused on identifying the effects of MeHg on primary MNs *in vitro*. Spinal cord MNs isolated from mice at postnatal day 4 – 6 were exposed to 0.1 – 1 μM MeHg *in vitro*. MeHg-induced alterations in $[Ca^{2+}]_i$ were measured using Ca^{2+} microfluorimetry. MeHg-induced biphasic increases in MN $[Ca^{2+}]_i$ at concentrations as low as 0.1 μM. Similar to the observed alterations in cerebellar granule cells (Limke et al. , 2003, Marty and Atchison, 1997) making MNs a highly sensitive target to MeHg. Disruption of $Ca^{2+}{}_i$ in MNs was mediated in part by N-methyl-D-aspartate (NMDA), α-amino-3-hydroxy-5-methyl-4-isoxazolepropionic acid (AMPA) and Kainate (KA) glutamate receptors. Decreases in $[Ca^{2+}]_i$ occurred after exposure to the AMPA/KA antagonist 6-cyano-7-nitroquinoxaline-2,3-dione (CNQX) and NMDA receptor antagonist dizocilpine (MK-801) (Ramanathan and Atchison, 2011).

At the level of the neuromuscular junction (NMJ), MeHg also has concentration-dependent effects. In phrenic-nerve-diaphragm preparation from adult rat, *in vitro* bath-applied MeHg caused irreversible alterations in synaptic transmission. Frequency of miniature end plate potentials (mEPPs) increased after 15 – 40 min at 20 μM MeHg; higher MeHg concentrations (100 μM) caused similar effects after 5 – 15 min (Atchison and Narahashi, 1982). Alterations in synaptic transmission are one of the characteristics of MeHg toxicity (Atchison, 2005b, Juang, 1976, Juang and Yonemura, 1975) and could be one of the mechanisms by which MeHg is leading to MN damage.

In a study focused in understanding MeHg effects on the innervation of motor and sensory neurons on muscle, adult rats were exposed to 2 mg/kg/day MeHg chronically for 5-weeks via intubation. Wallerian degeneration was found in the nerve innervating the extensor

digitorum longus muscle (EDL) (Yip and Riley, 1987). This observation is consistent with findings from patients from Minamata and Iraq, as well as the rodent studies previously discussed here. Degeneration of 13.7% motor end plates occurred, however, no atrophy of muscle fibers occurred as a result of the motor end plate degeneration. Degeneration occurred at the level of the sensory fiber (Yip and Riley, 1987). Thus, it is possible that sensory degeneration leads to altered MN communication and subsequently degeneration.

In addition to MeHg, inorganic Hg accumulates and leads to motor dysfunction in large MNs (Dietrich, Mantese, 2005, Møller-Madsen, 1990, 1991, Pamphlett and Waley, 1996). Though Hg^{2+} is not as toxic as MeHg, it is important to identify its effects at the cellular level, because low concentrations of MeHg are de-methylated in the brain of monkeys (Vahter et al. , 1994) and rodents (Suda and Hirayama, 1992, Suda et al. , 1992). $HgCl_2$ can also move in a retrograde fashion from the muscle nerve terminal into MN soma (Arvidson, 1992). In a study conducted in adult rats, a single intramuscular injection of 30 μg of $HgCl_2$ caused sensory and lower MN Hg accumulation. Although inorganic Hg accumulated in MN cell bodies no cell damage was detected (Arvidson, 1992). At the NMJ, $HgCl_2$ also inhibits synaptic transmission (Juang, 1976, Røed and Herlofson, 1994). Although $HgCl_2$ cannot cross the blood brain barrier as readily as MeHg, once it does, it causes similar effects, most importantly MN degeneration. MN dysfunction has been observed in the form of Amyotrophic Lateral Sclerosis (ALS)-like symptoms after $HgCl_2$ poisoning (Praline et al. , 2007), and because there has been no evidence of it being the causative agent of the disease, it is suggested that gene x environment interactions could play a role in the development of such disease. The same has been the case for MeHg (Johnson, Yuan, 2011, Roos et al. , 2006, Sutedja et al. , 2009).

ALS is the most common MN disease in humans. ALS patients' present symptoms that are similar to those observed after mercurial poisoning. Most importantly, several of the mechanisms involved in ALS-induced MN degeneration are similar to those observed after MeHg poisoning. Other important factors that can contribute to MN susceptibility to degeneration after environmental exposures and in ALS are: 1) low abundance of Ca^{2+} binding proteins such as calbindin D-28K and parvalbumin (Ince et al. , 1993, Palecek et al. , 1999); and 2) increase of Ca^{2+}-permeable AMPA receptors, which also occurs in normal human nervous system (Kawahara et al. , 2003). Therefore, if MNs have a predisposition to cell death by Ca^{2+}-mediated pathways, exposure to an environmental toxicant such as MeHg, which causes toxicity through Ca^{2+} dysregulation, would likely cause these cells to degenerate at a faster rate or exhibit toxicity earlier. This might have been the case in a study in which a mouse model carrying an ALS mutation, the superoxide dismutase 1 G93A (SOD1-G93A), were exposed to chronic low dose (1 and 3ppm) MeHg, *ad libitum* in water, and an earlier onset of ALS-like symptoms was observed (Johnson, Yuan, 2011). The superoxide dismutase 1 is a free radical scavenger protein that is present in mammals. In ALS, mutations in the SOD1 enzyme are present in both familial and sporadic forms of the disease. The SOD1-G93A mutation leads to an increase in expression of this enzyme. Its overexpression causes impaired function of the protein and a cascade of downstream events that cause MN cell death. SOD1-G93A animals have been well characterized and thus present a great model to use in ALS-related studies. Most importantly because in the sporadic and the familial form of ALS the mechanism of pathogenesis is indistinguishable, it presents a feasible model to study both sporadic and familial ALS.

In order to identify how MeHg was causing alterations in MNs in the SOD1-G93A mouse model, Ca^{2+} microfluorimetry experiments were performed in MNs from brainstem

hypoglossal nucleus. MeHg-induced increases in $[Ca^{2+}]_i$ were mediated in part by Ca^{2+}-permeable AMPA and KA receptors, as the increases in Ca^{2+} were reduced by the antagonist of Ca^{2+}-permeable AMPA receptors, 1-Naphthyl acetyl spermine trihydrochloride (NAS) and CNQX (Johnson, Yuan, 2011).

ii. Glutamate receptors as probable contributors of MeHg-induced Ca^{2+} dysregulation

Glutamate is the most abundant excitatory amino acid in the central nervous system. It acts on distinct types of receptors; ionotropic and metabotropic. I focus on the ionotropic glutamate receptors because they have been implicated in the degeneration of MNs in ALS (Kwak et al. , 2010, Spalloni et al. , 2012) and after MeHg exposure (Johnson, Yuan, 2011, Ramanathan and Atchison, 2011). Ionotropic glutamate receptors include NMDA, AMPA and KA receptors.

NMDA receptors are unique as they have both ionotropic and voltage-gated properties. For NMDA receptors to activate they need the depolarization of the cell, which will lead to the removal of a Mg^{2+} molecule from its pore, and the binding of a glutamate or NMDA and a glycine molecule. Once opened, NMDA receptors will allow the flow of Na^+, K^+, and Ca^{2+}, making them essential for excitatory neurotransmission. NMDA receptors are heterotetramers comprised of two NR1 and two NR2 (NR2A-D) subunits. In certain neuronal populations the receptor composition can be two NR1 and two NR3 subunits (Fig. 1.1) (Paoletti et al. , 2013).

NMDA receptors became the targets of study because they are the main ion channels involved in synaptic plasticity which is essential for cognitive functions, which are affected in rodent models after MeHg exposure. In a study in which rats were treated with a single dose of 8 mg/kg MeHg via oral gavage, alterations in cognitive functions occurred. To identify if the NMDA receptors were affected, mRNA expression of all the NMDA subunits was measured.

The NR2B subunit was up regulated in the hippocampus but not the frontal cortex, suggesting that alterations in cognitive functions could be associated with alterations in expression of specific NMDA receptor subunits in the hippocampus (Baraldi et al. , 2002). In another study that focused on understanding MeHg effects in spatial learning and memory oral exposure to 5 mg/kg/day MeHg for 7 days caused downregulation of the NR2A and NR2B subunits and increased expression of NR2C subunit in the hippocampus (Liu et al. , 2009). Based on these results it is evident that effects of MeHg on NMDA gene expression differ depending on the time of exposure, concentration and duration as demonstrated by Baraldi, Zanoli (2002) and Liu, Wang (2009). However, the important observation is that altered expression of NMDA receptor subunits does occur after MeHg exposure, and this could occur in other regions of the central nervous system thereby contributing to MeHg-induced cytotoxicity.

NMDA receptors also mediate cell death after MeHg exposure in the occipital cortex, hippocampus, cerebellum and brainstem (Miyamoto et al., 2001). Postnatal days 2, 16 and 60 rats were treated orally for 7 days to 10 mg/kg/day MeHg and MK-801 intraperitoneally. Mild levels of degeneration of neurons occurred in the brainstem at PND2 and 16. However co-administration of MK-801 decreased MeHg-induced effects (Miyamoto et al. , 2001). This study demonstrated that in the brainstem, a region rich in MNs, MeHg causes cell death by mechanisms that involve NMDA receptors.

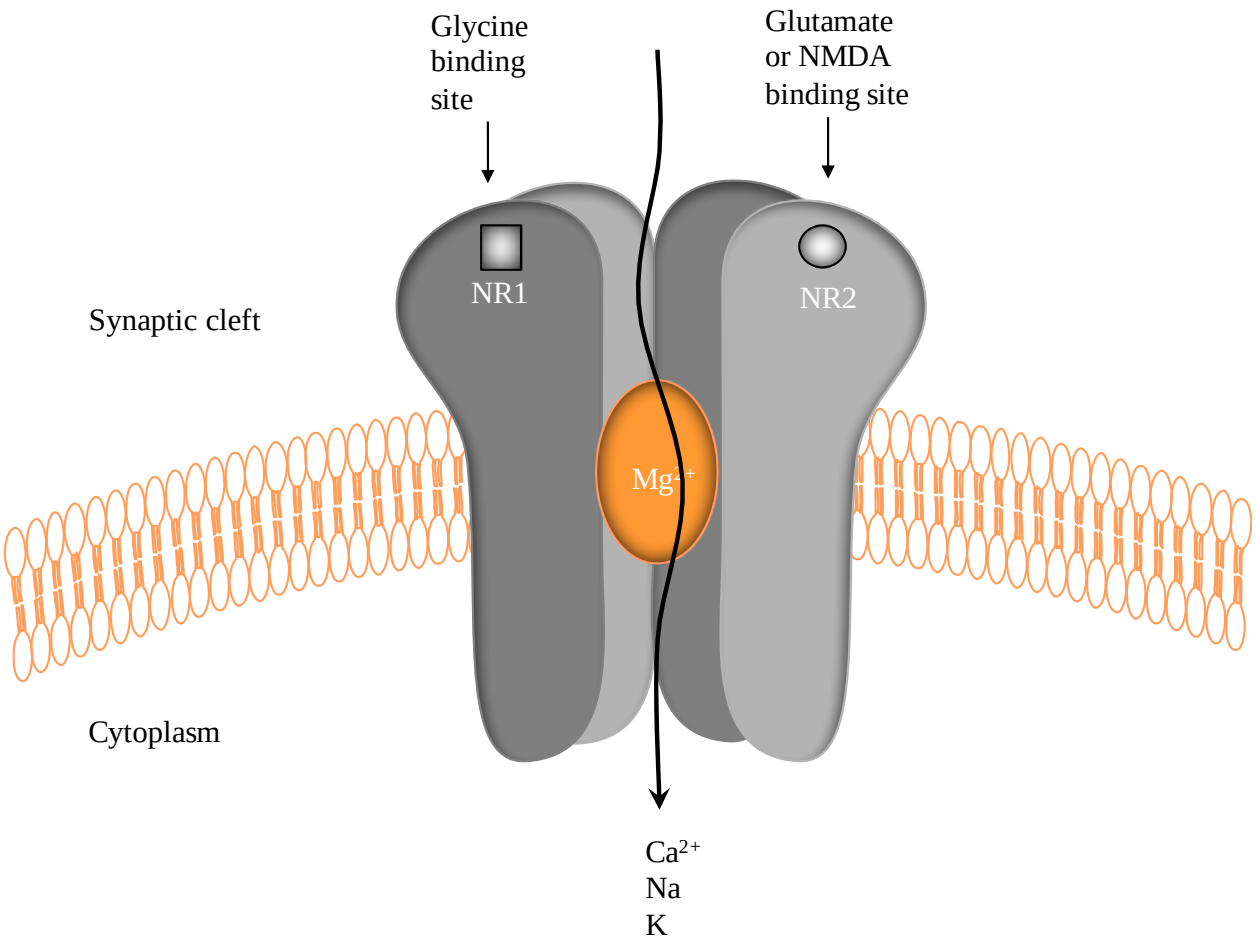

Figure 1.1. NMDA receptor structure and composition. NMDA receptor are heterotetramers comprised of two NR1 and two NR2 (NR2A-D) subunits. In certain neuronal populations, the receptor composition can be two NR1 and two NR3 subunits. For NMDA receptors to activate they need the depolarization of the cell, which will lead to the removal of a Mg^{2+} molecule from its pore, and the binding of a glutamate or NMDA and a glycine molecule. Once opened, NMDA receptors will allow the flow of Ca^{2+}, Na, and K.

An *in vitro* study in which human neuroblastoma SH-SY-5Y cells were exposed to 0.25 – 5 μM MeHg for 4 hr showed that MeHg causes necrotic cell death by Ca^{2+} pathways mediated in part by NMDA receptors. Exposure to MK-801 or the NMDA antagonist memantine (1-amino-3,5-dimethyl-adamantane) decreased MeHg-induced cell death (Ndountse and Chan, 2008). Thus, the previous studies demonstrate that NMDA receptors can contribute to MeHg-induced cell death as a result of the alterations in the expression of specific receptor subunits and/or by contribution of NMDA-mediated Ca^{2+} influx.

AMPA type glutamate receptors have also been associated with MeHg-induced toxicity. AMPA receptors are heterotetramers comprised of combinations of four subunits GluA1, GluA2, GluA3, and GluA4, also known as GluR1-4 or GluA1-4. Each subunit is encoded by a distinct gene. AMPA receptors are composed of dimeric dimers (Fig. 1.2). Each subunit confers a unique kinetic property to the AMPA receptors, as do the post transcriptional modifications such as RNA editing and alternative splicing (Bettler and Mulle, 1995, Bleakman and Lodge, 1998). AMPA receptors are activated by glutamate or the analog AMPA. AMPA receptors are typically permeable to Na^{+} and K^{+}, but not Ca^{2+}; this property is mediated by post-transcriptional RNA editing of the GluA2 subunit. AMPA receptors also undergo alternative splicing, which involves a change in the amino acid sequence that determines the electrophysiological properties of the receptor. Alternative splicing on AMPA receptors can lead to two splice variants, "*Flip*" or "*Flop*". The "*Flip*" form of the receptor desensitizes slowly while the "*Flop*" form desensitizes rapidly (Bettler and Mulle, 1995). Normally the GluA2 subunit is edited, giving AMPA receptors low permeability to Ca^{2+}. When the AMPA receptor does not have the GluA2 subunit or it contains the unedited form of the GluA2 (GluA2Q), they have high Ca^{2+} permeability (Fig. 1.3),

this alteration makes MNs susceptible to degeneration through Ca^{2+}-mediated pathways (Vandenberghe et al. , 2000).

RNA editing of the AMPA receptors occurs through the adenosine deaminase acting on RNA 2 (ADAR2) enzyme (Higuchi, 1993). ADAR2 is a double stranded deaminase that works specifically at the pore forming region of the GluA2 subunit known as the Q/R site (Fig. 1.3A). There the ADAR2 changes a glutamine (Q) codon for an arginine (R) codon. Normally the GluA2 is edited, giving AMPA receptors low permeability to Ca^{2+}. When the AMPA receptor contains the unedited form of the GluA2 (GluA2Q), they have high Ca^{2+} permeability (Fig. 1.3B). In AMPA receptors post transcriptional modifications have an important role in Ca^{2+} permeability and cell excitability. Therefore, it is important to identify if changes in these post transcriptional modifications are occurring after exposure to neurotoxicants, as these can contribute to susceptibility in cellular targets.

In ALS, increase levels of GluA2Q have been observed. Increases in GluA2Q levels can result from impaired function of the ADAR2. One way that ADAR2 function can be disrupted is by cleavage of its C terminal (Mahajan et al. , 2011). This can occur by glutamate excitotoxicity (overactivation of glutamate receptors) (Mahajan, Thai, 2011). Disruption in ADAR2 also leads to altered tetramerization of AMPA receptors. This can be occurring in MNs after chronic MeHg exposure.

Previous studies have shown that MeHg leads to increase glutamate release (Yuan and Atchison, 2007), impaired function of excitatory amino acid transporter EAAT2 (Aschner et al. , 2000) (impaired glutamate uptake), increased gene expression of GluA2 (presented in chapter 2) and increase in $[Ca^{2+}]_i$ (presented in chapter 3) (Johnson, Yuan, 2011, Limke et al. , 2004, Ramanathan and Atchison, 2011). These can be indicators of MeHg-induced alterations in the

RNA editing of the GluA2 subunit of AMPA receptors, leading to the observed alterations in $[Ca^{2+}]_i$ in MNs. However, this correlation has not been observed before and is one of the goals of this dissertation.

Alterations in glutamate reuptake and Ca^{2+} regulation in ALS and after MeHg exposures have been well documented (Aschner et al. , 2007, Atchison, 2005, Brookes, 1992, Grosskreutz et al. , 2010, Limke, Heidemann, 2004, Mutkus et al. , 2005). Most importantly, MeHg-induced alterations in $[Ca^{2+}]_i$ in MNs lead to early onset ALS-like phenotype in the superoxide dismutase 1 (SOD1-G93A) mouse (Johnson, Yuan, 2011). Using Ca^{2+} sensitive fluorophores and microscopy, it was determined that MeHg-induced alterations in MNs from the SOD1-G93A mice were moderated in part by Ca^{2+} permeable AMPA receptors. Although all of these findings shed light on the potential role of the AMPA receptors in MeHg-induced toxicity of MNs, there are still important gaps as to how these alterations occur. Thus, further studies are needed in order to characterize the role of this ion channel in MeHg-induced toxicity in MNs.

KA receptors are another group of ionotropic glutamate receptors that mediate fast excitatory neurotransmission in the central nervous system. These receptors are comprised of GriK1, GriK2, GriK3, GriK4 and GriK5 subunits arranged as a tetramer. Although KA receptors are less distributed in the nervous system than AMPA and NMDA they have shown to play a role in synaptic plasticity (Bettler and Mulle, 1995).

KA receptors had not been identified as potential contributors to MeHg-induced toxicity until recently. Ramanathan and Atchison, 2011, and Johnson et al., 2011 demonstrated that exposure to MeHg leads to increases in $[Ca^{2+}]_i$ in MNs that are mediated in part by KA receptors. Inorganic Hg was identified as an antagonist for KA receptors in the late eighties. In this study *Xenopus* oocytes expressing the human KA receptors were exposed to 1 μM Hg bath applied and

block of KA current was observed (Umbach and Gundersen, 1989). This study demonstrated that Hg can interact with the KA receptor and alter its function by blocking it. However, no further studies have been performed to characterize Hg or MeHg interaction with this receptor and the role it may play in MeHg-induced toxicity in neuronal cells.

Based on the literature discussed previously I aimed to demonstrate 1) that MNs are a target of MeHg toxicity and 2) that ion channels other than the well-studied $GABA_A$ receptor and the voltage gated Ca^{2+} channels (VGCCs) are mediating MeHg toxicity in neuronal cells and should be studied further. This led me to the rationale of this dissertation.

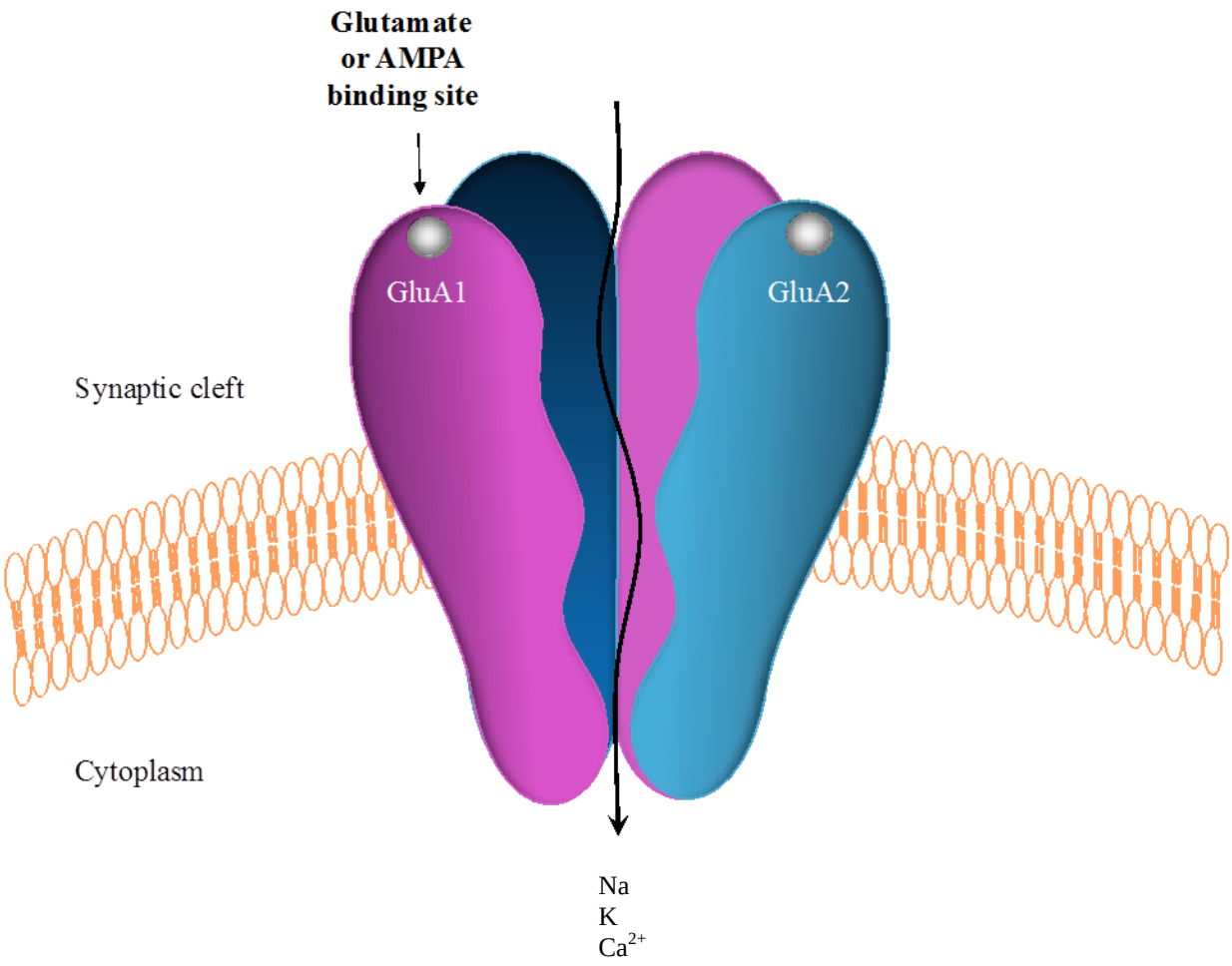

Figure 1.2. Subunit composition of the AMPA receptor. AMPA receptors are heterotetramers comprised of combinations of four subunits GluA1, GluA2, GluA3, and GluA4. Each subunit is encoded by a distinct gene. AMPA receptors are composed of dimeric dimers. Once glutamate or AMPA binds to the receptor it allows the flow of Na, K, and sometimes Ca^{2+}, depending on the subunit composition.

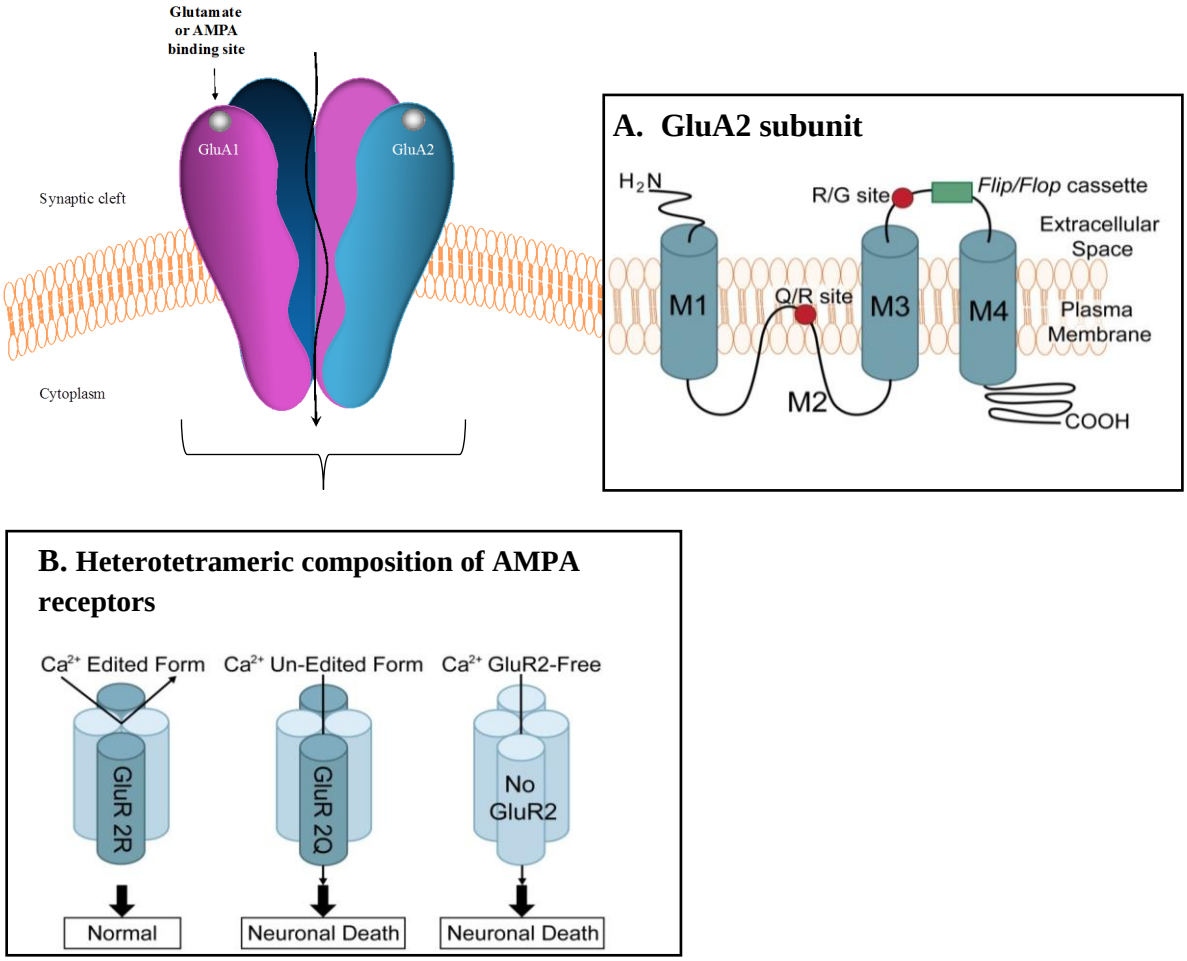

Figure 1.3. Post transcriptional modifications in the AMPA receptors determine their Ca^{2+} permeability as does the presence of the GluA2 subunit. AMPA receptors are typically permeable to Na and K, but not Ca^{2+}; this property is mediated by post-transcriptional RNA editing of the GluA2 subunit which occurs at the Q/R site of the GluA2 subunit (A). When GluA2 is not present in the receptor or when the unedited form (GluA2Q) is present in the receptor it confers Ca^{2+} permeability (B). Alterations in intracellular Ca^{2+} as a result of deficient RNA editing commonly lead to cell death. Figure modified from: (Kwak, Hideyama, 2010).

d. Rationale and specific aims

MeHg exposure alters $[Ca^{2+}]_i$ in MNs *in vitro* and *in vivo*. These are mediated in part by Ca^{2+} permeable AMPA receptors (Johnson, Yuan, 2011, Ramanathan and Atchison, 2011). However, the effects of MeHg in AMPA receptors have not been characterized nor the role these ion channels play in MeHg-induced Ca^{2+} alterations in MNs of human origin.

In spinal cord MNs abundance of Ca^{2+} permeable AMPA receptors is known. These cells also have low abundance of Ca^{2+} binding proteins. These two factors heighten the susceptibility of MNs to degenerate during insults that are mediated by Ca^{2+} pathways. This could have been the case in a study were MeHg-induced alterations in $[Ca^{2+}]_i$ in MNs led to early onset ALS-like phenotype in a superoxide dismutase 1 (SOD1-G93A) mouse (Ramanathan and Atchison, 2011). However, it is not known if mRNA levels of the RNA editing enzyme are decreased after MeHg exposure and decreased levels have been correlated with decrease GluA2 editing in ALS (Kawahara et al. , 2003). Also, we do not know if alterations in AMPA receptor expression occur after MeHg exposure contributing to the observed Ca^{2+} alterations.

All the previously mentioned studies have been performed in rodent models, thus we do not know if these findings could translate to what could occur in humans. The aim of the proposed experiments was to test the hypothesis that *alterations in Ca^{2+} permeability and expression of AMPA receptors, caused by MeHg exposure in rodent models, occur similarly in human induced pluripotent stem cell MNs (hiPSC-MN).* Our overarching hypothesis is that MeHg-induced alterations in $[Ca^{2+}]_i$ homeostasis in MNs are mediated by alterations in expression, function and RNA editing of the AMPA receptors. This hypothesis was tested in two specific aims:

Specific Aim 1. Does MeHg exposure affect AMPA receptor expression and Ca^{2+} permeability in MNs? The working hypothesis is that MeHg will alter the expression and Ca^{2+} permeability of the AMPA receptors, disrupting Ca^{2+} homeostasis leading to cell death.

Specific Aim 2. Will MeHg exposure alter Ca^{2+} homeostasis in hiPSC-MNs? If so, is this mediated by AMPA receptors? The working hypothesis is that MeHg exposure will impair the function and expression of AMPA receptors and alter the intracellular Ca^{2+} concentrations as a result of these alterations.

To address these aims I used two approaches. First, I sought to determine gross developmental and motor alterations, and global changes in the AMPA receptor expression in mice to identify global actions of MeHg toxicity beyond MNs (Chapter two). The second strategy was to examine at the level of the MN itself whether alterations in Ca^{2+} homeostasis and AMPA receptor expression occurred and if they were as a result of MeHg exposure (Chapter three).

e. Model Systems

i. NSC34 cell model

NSC34 cells are a hybrid between embryonic spinal cord MNs and neuroblastoma cells from mice (Cashman et al. , 1992). They have been developed by fusion of embryonic spinal cord MNs and neuroblastoma cells from mice. These cells can be used in their undifferentiated or differentiated states. Differentiated NSC34 cells express MN markers choline acetyl transferase (ChAT), non-phosphorylated neurofilament H (SMI32), microtubule associated protein (MAP2) and vesicular acethylcholine transporter (VAChT) among others (Cashman, Durham, 1992, Maier et al. , 2013). They also express functional glutamate receptor AMPA and NMDA (Eggett et al. , 2000). Because primary spinal cord MNs from post-natal mice are very difficult to isolate this MN cell line has been used extensively for *in vitro* MN studies. NSC34 cells have also been extensively used as an *in vitro* model for ALS (Babetto et al. , 2005, Fukada et al. , 2004, Gomes et al. , 2010, Hemendinger et al. , 2008, Lu et al. , 2012, Raimondi et al. , 2006, Sathasivam et al. , 2005) and once to study MeHg toxicity (Chapman and Chan, 1999). Differentiated NSC34 cells were used in Chapter 3 to optimize MeHg concentrations and techniques used in our spinal cord MN *in vitro* experiments before moving to the human MN cell model.

ii. Human induced pluripotent stem cell derived motor neurons (hiPSC-MNs)

Human induced pluripotent stem cells derived MNs (hiPSC-MNs) were used as our human MN cell model. The hiPSC-MNs used for our studies were purchased terminally differentiated as MNs from iX Cells Biotechnologies (San Diego, CA). These cells were the first hiPSC-MNs commercially available and came into the market in Spring 2016. Thus, there are no current publications with them or their characterization. I took advantage of this opportunity and

established a data sharing agreement with iX Cells Biotechnologies. We used hiPSC-MNs in Chapter three to characterize MeHg effects in human MNs, identify if Ca^{2+}_i alterations occur after acute MeHg exposure and identify if AMPA receptors are playing a role in the observed alterations.

B) Techniques

a. Intracellular Ca^{2+} measurements *in vitro*

MeHg causes alteration in $[Ca^{2+}]_i$ and these alterations contribute to MeHg-induced cell death in multiple neuronal cell types. These alterations can be measured by different techniques including single cell Ca^{2+} microfluorimetry. This technique allows us to measure alterations in Ca^{2+}_i in individual cells in real-time allowing us to identify changes that could precede cell death.

Ratiometric Ca^{2+} measurements were performed using Fura-2AM, an intracellular Ca^{2+} fluorophore (Marty and Atchison, 1997). The AM group allows Fura-2 to enter the cells and be cleaved by endogenous esterase's, therefore remaining in the cell and serving as an indicator of $[Ca^{2+}]_i$. Fura-2 excitation wavelengths are at 340 nm and 380 nm and the emitted fluorescence is measured at 505 nm. Fluorescence at 340 nm indicates the bound form of Fura-2 (Fura-2 + cation) whereas that at 380 nm indicates the unbound form of Fura-2 (Fura-2 unbound from cation). The ratio of fluorescence at 340/380 indicate increases in $[Ca^{2+}]_i$ (Grynkiewicz, Poenie, 1985). Although Fura-2AM is a very sensitive technique to monitor changes in $[Ca^{2+}]_i$, this fluorophore also has high affinity for other divalent cations including Zn^{2+}. Thus, what was measured in Chapter three are relative and not absolute changes in $[Ca^{2+}]_i$.

CHAPTER TWO: LOW LEVEL METHYLMERCURY EXPOSURE ALTERS mRNA LEVELS OF GLUTAMATE RECEPTORS AND VOLTAGE GATED CALCIUM CHANNELS IN THE CEREBELLUM AND BRAINSTEM OF THE DEVELOPING RAT

A) Abstract

Ion channels are especially sensitive to methylmercury (MeHg) toxicity. Ionotropic receptors such as N-methyl-D-aspartate (NMDA), α-amino-3-hydroxy-5-methyl-4-isoxazolepropionate (AMPA), and several types of voltage gated Ca^{2+} channels (VGCC) are some of the main targets, resulting in alterations on synaptic transmission and intracellular calcium $[Ca^{2+}]_i$ homeostasis. MeHg induced Ca^{2+} dysregulation leads to increased release of neurotransmitters, alterations in ion channel function, alterations in Ca^{2+} reuptake, and cell death. One characteristic clinical sign of MeHg toxicity is motor dysfunction. MeHg-induced alterations in Ca^{2+} homeostasis in motor neurons (MNs) is mediated by several glutamate receptors and VGCCs. All these events may contribute to the observed motor dysfunction. However, effects of MeHg on MNs have not been characterized. To identify possible mechanisms by which MeHg could be leading to Ca^{2+} dysregulation and motor dysfunction, we sought to determine the effects of MeHg on gene expression of AMPA, NMDA and VGCC subunits in the cerebellum and brainstem regions of rats. Comparing expression of these genes can reveal whether MeHg exposure results in lasting changes in gene expression of nerve membrane proteins whose function is affected by MeHg in cerebellum and brainstem. Postnatal day 5 rat pups were treated with 0.75 and 1.5 mg/kg/day MeHg. Treatment was maintained for 15 or, 30 days, and then stopped for a washout period of 30 days (PND 65). Quantitative real time PCR on reverse transcript (cDNA) of RNA isolated from 10 mg of cerebellum and brainstem was used to assay the transcript level of the target protein genes. Our results demonstrate that effects of MeHg at the mRNA level are more pronounced in the brainstem than in the cerebellum. These results suggest that brainstem can compensate for MeHg effects and the cerebellum does not, and thus is more susceptible to cell death than the brainstem.

B) Introduction

Methylmercury (MeHg) is a prevalent environmental neurotoxicant that affects the central nervous system (CNS) following acute and chronic exposure (Atchison, 2005). Characteristic clinical signs of MeHg poisoning include visual impairment, muscle weakness and ataxia. The developing nervous system has demonstrated high susceptibility to MeHg by being altered by this organo-metal in very low concentrations. The specific mechanism by which MeHg affects the CNS has not been elucidated, however previous studies have shown that it has cell specificity (Clarkson and Magos, 2006). Cellular targets of MeHg include cerebellar granule cells (CGC) (Hunter and Rusell,1954), astrocytes (Aschner, Yao, 2000) and motor neurons (MNs) (Ramanathan and Atchison, 2011). In these cell populations MeHg alters Ca^{2+} homeostasis and leads to cell death *in vitro* and *in vivo* (Johnson et al. , 2011, Ramanathan and Atchison, 2011). Ca^{2+} dysregulation is one of the main pathways by which MeHg leads to cell death (Limke, Heidemann, 2004, Yuan and Atchison, 2007).

Intracellular calcium $[Ca^{2+}]_i$ regulation is essential for numerous cellular functions, including neurotransmitter release and cell migration. Voltage dependent Ca^{2+} channels (VGCC) play an important role in these processes. Electrophysiological studies performed in cerebellar granule cells show that MeHg affects ion channels differentially, with VGCCs and gamma-aminobutyric acid A ($GABA_A$) receptors being the most susceptible to its toxicity (Ramanathan and Atchison, 2011, Yuan and Atchison, 2005). MeHg impairs the function of VGCCs and inhibitory $GABA_A$ receptors, leading to a complete block of the currents in a concentration and time dependent manner (Hajela et al. , 2003, Herden et al. , 2008, Peng et al. , 2002, Yuan and Atchison, 2005, Yuan and Atchison, 2003). Interestingly, *in vitro* studies show that blockage of VGCCs with specific antagonists delay MeHg-induced increase in $[Ca^{2+}]_i$ (Limke, Heidemann,

2004, Marty and Atchison, 1997), suggesting the involvement of VGCCs on MeHg-induced alterations in $[Ca^{2+}]_i$. Thus, alteration in $[Ca^{2+}]_i$ and ion channel function play an important role in MeHg-induced cytotoxicity.

MeHg alterations in Ca^{2+} homeostasis has been the focus of many studies that have identified several potential mechanisms by which this occurs. Limke et al. (2003) found that one way MeHg leads to increase in $[Ca^{2+}]_i$ is by interacting with the muscarinic receptor M3, activating inositol-1,3,4- triphosphate receptor (IP3R) and leading to release of Ca^{2+} from intracellular stores (Limke, Bearss, & Atchison, 2004; Limke T.L., 2003). MeHg inhibits astrocytic glutamate transporters (Aschner, Syversen, Souza, Rocha, & Farina, 2007), increasing glutamate in the synapse; possibly leading to activation of N-methyl-D-aspartate (NMDA) and α-amino-3-hydroxy-5-methyl-4-isoxazole propionic acid (AMPA) receptors, ultimately leading to an increase in $[Ca^{2+}]_i$. It has also been shown that glutamate receptors AMPA, NMDA and kainate (KA) contribute to MeHg-induced increases in Ca^{2+}, specifically in MNs (Ramanathan and Atchison, 2011). Therefore, selective effects of MeHg on certain ion channels and receptors may be responsible for MeHg selective neurotoxicity. However, the extent to which MeHg disrupts ion channel function and Ca^{2+} homeostasis via alterations in expression of genes that influence these processes has not been examined and is the focus of the present study.

Previous studies focused on gene expression alterations as a result of MeHg exposure have used techniques such as microarray, semi quantitative PCR and serial analysis of gene expression (SAGE) to identify cluster of genes that could be involved in MeHg-induced cell death (Cambier et al., 2010). These studies showed that MeHg causes alterations in the expression of Ca^{2+} binding proteins in skeletal muscle of zebrafish (Cambier et al., 2010), increased expression of genes involved in Ca^{2+} homeostasis, cell adhesion, signal transduction,

the ubiquitin-protease pathway, detoxification (Jayashankar et al., 2012; Shimada et al., 2010) and altered expression of NMDA receptors (Liu, Wang, Zhang, & Zhou, 2009; Ndountse & Chan, 2008). However, a direct correlation of the effects of MeHg on voltage gated and ligand gated ion channels in gene expression studies has not been done. To ascertain the effects of MeHg on these key genes we measured expression levels of known sensitive targets to MeHg toxicity such as the VGCCs, NMDA, and AMPA receptors. We chose to measure expression levels of the pore-forming α1 subunit of the P/Q type (α_{1A}), N type (α_{1B}), L type (α_{1C}) and R type (α_{1E}) VGCCs because this subunit is essential for VGCC function (Catterall, 2011). Because alterations in expression of NMDA receptors have been implicated in MeHg-induced cytotoxicity (Baraldi et al. , 2002, Liu et al. , 2009, Ndountse and Chan, 2008, Ramanathan and Atchison, 2011, Xu et al. , 2013) and AMPA receptors contribute to MeHg-induced increases in $[Ca^{2+}]_i$ in MNs (Ramanathan and Atchison, 2011), they were selected as targets in our study. In summary, our approach is focused on understanding the differences in susceptibility to MeHg toxicity of the cerebellum compared to the brainstem, by measuring gene expression profiles of these key genes in each tissue.

C) Materials and methods

a. Chemicals

Methylmercuric (II) chloride (MeHg) was purchased from ICN Biomedical Inc. (Costa Mesa, CA). A stock solution used for injections was prepared with physiological saline solution (0.9% NaCl) to a final concentration of 4 mg/ml. Dilutions for injections were prepared daily using the 4 mg/ml MeHg stock solution.

b. Animals and MeHg exposure

All animal procedures were approved by the Institutional Animal Use and Care Committee (IACUC) at Michigan State University and were in accordance with the National Institutes of Health guidelines. Forty post-natal day four (PND 4) male Sprague Dawley rats along with dams were purchased from Charles River Laboratories (Wilmington, MA). Animals were housed under standard conditions (12:12 light/dark cycle, normal food and water *ad lib*). Pups were housed with the dam until PND 21, and then housed individually. MeHg exposure started at postnatal day 5 (PND 5) and was via daily subcutaneous injection. Although the most common form of MeHg exposure is orally, through contaminated sea food, we chose to do our exposures via subcutaneous injections because it was the most practical way to dose PND 5 pups. PND 5 rat pups were divided into three groups; control (0.9% NaCl), 0.75 mg/kg/day and 1.5 mg/kg/day MeHg. Daily injections were given for either 15 (through PND 20), or 30 days (through PND 35). Another group that was given injections daily for 30 days was kept for a "washout" period of 30 days without any further treatment (through PND 65). The "washout" period was used to determine whether MeHg effects on gene expression were reversible. Weight, behavior and general health were monitored starting on PND 5 until euthanized on PND 20,

PND 35 or PND 65. Cerebellar and brainstem tissue were dissected, excised and immediately frozen in liquid nitrogen, and kept at -80^{O}C until use.

c. Neurodevelopment

Neurodevelopment was assessed daily starting on PND 5. During the first week, the time to open the eyes, fur development and incisor presence was assessed. Body weight was taken every day for the first thirty days of treatment and every other day thereafter until the day of euthanasia.

d. Surface righting reflex and hind limb cross

Surface righting reflex and hind limb crossing were assessed daily for the thirty days of treatment. The righting time was performed by placing the animal on his back and measuring how long he took to turn to the upright position. Hind limb crossing was assessed by lifting the rat by the tail 8 inches from the surface and observing spacing between the hind limbs. The measurements were as follows: No hind limb cross (0), partial hind limb cross = limbs crossing or approaching midline (1), and full cross = both limbs crossing midline (2).

e. RNA isolation

Total RNA and protein were isolated, from a sagittal slice of the cerebellum (10 mg) or a section of the brainstem region where the hypoglossal nucleus and the dorsal motor nucleus of vagus are located, following the TRI reagent (Molecular Research Center; Cincinnati, OH) manufacturer's protocol. The concentration and integrity of the RNA was assessed spectrophotometrically in the Nanodrop-2000 (Thermo-Scientific; Pittsburg, PA) and by denaturing gel electrophoresis (Aranda, LaJoie, & Jorcyk, 2012). A ratio of 1.9-2.0 at 260/280 nm absorbance was considered appropriate.

f. Reverse transcription PCR

Isolated total RNA was diluted to a final concentration of 2 µg/ml. Reverse transcription PCR was performed using the High Capacity cDNA Reverse Transcription Kit protocol (Applied Biosystems; Grand Island, NY), with thermal conditions of: 85 ^{o}C for 15 min, 37 ^{o}C for 120 min and 80 ^{o}C for 5 min. The purity and concentration of the cDNA was assessed using the ND-2000. A ratio of 1.8 at 260/280 nm absorbance was considered pure.

g. Quantitative real-time PCR (qPCR)

Housekeeping genes were selected after analyzing the expression in treated and untreated samples, and determining that the expression was unaffected by the conditions using NormFinder (Andersen et al. , 2004).

Real time PCR was performed using an ABI Fast 7500 thermal cycler following the TaqMan gene expression assay protocol (Applied Biosystems, Grand Island, NY), with thermal cycler conditions of: 50 ^{o}C for 2 min, 95 ^{o}C for 10 min, followed by 40 cycles (95 ^{o}C for 15 s and 60 ^{o}C for 1 min). TaqMan gene-specific primers that were used are listed in table 1. Transcript expression profiling was performed in triplicates for each sample and the threshold cycle values were averaged. A concentration of 2.25 µg was used as the input for each sample, to control for variability. Transcript expression levels were normalized to GAPDH and βactin (housekeeping genes), and the untreated control. The results are presented as fold change in expression compared to controls, calculated for each gene following the $2^{\Delta\Delta Ct}$ Livak method (Livak & Schmittgen, 2001).

h. Statistical analysis

Statistical analysis was performed using GraphPad Prism® software version 6 (GraphPad Software, Inc., La Jolla, CA) to draw comparisons among groups using two-way analysis of

variance (ANOVA) for MeHg gene expression studies. Bonferroni's test was performed for post hoc comparisons. Statistical significance was considered for values $p \leq 0.05$.

Table 1.1. Genes and accession number of the TaqMan primers used in rat quantitative real-time PCR experiments.

Gene	Gene name	Gene Bank ID	Accession number
Endogenous controls (housekeeping genes)			
Actb	Actin, beta	NM_031144.2	Rn00667869_m1
Gapdh	Glyceraldehyde-3-phosphate Dehydrogenase	NM_017008.3	Rn01775763_g1
Glutamate AMPA receptor subunits			
Gria1	GluA1 subunit	NM_031608.1	Rn00709588_m1
Gria2	GluA2 subunit	NM_017261.2	Rn00568514_m1
Gria3	GluA3 subunit	NM_032990.2	Rn00583547_m1
Gria4	GluA4 subunit	NM_001113184.1	Rn00568544_m1
Glutamate NMDA receptor subunits			
Grina	N-methyl D-aspartate 1	NM_153308.4	Rn00596289_g1
Grin2a	N-methyl D-aspartate 2A	NM_012573.3	Rn01424654_m1
Grin2b	N-methyl D-aspartate 2B	NM_012574.1	Rn00680474_m1
Grin2c	N-methyl D-aspartate 2C	NM_012575.3	Rn00561364_m1
Voltage gated calcium channel (VGCC), alpha 1 subunit			
Cacna1a	P/Q type VGCC, $\alpha 1_A$ subunit	NM_012918.3	Rn01512405_m1
Cacna1b	N type VGCC, $\alpha 1_B$ subunit	NM_147141.1	Rn00595911_m1
Cacna1c	L type VGCC, $\alpha 1_C$ subunit	NM_012517.2	Rn00709287_m1
Cacna1e	R type VGCC, $\alpha 1_E$ subunit	NM_019294.2	Rn00494444_m1

D) Results

a. Animal health and behavior was not affected by low-dose MeHg exposure

Rat body weight was monitored daily for the treatment period to determine if MeHg exposure altered normal growth weight gain and no differences were found (Fig. 2.1). Neurodevelopment was assessed during the first week of treatment, the time to open the eyes, fur development and incisor presence were monitored and no changes were found between controls and treated rats. Motor reflex was measured in the form of righting reflex as an indirect measurement of motor dysfunction because due to the age of our rats it was difficult to address with other methods. No changes were found in the form of righting reflex in our study (Fig. 2.2). MeHg alters motor coordination and hind limb strength (Dietrich et al. , 2005 Montgomery et al. , 2008). In our exposure paradigm, no alterations were found consistently. Hind limb cross was performed to measure motor impairment indirectly. Rats exposed to MeHg for 15 days displayed hind limb cross starting at day 9 and day 11 for 0.75 mg/kg/day MeHg exposure, and at day 15 for the 1.5 mg/kg/day MeHg exposure (Fig. 2.3A). In the group exposed to MeHg for 30 days several rats displayed partial or full hind limb cross at day 10, 12 or 16 for 0.75 mg/kg/day MeHg and day 18, 19 and 20 for the 1.5 mg/kg/day MeHg exposure (Fig. 2.3B). Taken together the data indicate that our low-dose exposure paradigm does not cause significant behavioral deficits in the animals in our study.

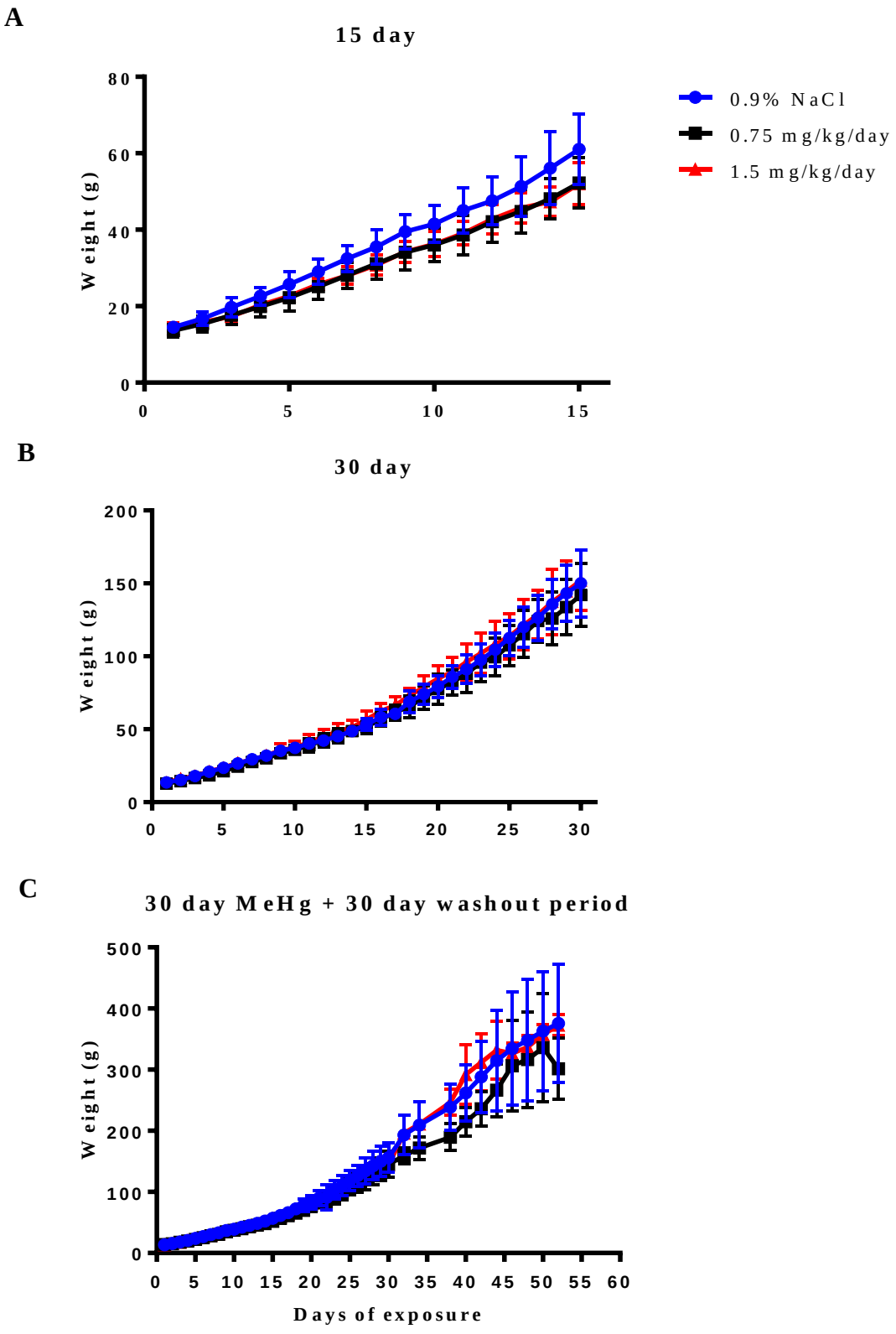

Figure 2.1. Low dose chronic MeHg exposure does not affect body weigh in Sprague Dawley rats. Sprague Dawley rats were exposed to 0, 0.75 or 1.5 mg/kg/day MeHg for 15, 30,

Figure 2.1 (cont'd) or 30 day + 30 day washout period. Rats were weighed throughout their exposure period, every day for the first 30 days and three times a week afterwards. The mean weight per day was determined. (A) Fifteen, (B) Thirty-day or (C) Thirty-day and thirty-day washout period exposure did not alter the rats body weight. Two-way ANOVA, Bonferroni post-test $p < 0.05$. ($n \geq 5$). Data are represented as mean ± SEM.

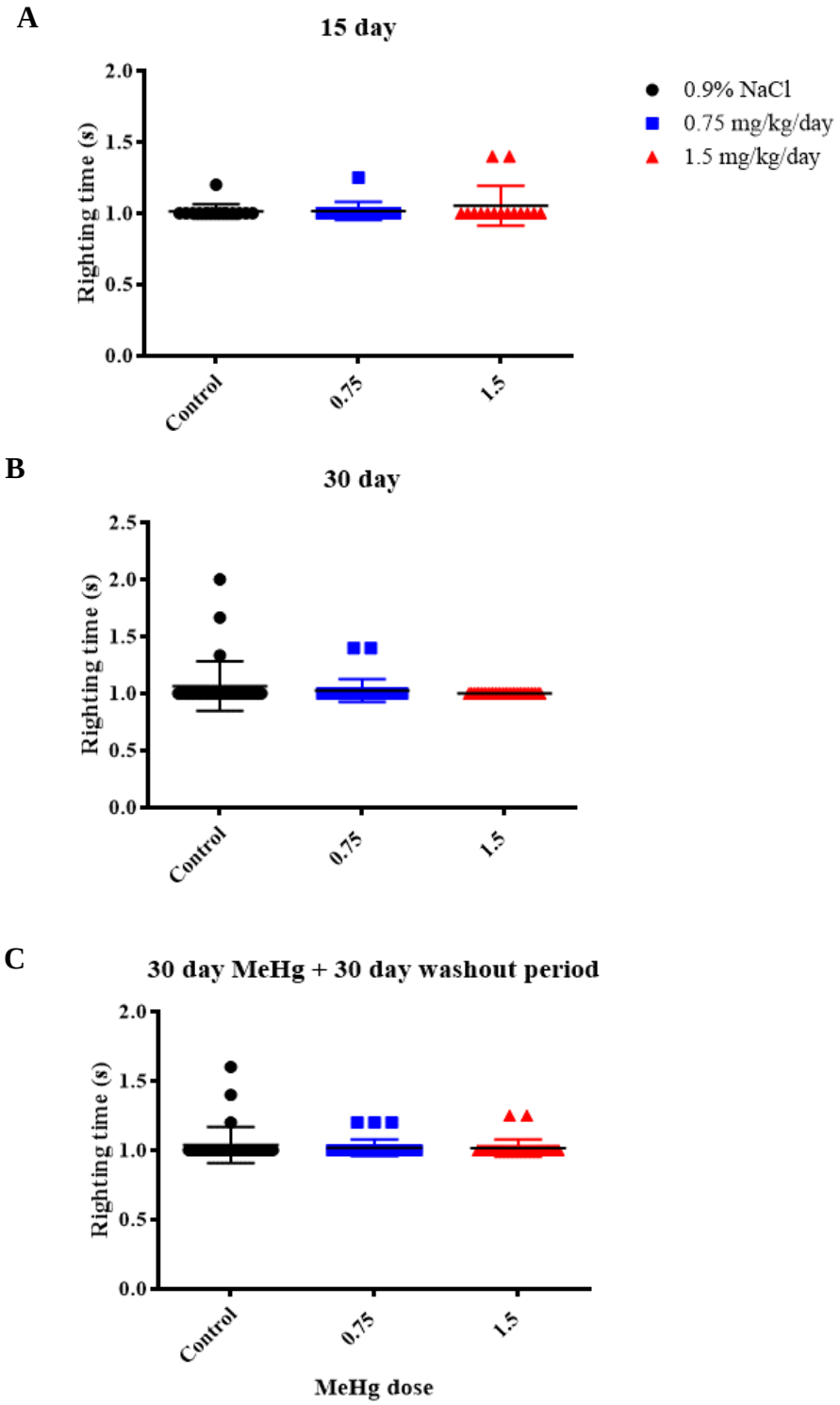

Figure 2.2. MeHg effects on righting reflex in the developing rat. Sprague Dawley rats were exposed to 0, 0.75 or 1.5 mg/kg/day MeHg for 15, 30, or 30 day + 30 day washout period. Righting reflex was measured for each group dosed for a period of 15 or 30 days.

Figure 2.2 (cont'd) Individual times are represented. (A) Fifteen, (B) Thirty-day or (C) Thirty-day and thirty-day washout period exposure did not alter the rats righting time. Data are represented as mean ± SEM, ($n \geq 5$).

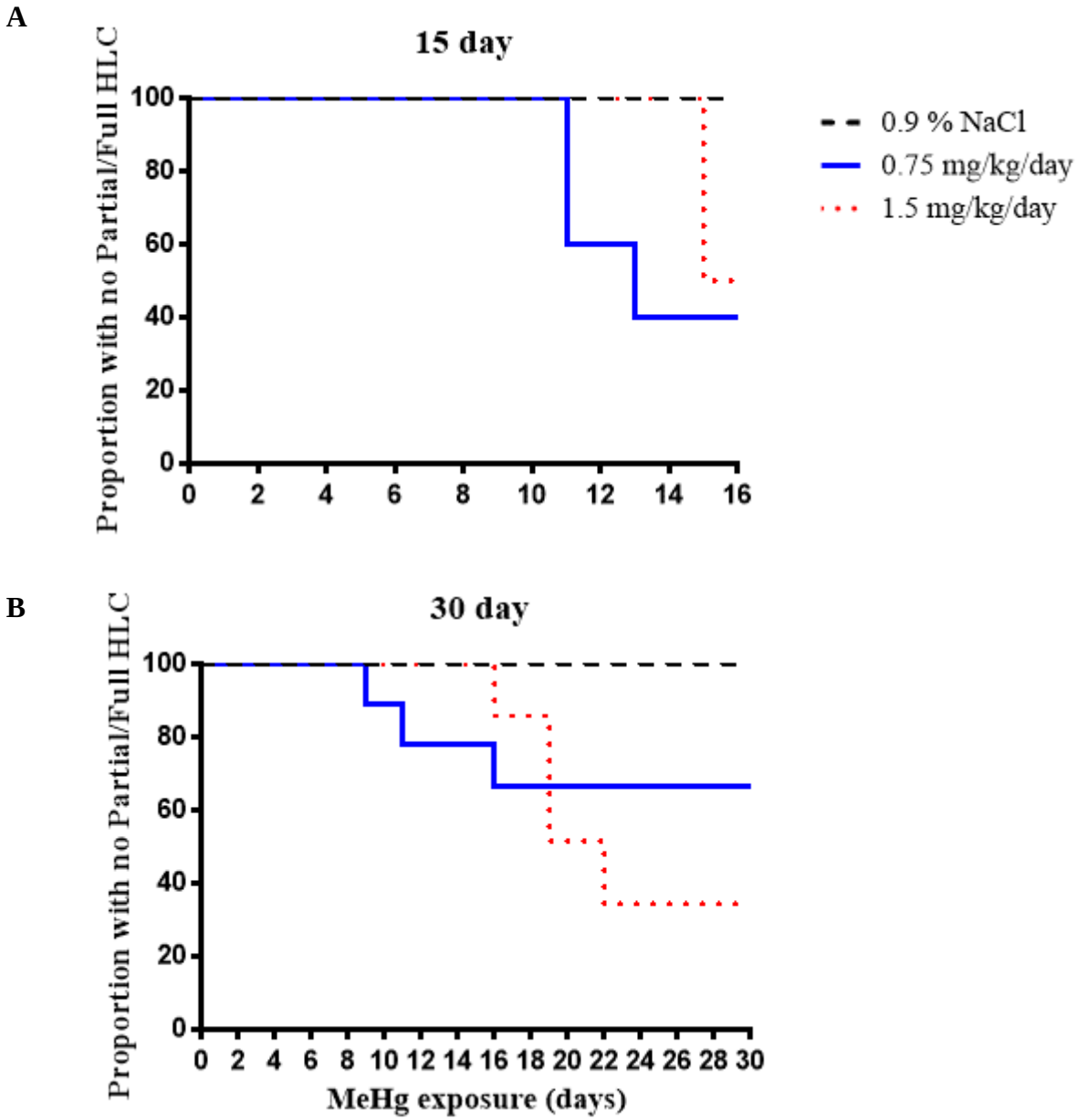

Figure 2.3. MeHg effects on hind limb cross in the developing rat. Sprague Dawley rats were exposed to 0, 0.75 or 1.5 mg/kg/day MeHg for 15, 30, or 30 day + 30 day washout period. Hind limb cross was throughout their exposure period, every day for the first 30 days. Values are represented as the proportion of no, partial, or full hind limb cross per group after (A) Fifteen, or (B) Thirty-day MeHg exposure, ($n \geq 5$).

b. MeHg has greater effects on AMPA receptor subunit expression in brainstem of rats than cerebellum

The role of the AMPA receptors in MeHg-induced cytotoxicity is not yet understood; however, these receptors have been associated with the increase in $[Ca^{2+}]_i$ in brainstem and spinal cord MNs after MeHg exposure (Johnson et al. , 2011, Ramanathan and Atchison, 2011). Thus, we sought to identify whether changes in gene expression levels of the four subunits that compose AMPA receptors occur after MeHg exposure. Identifying changes in message levels of the subunits that compose this receptor can help understand the physiological changes observed after MeHg exposure. Exposure to 0.75 mg/kg/day MeHg had a significant effect in all the GluA subunits studied compared to 15 after 30 day exposure in brainstem of rats (Fig. 2.4A). There was also a significant difference of all the subunits expression when comparing 30 with 30 day + 30 day wp (Fig. 2.4A). In the cerebellum 0.75 mg/kg/day MeHg exposure led to a significant difference when comparing 15 with 30 day exposure of the GluA2 and GluA3 subunits. Comparison between 30 and 30 day + 30 day wp exposure had a significant difference for the GluA2 subunit (Fig. 2.4B). In the brainstem higher MeHg concentration, 1.5 mg/kg/day caused a significant difference in the GluA1, GluA2 and GluA4 subunits when we compared the 15 with the 30 day exposure. Comparison between 30 and 30 day + 30 day wp exposure had a significant difference in the GluA2, GluA3 and GluA4 (Fig. 2.4C). However, in the cerebellum the expression changes were not as pronounced and there was only a significant difference in the GluA3 subunit when comparing 15 with 30 day exposure (Fig. 2.4D).

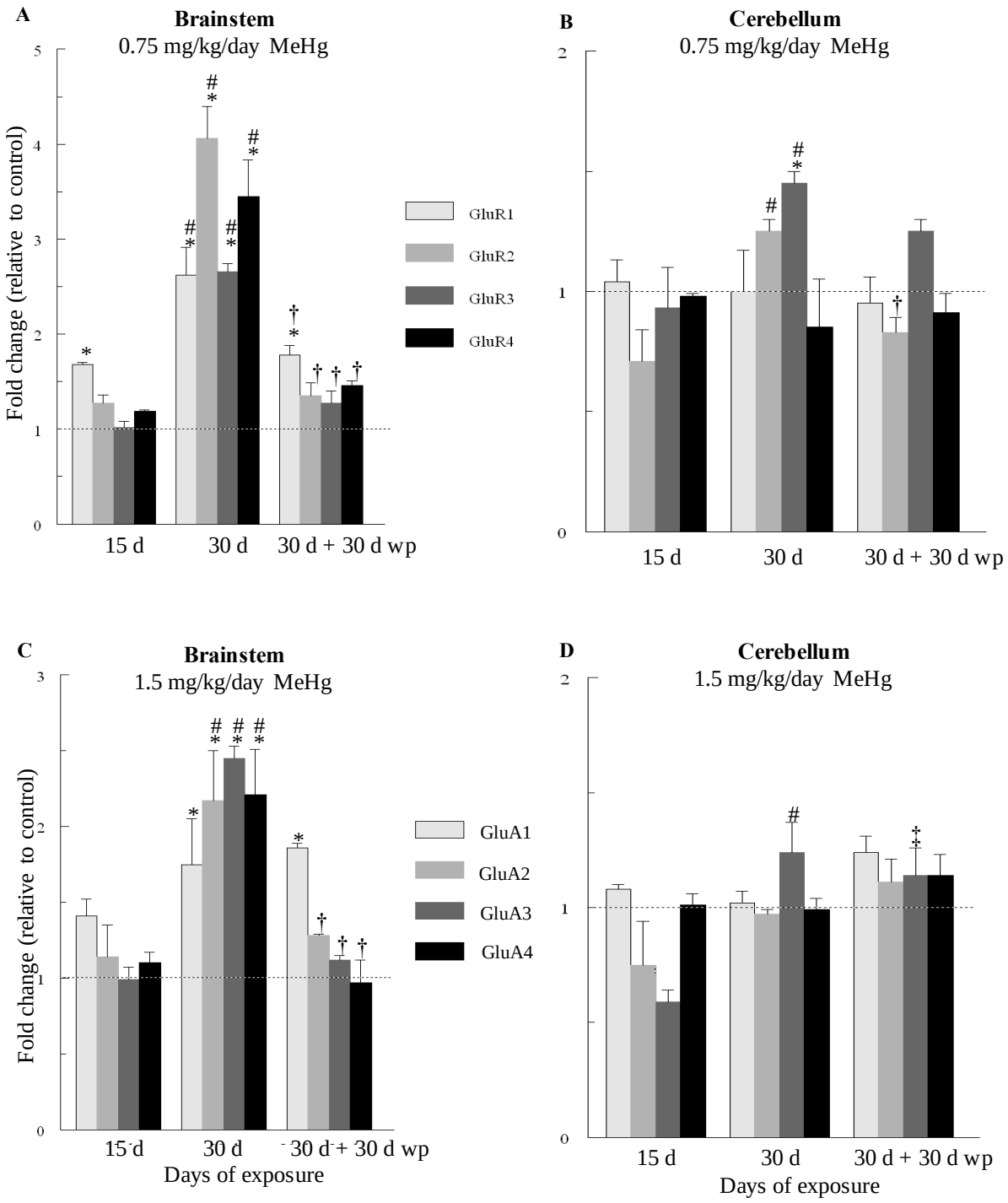

Figure 2.4. Relative expression of AMPA receptor subunits after MeHg exposure. AMPA receptor GluA 1- 4 subunit expression in brainstem after 0.75 (A) or 1.5 mg/kg/day MeHg exposure (C) for 15 day (15 d), 30 day (30 d) or 30 day + 30 day washout period (30 d + 30 d wp). Expression of GluA subunits in cerebellar tissue after 0.75 mg/kg/day MeHg (B) and 1.5 mg/kg/day MeHg (D). * indicates a significant difference from control (0.9 % NaCl) ($p \leq 0.05$).

Figure 2.4 (cont'd) Control value =1 after normalization with the endogenous control. # indicates a significant difference between 15 and 30 d exposure ($p \leq 0.05$), ‡ indicates a significant difference between 15 and 30 d + 30 d wp exposure ($p \leq 0.05$), and † indicates a significant difference between 30 and 30 d + 30 d wp exposure ($p \leq 0.05$). Values are represented as mean ± SEM (n = 4, four biological replicates per group).

c. MeHg alters NMDA receptor subunit expression in cerebellum and brainstem of rats

MeHg alters gene expression of NMDA receptor subunits in the hippocampus and cortex of rodents which has been associated with impaired cognitive behavior (Baraldi, Zanolo, 2002, Gao et al. , 2008, Liu, Wang, 2009). Alterations have also been observed in a dopaminergic human cell line of neuroblastoma origin, SHSY5Y (Ndountse and Chan, 2008). To identify if changes in gene expression after MeHg exposure occur in the brainstem and cerebellum we chose the NMDA receptor subunits NR1, which is the most abundant subunit and glycine binding subunit; and the NR2A subunit which is the glutamate binding subunit (Paoletti et al. , 2013). A functional channel requires NR1 and an NR2 subunit. In brainstem tissue of animals exposed to 0.75 mg/kg/day MeHg a significant difference in the NR1 and NR2A subunits was observed when comparing 15 with 30 day, and 30 day with 30 day + 30 day wp exposure (Fig. 2.5A). Similar exposure in the cerebellum did not have any significant changes in the NMDA receptor subunits studied (Fig. 2.5B). Exposure to 1.5 mg/kg/day MeHg in the brainstem caused a significant difference in the NR1 and NR2A subunit when comparing 15 with 30 day and the 30 with the 30 day + 30 day wp exposure (Fig. 2.5C). The cerebellum showed a significant difference for the NR1 subunit when comparing the 15 with the 30 day and the 30 with the 30 day + 30 day wp exposure (Fig. 2.5D).

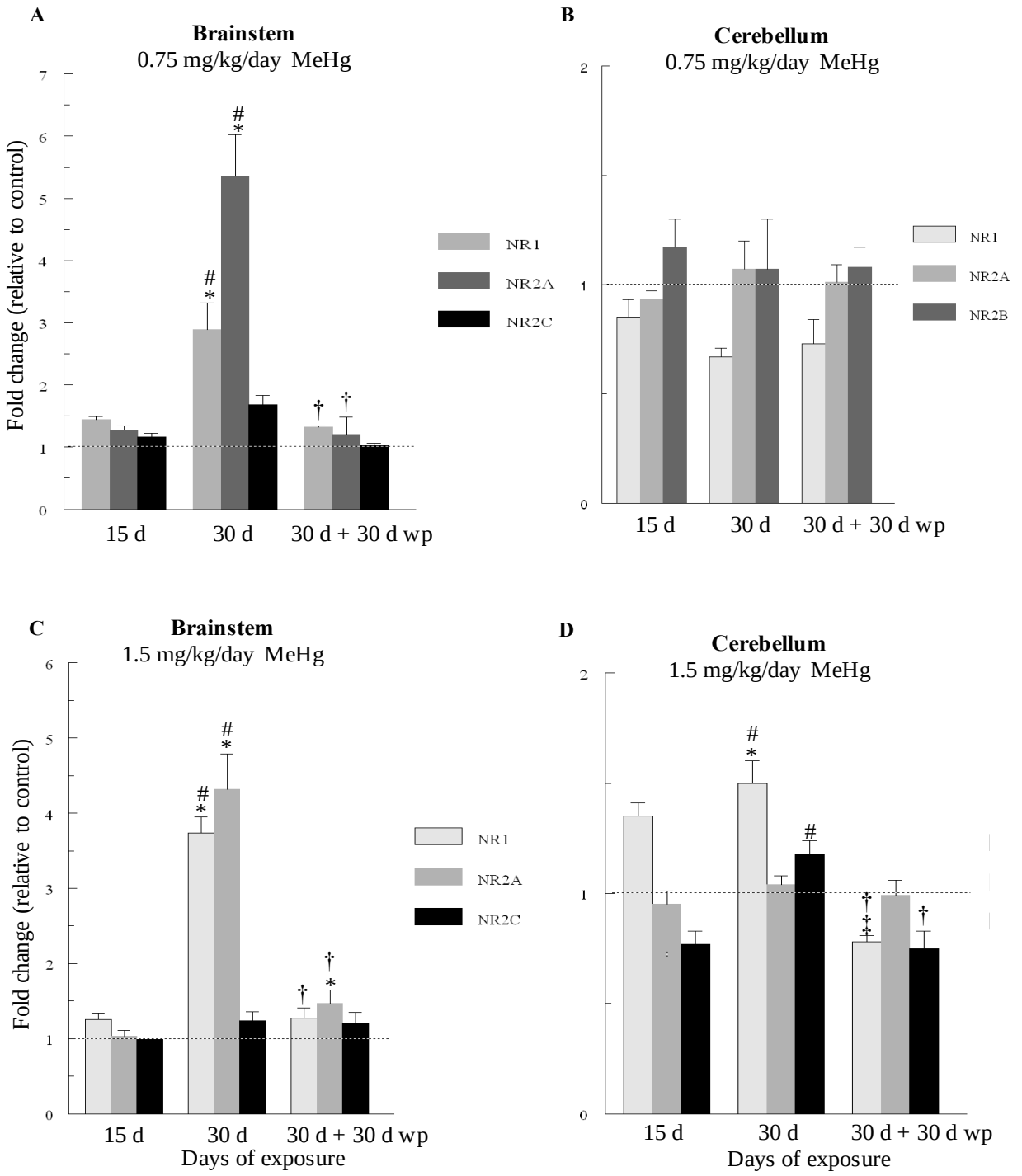

Figure 2.5. Relative expression of NMDA receptor subunits after MeHg exposure. NMDA receptor NR1, NR2A and NR2C subunit expression in brainstem after 0.75 (A) or 1.5 mg/kg/day MeHg exposure (C) for 15 day (15 d), 30 day (30 d) or 30 day + 30 day washout period (30 d + 30 d wp). Expression of NR1, NR2A and NR2B subunits in cerebellar tissue after

Figure 2.5 (cont'd) 0.75 mg/kg/day MeHg (B) and NR1, NR2A and NR2C after 1.5 mg/kg/day MeHg exposure (D). * indicates a significant difference from control (0.9 % NaCl) ($p \leq 0.05$). Control value =1 after normalization with the endogenous control. # indicates a significant difference between 15 and 30 d exposure ($p \leq 0.05$), ‡ indicates a significant difference between 15 and 30 d + 30 d wp exposure ($p \leq 0.05$) , and † indicates a significant difference between 30 and 30 d + 30 d wp exposure ($p \leq 0.05$). Values are represented as mean ± SEM (n = 4, four biological replicates per group).

d. MeHg exposure has greater effects on mRNA expression of VGCC a1 subunits in brainstem than in cerebellum of rats

VGCCs contribute to MeHg-induced increases in $[Ca^{2+}]_i$ in cerebellar cells and MNs (Marty and Atchison, 1997, Ramanathan and Atchison, 2011). However, functional studies have also demonstrated that MeHg alters their function (Hajela, Peng, 2003, Peng et al. , 2002, Shafer and Atchison, 1991, Shafer et al. , 1990, Sirois and Atchison, 2000, Yuan et al. , 2005) mainly by causing an irreversible blockage. Because effects of MeHg on gene or protein expression of these channels have not been performed we chose these for our study, mainly because of the important role they play in MeHg-induced toxicity in neuronal cells. Effects of MeHg exposure on gene expression of VGCCs was evaluated by quantifying gene expression of the α1 pore forming subunit of the P/Q type (α_{1A}), N type (α_{1B}), L type (α_{1C}) and R type (α_{1E}) VGCCs. A comparison study was performed on the subunits expression and the days of exposure. In the brainstem 0.75 mg/kg/day MeHg exposure comparison between 15 and 30 day showed a significant difference between the α1C and α1E subunits, however the comparison between the 30 vs 30 day + 30 day wp exposure showed a significant difference between the α1A, α1C, and α1E subunits (Fig. 2.6A). In the cerebellum, the same exposure showed a significant difference in the α1A and α1E when comparing 15 with 30 day + 30 day wp days, and 30 vs 30 day + 30 day wp (Fig. 2.6B). The higher MeHg exposure, 1.5 mg/kg/day in the brainstem showed a significant difference between α1B, α1C, and α1E when comparing 15 with 30 day exposure and 30 with 30 day + 30 day wp exposure. The α1A subunit was significantly different in the 30 vs 30 day + 30 day wp comparison (Fig. 2.6C). Cerebellar α1 subunit expression after 1.5 mg/kg/day did not show any statistically significant changes in gene expression when compared among groups (Fig. 2.6D).

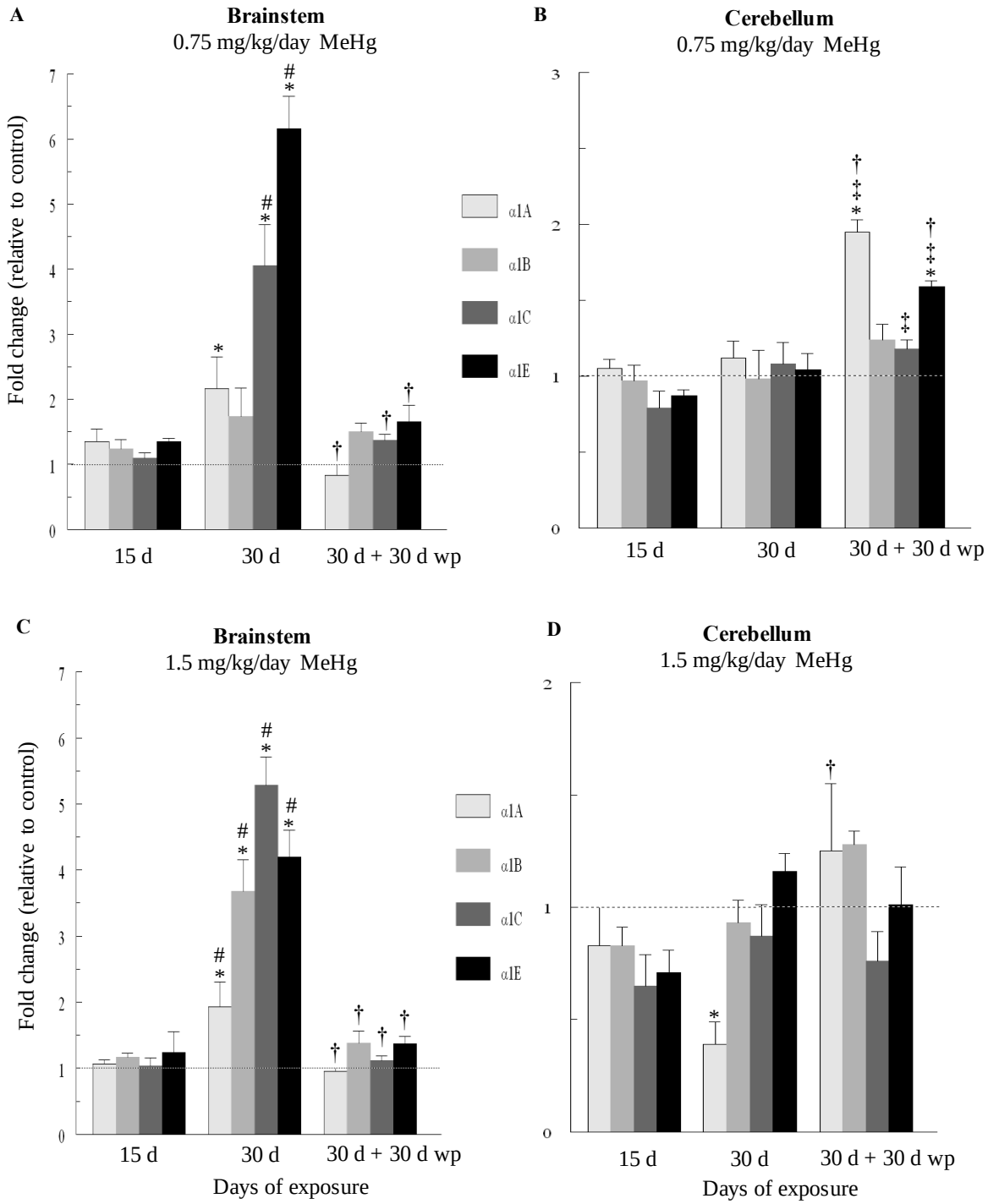

Figure 2.6. Relative expression of VGCC α1 subunit after MeHg exposure. VGCC α1 subunit expression in brainstem after 0.75 (A) or 1.5 mg/kg/day MeHg exposure (C) for 15 day (15 d), 30 day (30 d) or 30 day + 30 day washout period (30 d + 30 d wp). Expression of α1A (P/Q type), α1B (N-type), α1C (L-type), and α1E (R-type) VGCC subunits in cerebellar tissue

Figure 2.6 (cont'd) after 0.75 mg/kg/day MeHg (B) and 1.5 mg/kg/day MeHg exposure (D). * indicates a significant difference from control (0.9 % NaCl) ($p \leq 0.05$). Control value =1 after normalization with the endogenous control. # indicates a significant difference between 15 and 30 d exposure ($p \leq 0.05$), ‡ indicates a significant difference between 15 and 30 d + 30 d wp exposure ($p \leq 0.05$), and † indicates a significant difference between 30 and 30 d + 30 d wp exposure ($p \leq 0.05$). Values are represented as mean ± SEM (n = 4, four biological replicates per group).

E) Discussion

The purpose of this study was to determine whether chronic low dose MeHg exposure during development leads to changes in the mRNA levels of ion channels that contribute to $[Ca^{2+}]_i$ alterations in known susceptible brain regions. Our study focused on identifying the changes that occur at the mRNA level in the cerebellum and the hypoglossal nucleus region of the brainstem. Cerebellar granule cells are the most abundant cells in the cerebellum and are known to be the most susceptible cell type to MeHg toxicity (Hunter and Russell, 1954). The brainstem hypoglossal nucleus is a region rich in MNs, another cell type that is susceptible to MeHg toxicity (Moller-Madsen, 1990b, 1991). Although MNs are not one of MeHg primary targets, toxicity occurs after MeHg exposure and Ca^{2+} mediated pathways contribute to this toxicity (Ramanathan and Atchison, 2011). However, the mechanisms underlying these events have not been well characterized.

Based on previous findings we know that MeHg leads to degeneration of cerebellar granule cells at acute and chronic exposures and at very low concentrations. In our study we selected low doses which could be relevant to toxicological exposures that can occur throughout one's lifetime. We hypothesized that these low-dose exposures to MeHg were going to cause a pronounced alteration in gene expression in the cerebellum compared to the brainstem of developing rats. This, represented as an increase in the mRNA levels of the receptors studied as a mechanism of compensation for MeHg effects mostly on cerebellar granule cells. However, our findings demonstrated that MeHg effects were greater in the brainstem hypoglossal region by having a significant increase (2.5 - 5-fold) in the expression of all the receptors studied, mostly after 30 d MeHg exposure, this was not observed in the cerebellum.

In cerebellar granule cells AMPA receptors do not contribute to MeHg-induced $[Ca^{2+}]_i$ alterations, at least as demonstrated by an acute low dose *in vitro* exposure. VGCCs play a major role in these alterations (Marty and Atchison, 1997). This could be one of the reasons why in the cerebellum we did not have significant changes in the expression of AMPA receptor subunits at 15 d after both 0.75 or 1.5 mg/kg/day MeHg exposure. After the 30 d exposure increase in expression of the GluA2 at 0.75 mg/kg/day and increase in GluA3 at both concentrations occurred. This could be due to the increase in neurotransmitter release known to occur after MeHg exposure (Yuan and Atchison, 2007), as AMPA receptor subunit expression can be modulated and upregulated based on activation patterns (Henley and Wilkinson, 2016).

NMDA receptor gene expression is altered in the cortex (Baraldi, Zanoli, 2002, Liu, Wang, 2009) and SHSY5Y neuroblastoma cells (Ndountse and Chan, 2008) after MeHg exposure. They also contribute to MeHg-induced cell death observed in the brainstem and cerebellum of rats after 7 days, 10 mg/kg/day exposure. This is known because exposure to NMDA receptor antagonist, MK801, reduced cell death on these regions (Miyamoto et al. , 2001). NMDA receptors are essential for synaptic plasticity which underlies learning and memory. MeHg alters learning and memory as well as neurobehavioral development in rodents and humans, and that is the main reason they have been the targets of study. In our study we observed a significant increase of the NR1 and NR2A in the brainstem and these remained significantly increased after 30 day washout period. In the cerebellum, significant increase in the NR1 and NR2C was observed. Increase expression in the NR2B and NR2C have been observed in the hippocampus (Liu, Wang, 2009) after MeHg exposure. Thus, although in cerebellum alteration in expression of the NR2C was similar to that observed in cortex, our other results could indicate that effects of MeHg in NMDA receptor subunit expression are different

depending on the region of the nervous system where it is measured. Although the NR1, 2A and 2B are the most abundant NMDA subunits in the brain.

MeHg effects on VGCCs have been extensively studied. MeHg exposure leads to a complete block of the current in a concentration and time dependent manner (Hajela, Peng, 2003, Herden, Pardo, 2008, Peng, Hajela, 2002, Yuan and Atchison, 2005, Yuan and Atchison, 2003). Interestingly, *in vitro* studies show that blockage of VGCCs with specific antagonists delay MeHg-induced increase in $[Ca^{2+}]_i$ (Limke, Heidemann, 2004a, Marty and Atchison, 1997a), suggesting that VGCCs play a role in these alterations. This has also been observed in MNs (Ramanathan and Atchison, 2011). In our study we observed a significant upregulation of all the α1 subunits studied after 30 day exposure in the brainstem of rats. An increase in expression was also observed for all of the subunits in the cerebellum tissue only in the 0.75 mg/kg/day MeHg exposure and after the 30 d washout period. These results are consistent with our hypothesis that MeHg effects in the VGCCs in cerebellar granule cells can lead to an increase in expression of the VGCCs, in this case observed at the mRNA levels. Another important finding is that in the cerebellum the effects seen only after the 30 d washout period could indicate MeHg delayed effects in this region. In mice MN contribution of VGCC (L and N-type) to MeHg-induced increase in $Ca^{2+}{}_i$ occurs (Ramanathan and Atchison, 2011). Increase in expression of these VGCC type could be occurring and thus contribute to the observed alterations. Effects at the protein levels should be studied to identify if this is the case.

Ca^{2+} permeable ion channels play an important role in MeHg-induced Ca^{2+} dysregulation in neuronal cells. Our findings contribute to the understanding of how MeHg could be leading to alterations in Ca^{2+} homeostasis, which could be in part due to the alterations in gene expression of Ca^{2+} permeable ion channels. Functional electrophysiological studies and protein expression

studies would have to be made with these conditions to identify what the changes observed at the gene level could be indicating at the functional level mostly in the brainstem region.

CHAPTER THREE: CHARACTERIZING METHYLMERCURY EFFECTS ON SPINAL CORD MOTOR NEURONS USING HUMAN INDUCED PLURIPOTENT STEM CELL DERIVED MOTOR NEURONS

A) Abstract

Motor dysfunction is one of the primary signs of methylmercury (MeHg) poisoning. Many studies have implicated the motor dysfunction primarily to the degeneration of cerebellar granule cells. However, studies on rodents have demonstrated that motor neurons (MNs) accumulate MeHg and once the cells become saturated with MeHg degeneration and ataxia are observed. Also, that α MNs seem to be more susceptible to degenerate and accumulate MeHg than β MNs, however, the mechanism of toxicity of MeHg on MNs is unknown. *In vitro* studies using mouse spinal cord MNs showed that MeHg alters intracellular Ca^{2+} $[Ca^{2+}]_i$ in these cells. The use of an α-amino-3- hydroxy-5-methyl-4-isoxazolepropionic acid (AMPA) receptor antagonist CNQX delayed the observed increases in $[Ca^{2+}]_i$ suggesting AMPA receptors contribute to these alterations. AMPA receptors are not normally permeable to Ca^{2+}, but changes in the expression of the receptor GluA2 subunit or its RNA editing enzyme, adenosine deaminase acting on RNA2 (ADAR2), lead to their Ca^{2+} permeability. The goals of this study were two-fold: The first was to optimize MeHg concentrations and techniques used in spinal cord MNs experiments *in vitro* using the NSC34 cell line before moving to the human induced pluripotent stem cell MN (hiPSC-MN) model. The information gathered from the first goal was used to perform the second goal which was to characterize the effects of MeHg on cell viability, gene expression of the AMPAR and ADAR2, and $Ca^{2+}{}_i$ alterations in hiPSC-MNs. This allowed me to identify if changes like those observed in rodent MNs or in the NSC34 MN cell line occur in hiPSC-MNs. The primary goal of this study was to characterize the effects of MeHg on hiPSC-MNs, to identify what occurs in human MNs after low dose acute MeHg exposure. DIV 7 hiPSC-MNs were exposed to 0, 0.1, 0.2, 0.5, 1 and 1.5 µM MeHg. Cells were divided into two groups. One group was perfused with MeHg at the indicated concentrations for ratiometric Ca^{2+}

measurement experiments and another group was exposed to MeHg for 1 hr and delayed toxicity was assessed after 24 hr, this was used for cell viability and gene expression studies. Quantitative real-time PCR was performed on reverse transcript (cDNA) of RNA isolated from hiPSC-MNs to study glutamate receptor expression. AMPA receptor GluA1 - 4 subunits, and the ADAR2 enzyme genes were measured from treated and untreated cells. Intracellular Ca^{2+} ($[Ca^{2+}]_i$) alterations were measured with a ratiometric Ca^{2+} fluorophore, Fura 2-AM. Delayed MeHg effects in hiPSC-MNs include a concentration dependent cell death, and AMPA and ADAR2 gene expression alterations assessed 24 hr post MeHg exposure. The results from this study demonstrate for the first time that 1) MeHg alters $[Ca^{2+}]_i$ in human MNs 2) alteration in $[Ca^{2+}]_i$ are being mediated by ionotropic glutamate AMPA receptors 3) alterations in gene expression of AMPA receptors and ADAR can be contributing to these alterations. These results of this study contribute to the understanding of MeHg effects in human MNs.

B) Introduction

Motor dysfunction is a preeminent sign of methylmercury (MeHg) toxicity in humans (Bakir, Damluji, 1973, Ekino et al. , 2007). Developmental and adult MeHg exposure lead to ataxia and the mechanisms by which it occurs is not well understood. Degeneration of the cerebellar granule cells has been characterized as a key factor leading to the observed motor dysfunction in rodents and humans (Clarkson and Magos, 2006).

Effects of MeHg on motor neurons (MNs) have not been characterized and this cell type is not one of the main targets of its toxicity. However, in the early 1990s several studies focused on understanding MeHg effects in MNs because Hg and MeHg had been associated to the development of MN disease amyotrophic lateral sclerosis (ALS) (Johnson, Yuan, 2011, Praline et al. , 1990, Roos, Vesterberg, 2006, Sutedja, Veldink, 2009). Using rodent models it was shown that MeHg 1) accumulates and degenerates α MNs and not medium or small MNs in the spinal cord, 2) when MNs become saturated with MeHg ataxia is observed and 3) neurophagia, atrophy and degeneration is observed in the anterior horn in the lumbar region of the spinal cord (Moller-Madsen, 1990, 1991). These studies were pathological studies, where the identification of the molecular mechanisms by which MeHg was damaging the cells was not of importance.

Only two studies have focused on identifying the effects of methylmercury (MeHg) in MNs *in vitro*. The first study used NSC34 cells which are a hybrid between mouse embryonic spinal cord MNs and neuroblastoma cells and are considered a surrogate model for spinal cord MNs (Cashman, Durham, 1992, Eggett, Crosier, 2000, Maier, Böhm, 2013). In this study exposures to mercuric chloride ($HgCl_2$) and MeHg were made to identify their toxicity and they concluded that 1) MeHg was more toxic than Hg (LD_{50} of 1.74 µM compared to Hg 7.95 µM), and 2) concentration-dependent cell death occurred after 48 hr of exposure to both mercurials

(Chapman and Chan, 1999). The second and more recent study used primary MNs isolated from spinal cord of mice PND 4 - 7. The focus of this study was to identify if acute MeHg exposure led to alterations in intracellular Ca^{2+} (Ca^{2+}_i) and identify ion channels that could contribute to the observed alterations. When exposed to low concentrations (0.1 - 1.5 μM) of MeHg acutely (~1 hr), spinal cord MNs of mice showed alterations in $[Ca^{2+}]_i$. Disruption in $[Ca^{2+}]_i$ was mediated in part by ionotropic glutamate receptors NMDA and AMPA (Ramanathan and Atchison, 2011). Taken together these studies demonstrated that MNs degenerate after exposure to MeHg and this can be as a result of the observed alterations in $[Ca^{2+}]_i$ that are mediated by ionotropic glutamate receptors. However, no further studies have been performed to characterize the role of the ionotropic glutamate receptors in MeHg-induced toxicity in MNs. Also, no other studies have used either NSC34 cells or human induced pluripotent stem cell MNs (hiPSC-MNs) to study MeHg-induced Ca^{2+} toxicity in this cell type.

This presented a new and unexplored area to conduct research focused on the effects MeHg could have in MNs of human origin and identify the role ionotropic glutamate receptor AMPA could have in MeHg-induced toxicity in this cell population. The goals of this study were two-fold. The first was to optimize MeHg concentrations and techniques used in our spinal cord MNs experiments *in vitro* using the NSC34 cell line before moving to the human induced pluripotent stem cell MN (hiPSC-MN) model. In this first part, I also wanted to identify if cell viability and gene expression alterations in AMPA receptors occurred after low dose MeHg exposure. Using the information gathered from the first goal I moved onto my second goal which was to characterize the effects of MeHg on cell viability, gene expression of AMPA receptors, ADAR and Ca^{2+}_i alterations in the hiPSC-MNs. This allowed me to identify if changes like those observed in rodent MNs or in the NSC34 MN cell line occur in hiPSC-MNs.

Thus, I hypothesized that MeHg was going to cause a concentration dependent cell death of MNs, and alteration in Ca^{2+} homeostasis was going to occur in a biphasic manner as it has been observed in several other cell types including cerebellar granule cells and primary spinal cord MNs from mice (Edwards, Marty, 2005, Marty and Atchison, 1997, Ramanathan and Atchison, 2011). Because our lab has identified in multiple models, including mouse spinal cord MNs, MeHg-induced alterations in $[Ca^{2+}]_i$, I hypothesized that this was going to occur in hiPSC-MNs and it was going to be mediated in part by AMPA receptors. Thus, I focused on identifying these changes and the role AMPA receptors could have on these alterations.

AMPA receptors are not Ca^{2+} permeable, this property is observed in the absence of the GluA2 subunit or an alteration in a post transcriptional process called RNA editing of this subunit (Bettler and Mulle, 1995). RNA editing alterations can occur by multiple mechanisms. One of the mechanisms is by the cleavage of its C terminal by glutamate excitotoxicity (Mahajan, Thai, 2011). This is the over activation of AMPA receptors due to the increase of glutamate being released by neighboring cells. Another mechanism is by the decrease in expression of the RNA editing enzyme ADAR2 (Kawahara, Ito, 2003).

Spinal cord MNs normally express Ca^{2+} permeable AMPA receptors (Kawahara et al. , 2003). This can heighten their susceptibility to degeneration when exposed to toxicants which mechanisms of action are through Ca^{2+} mediated pathways. MNs also have low abundance of Ca^{2+} binding proteins such as Calbindin D28K. This can also contribute to a higher susceptibility to MeHg toxicity. These characteristics strengthen my hypothesis of what could occur in hiPSC-MNs after MeHg exposure.

The results of this study demonstrate that exposure to low concentrations of MeHg (0.5 - 1.5 µM) lead to a concentration dependent cell death of NSC34 cells and hiPSC-MNs. Also,

alterations in mRNA expression of AMPA receptors after MeHg exposure is observed. Most importantly MeHg-induced increase in $[Ca^{2+}]_i$ was observed in hiPSC-MNs and these alterations were mediated in part by Ca^{2+} permeable AMPA receptors.

C) Materials and methods

a. Materials

Methylmercury chloride (MeHg) was purchased from ICN Biomedical Inc. (Costa Mesa, CA). Dubelco's modified eagle's medium (DMEM), Ham's F12, fetal bovine serum (FBS), penicillin/streptomycin, trypsin-EDTA (0.25%), and 0.4% trypan blue were purchased from Thermo Scientific (Invitrogen, Grand Island, NY). Calcein acetoxymethylester (calcein AM) and ethidium homodimer-1 (EthD-1) were purchased as a cell viability kit from Molecular Probes (Invitrogen, Eugene, OR). Poly-D-lysine, Poly-L-ornithine, laminin, CNQX, NAS, AMPA, paraformaldehyde, triton X-100, Fura-2AM and Ethylene glycol-bis (β-aminoethylether) N,N,N',N'-tetra acetic acid (EGTA) were purchased from Sigma-Aldrich (St. Louis, MO). Normal goat serum and mounting medium Vecta shield with nuclear DNA stain 4, 6-diamino-2-phenylinndole (DAPI) were purchased from Vector Labs (Burlingame, CA). TRI reagent was purchased from Molecular Research Center (Cincinnati, OH). Cell counting slides for Bio-Rad TC20 were purchased from Bio-Rad (Hercules, CA). TPEN was purchased from Millipore (Billerica, MA).

Antibodies used in the immunocytochemistry performed in NSC34 cells were: mouse anti-non-phosphorylated neurofilament heavy 200 (SMI32) (Abcam; Cambridge, MA), rabbit anti-choline acetyltransferase (ChAT) and rabbit anti-ionotropic glutamate receptor 2 subunit (GluA2) purchased from Millipore (Temecula, CA). Secondary antibodies goat anti-mouse

Alexa Fluor 488, goat anti-rabbit Fitc-31583 or goat anti-rabbit Alexa Fluor 594 obtained from Fisher (Rockford, IL) were used.

Antibodies used in hiPSC-MNs were: rabbit anti-glutamate receptor subunit 1 (GluA1), rabbit anti-GluA2, rabbit anti-adenosine deaminase acting on RNA2 (ADAR2) conjugated with Alexa Fluor 488, and chicken anti-neurofilament heavy-200 (NFH) obtained from Abcam; Mouse anti-neuronal specific nuclear protein NeuN (NeuN) purchased from Millipore; Secondary antibodies used were donkey anti-mouse Alexa Fluor 405, goat anti-rabbit Alexa Fluor 488 and goat anti-chicken Alexa Fluor 594 obtained from Abcam.

b. Chemicals and solutions

MeHg stock solution used for experiments was prepared with double-distilled water to a concentration of 10 mM. MeHg exposure solutions for NSC34 cells were prepared in NSC34 cell culture media without antibiotics (penicillin and streptomycin) to a final concentration of 0.5, 1 or 1.5 μM MeHg. Solutions used for hiPSC-MN exposures were prepared in HEPES Buffer Saline (HBS). All exposure solutions were prepared the day of the experiment using MeHg stock solution that was never older than 30 days. TPEN, CNQX, NAS and AMPA were prepared as 10 mM stock solutions in double distilled water. Dilutions were made from these stocks on HBS for the performed experiments.

Experimental solutions for immunocytochemistry, including 4% (w/v) paraformaldehyde and the 10% (v/v) normal goat serum, were prepared in Phosphate Buffer Saline (PBS). PBS contained (in mM) 137 NaCl, 2.7 KCl, 1.4 NaH_2PO_4, and 4.3 Na_2HPO_4, pH 7.4 (Pardo et al. , 2006). Solutions used in all other experiments were made in HBS. HBS contained (in mM) 150 NaCl, 5.4 KCl, 1.8 $CaCl_2$, 0.8 MgSO4 , 20 d-glucose, and 20 Hepes (free acid), pH 7.3 (Marty

and Atchison, 1997). HBS pH was 7.3 with TRIS. Ca^{2+} free HBS was prepared similarly to HBS without $CaCl_2$ and addition of 20 μM EGTA was performed.

c. NSC34 cell culture

Undifferentiated NSC34 cells were purchased from Cedarlane Laboratories LLC (Burlington, NC). Undifferentiated NSC34 cells were cultured in DMEM, 10% (v/v) FBS and 1% (v/v) penicillin/streptomycin. Differentiated NSC34 cells were cultured in DMEM/Ham's F12 (1:1), 1% (v/v) FBS and 1% (v/v) penicillin/streptomycin (Eggett, Crosier, 2000) at a concentration of 1.2 x 10^5 cells/ml. Differentiated cells were passaged every 72 hr and were trypsinized for dislodging them from the culture flasks. Cells were plated in poly-d-lysine (40 μg/ml) coated 35 mm polystyrene culture dishes or flasks and incubated at 37 °C and 5% CO_2. On DIV 3 MeHg exposure occurred and after 24 or 48 hr post exposure all experiments were performed. Cells used for our experiments were from passage 5 - 15 at which time point expression of AMPA receptor subunit GluA2 was observed. Cells from the same passage were used for control and MeHg exposure in each experiment. Each experiment was conducted in triplicate.

d. Human induced pluripotent stem cell derived motor neuron cell culture (hiPSC-MNs)

HiPSC-MNs and their culture media (motor neuron maintenance medium®) were purchased from iX Cells Biotechnologies (San Diego, CA). These cells are derived from peripheral blood of an adult male and have been differentiated into MNs by episomal reprograming. They have been cryopreserved after being terminally differentiated into MNs. Because they are from human origin they were screened by the provider (iX Cells Biotechnologies) and were negative for HIV-1, hepatitis B and hepatitis C virus.

For plating, hiPSC-MNs were thawed for 1 min in a 37 ^{o}C water bath, then immediately 1 ml of human MN maintenance medium was added to the tube. The cell suspension was added into a 15 ml conical tube containing 4 ml of MN maintenance medium®. Cells were centrifuged for 3 min at 3,000 rpm to remove any trace of dimethyl sulfoxide (DMSO). Supernatant was removed and cells were resuspended in 2 ml of MN maintenance medium®. Approximately 1.2 x 10^5 cells/ml were cultured in MN maintenance medium® on pre-coated Poly-L-Ornitine (20 µg/ml) and laminin (5 µg/ml) 25 mm glass coverslips in 35 mm dishes. Cell quantification was performed with trypan blue in the Bio-Rad TC20 automated cell counter. Cells were incubated at 37 ^{o}C in an environment containing 5% CO_2. After 48 hr of incubation (DIV 2) 50% of the medium was changed for fresh MN maintenance medium®. Fifty percent of the medium was changed every 72 hr. Cells developed MN phenotype after the first 24 hr (DIV 1) *in vitro*. After 6 DIV they express all MN markers including ChAT, NFH and NeuN.

MeHg exposure for hiPSC-MNs occurred at DIV 7. Cells were exposed to MeHg in HBS for 1 hr to five different concentrations (0.1, 0.2, 0.5, 1 and 1.5 µM). These concentrations are toxicologically relevant and *in vitro* they present Ca^{2+} alterations in MNs (Ramanathan and Atchison, 2011). Using these concentrations allows for a comparison with what has been previously observed on mouse MNs.

e. NSC34 cell viability assessment via Trypan Blue cell exclusion assay

Cell viability experiments in NSC34 cells were performed using 0.4% trypan blue. After exposure to MeHg cells were removed from the culture dishes by washing them out with their own media. Cells were then centrifuged for 3 min at 12,000 rpm. The pellet was re-suspended with 150 µl of new media. Then 20 µl of the cell suspension was mixed with 20 µl of trypan blue

dye and placed in a cell counting slide for Bio-Rad TC20. Cells were then counted in a Bio-Rad TC20 automatic cell counter and dead, live and percentage of viable cells was recorded.

f. HiPSC-MNs cell viability assessment via calcein-AM/ethidium homodimer-1 cytotoxicity assay

Calcein-AM/ EthD-1 assay was used to assess cell viability in hiPSC-MNs following the established protocol by Marty and Atchison, 1998. Briefly, hiPSC-MNs were rinsed three times with HBS. Cells were then exposed to MeHg in HBS at a concentration of 0, 0.1, 0.2, 0.5, 1.0 or 1.5 µM for 1 hr, after which MeHg was removed and replaced with MN maintenance medium. The duration of MeHg exposure (1 hr) was selected after an increase in $[Ca^{2+}]_i$ was observed in hiPSC-MNs after exposure to the previously mentioned concentrations and no significant cell viability or cellular damage at the structural level was observed. Cell viability was assessed 24 hr post exposure, this mainly due to the turnover rate of the AMPA receptors (18-23 hr) (Huh, Wenthold, 1999) and the known delayed effects of MeHg on neuronal cells including MNs (Moller-Madsen, 1990, 1991, Rice, 1996). After 24 hr cells were incubated with 0.1 µM calcein AM and 0.5 µM ethidium homodimer-1 for 30 min at 37^{o}C. After incubation cells were rinsed with 1X HBS and then imaged in a Nikon Eclipse fluorescent microscope. Cell viability was calculated by counting the amount of live and dead cells from three different regions in each dish and averaging it. Then the following formula was used to calculate the percent viability.

$$\text{Percent viability} = \frac{\text{Total cells} - \text{Dead cells}}{\text{Total cells}} \times 100$$

g. Immunocytochemistry for SMI32, ChAT and GluA2 in NSC34 cells

Differentiated DIV 3 NSC34 cells were rinsed with PBS three times and fixed in 4% (w/v) paraformaldehyde in PBS for 30 min at room temperature. After washing, the cells were incubated in 0.1% (v/v) Triton-X for 30 min at room temperature. Afterwards, to prevent

nonspecific binding, cells were blocked with 10% (v/v) normal goat serum in PBS for 30 min. Cells were then rinsed with PBS three times and rabbit anti-SMI32 (1:1000), rabbit anti-ChAT (1:500) or rabbit anti-GluA2 (1:100) primary antibody was added. After an overnight (24 hr) incubation at 4 °C cells were washed in PBS three times and anti-rabbit Alexa Fluor 488 (1:200), anti-rabbit Fitc-31583 (1:200) or anti-rabbit Alexa Fluor 594 (1:200) secondary antibody was applied and incubated for 2 hr in the dark at room temperature. Cells were rinsed in PBS three times and mounted to glass slides with hard mount medium Vecta Shield containing the nuclear DNA stain 4, 6-diamino-2-phenylindole (DAPI) and were set to dry for 15 min at room temperature before examining. Images were collected using a Nikon Eclipse Ti fluorescence microscope and analyzed using a NIS Elements BR Software.

h. Immunocytochemistry for MN markers in hiPSC-MNs

The same protocol used for NSC34 cells was performed except the mounting medium reagents used. Cells labeled with one or two antibodies were mounted with Vecta Shield that contained DAPI (Vector labs). Cells labeled with three antibodies were mounted with prolong anti fade mounting medium (Life Technologies). Images were collected using an Olympus FV1000 confocal microscope equipped with Fluoview viewer FV10 3.1 software. The antibodies used for this study are: rabbit anti- GluA1 (1:100) and rabbit anti-GluA2 (1:50), the most common AMPA receptor subunits in MNs, rabbit anti-ADAR2 (1:200), mouse anti-NeuN (1:100), chicken anti-NFH (1:2500), and rabbit anti- ChAT (1:200). Secondary antibodies used were donkey anti-mouse Alexa Fluor 405, goat anti-rabbit Alexa Fluor 405, goat anti-rabbit Alexa Fluor 488, goat anti-chicken Alexa Fluor 594 at a dilution of 1:200.

i. Single-cell Ca^{2+} microfluorimetry

Ratiometric Ca^{2+} imaging was performed using Fura-2 acetoxy methyl ester (Fura-2AM), an intracellular Ca^{2+} fluorophore (Grynkiewicz et al. , 1985). Increases in $[Ca^{2+}]_i$ were monitored from the cell soma of 6 - 10 hiPSC-MNs per dish. Using a Nikon Diaphot microscope coupled to an Ionoptix system (Ionoptics; Milton, MA) and temperature regulated (37^oC) perfusion system (2 ml/min). HiPSC-MN were rinsed three times with HBS and incubated with 3 µM Fura-2AM in HBS for 40 min at 37^oC (Ramanathan and Atchison, 2011). After incubation, the cells were rinsed by perfusion for 15 min with HBS and the recordings started, this step is to allow the de-esterification of the fluorophore and the removal of unattached cells. The first five minutes were recorded with HBS, then the cells ability to buffer Ca^{2+} was determined by doing a 1 – 1.5 min exposure to 40 mM KCl. Healthy cells had a rapid depolarization that was reversed after KCl removal. There was a 5 min wash with HBS after KCl exposure to allow the cells to reach baseline. For experiments performed with antagonists the cells where exposed to 20 µM CNQX (Ramanathan and Atchison, 2011) or 50 µM NAS (Johnson et al. , 2011) for 10 min then perfused with CNQX or NAS with MeHg simultaneously, and fluorescence at 340/380 measured continually for at least 60 min. Increase in the 340/380 ratio indicates increase in $[Ca^{2+}]_i$.

j. RNA isolation from cells

Total RNA and protein was isolated from cells using phase separation following the TRI reagent (Molecular Research Center; Cincinnati, OH) manufacturer's protocol. After isolation, total RNA was diluted in ultrapure distilled water (Sigma-Aldrich) and was incubated for 1 hr in 30 µl/v of DNaseI. The concentration and integrity of the RNA was assessed spectrophotometrically in the Nanodrop-2000 (Thermo-Scientific; Pittsburg, PA) and by

denaturing gel (Aranda et al. , 2012). A ratio of 1.9-2.0 at 260/280 nm absorbance was considered acceptable.

k. Reverse transcription PCR (RT-PCR)

Isolated total RNA was adjusted to a final concentration of 1 µg/µl. Two step reverse transcript PCR was performed by cDNA synthesis using the High Capacity cDNA Reverse Transcription Kit (Applied Biosystems; Grand Island, NY), with thermal conditions of: 85 ^{o}C for 15 min, 37 ^{o}C for 120 min and 80 ^{o}C for 5 min. The purity and concentration of the cDNA was assessed using the ND-2000. A ratio of 1.8 at 260/280 nm absorbance was considered acceptable.

l. Quantitative real-time PCR (qPCR)

Quantitaitve real time PCR was performed with the reserve transcript (cDNA) using a Step One Plus thermal cycler following the TaqMan gene expression assay protocol (Applied Biosystems, Grand Island, NY), with thermal conditions of: 50 ^{o}C for 2 min, 95 ^{o}C for 10 min, followed by 40 cycles (95 ^{o}C for 15 s and 60 ^{o}C for 1 min). The primers used are shown on table 3.1 for NSC34 cells table 3.2 for hiPSC-MNs and were purchased from (Life Technologies). Gene expression was performed in triplicate for each sample and the threshold cycle values were averaged. A concentration of 1 µg/µl was used as the input for each sample, to control for variability. The total volume of the reaction was 25 µl. Gene expression levels were normalized to GAPDH and βactin (housekeeping genes), and the untreated control. The results are presented as relative mRNA levels compared to controls, calculated for each gene following the $2^{\Delta\Delta Ct}$ Livak method (Livak and Schmittgen, 2001).

Table 3.1. Genes and accession number of the primers used in real-time PCR for the mouse hybrid cell line NSC34.

Gene	Gene name	GeneBank ID	Accession number
Endogenous controls (housekeeping genes)			
Actb	Actin, beta	NM_007393.3	Mm00607939_s1
Gapdh	Glyceraldehyde-3-phosphate dehydrogenase	NM_008084.2	Mm99999915_g1
Glutamate AMPA receptor subunits			
Gria 1	GluA1 subunit	NM_001113325.2	Mm00433753_m1
Gria2	GluA2 subunit	NM_001039195.1	Mm00442822_m1
Gria3	GluA3 subunit	NM_016886.3	Mm00497506_m1
Gria4	GluA4 subunit	NM_001113180.1	Mm00444754_m1
RNA editing enzyme			
ADARB1	Adenosine deaminase acting on RNA 2	NM_001024837.2	Mm00504621_m1

Table 3.2. Genes and accession number of the primers used in real-time PCR for the hiPSC-MNs.

Gene	Gene name	GeneBank ID	Accession number
Endogenous controls (housekeeping genes)			
Actb	Actin, beta	NM_001101.3	Hs01060665_g1
Gapdh	Glyceraldehyde-3-phosphate dehydrogenase	NM_001256799.2	Hs02758991_g1
Glutamate AMPA receptor subunits			
Gria 1	GluA1 subunit	NM_000827.3	Hs00181348_m1
Gria2	GluA2 subunit	NM_000826.3	Hs00181331_m1
Gria3	GluA3 subunit	NM_000828.4	Hs01557466_m1
Gria4	GluA4 subunit	NM_000829.3	Hs00898778_m1
RNA editing enzyme			
ADARB1	Adenosine deaminase acting on RNA 2	NM_001112.3	Hs00953724_m1

m. Data analysis and statistics

Each experiment was performed in triplicates and the $n \geq 3$ unless indicated otherwise. Statistical analysis was performed using GraphPad Prism software version 6 (GraphPad Software, Inc., La Jolla, CA). For cell viability comparison among groups were performed using One-Way ANOVA and Tukey's post hoc test. For Fura-2AM comparisons among groups were performed using Two-Way ANOVA and Bonferroni's post hoc test. Statistical significance is considered for values $p \leq 0.05$.

D) Results

a. Differentiated DIV 3 NSC34 cells express MN markers SMI32, ChAT and glutamate receptor subunit GluA2

Differentiated NSC34 cells have been extensively used for studying amyotrophic lateral sclerosis (ALS) mechanism of pathogenesis (Babetto, Mangolini, 2005, Fukada, Zhang, 2004, Raimondi, Mangolini, 2006, Sathasivam, AJ, 2005). They have been characterized for the presence of MN markers and function (Cashman, 1990). Expression and function of the ionotropic glutamate receptors AMPA and NMDA has also been identified in these cells (Cashman, Durham, 1992, Eggett, Crosier, 2000). However, these studies have used differentiated NSC34 cells that have been in culture for more than 7 days (Eggett, Crosier, 2000). Hybrid cell lines can differ in the presence of neuronal markers or ion channels based on their cell culture components, differentiation states, and passage number. Although NSC34 cells have been extensively used, most of the studies have obtained these cells from Dr. Neil Cashman, the scientist that developed them (Cashman, Durham, 1992). In most studies, they have been differentiated once and cultured for at least 7 days before use.

NSC34 cells used in this study were purchased undifferentiated from Cedarlane laboratories. To identify if these cells expressed the cellular markers of MNs described in the literature, immunocytochemistry was performed. First NSC34 cells were differentiated using the serum deprivation protocol, by reducing the amount of the FBS from 10% (v/v) to 1% (v/v) (Eggett, Crosier, 2000) and passaged 5 to 15 times differentiated. Identification of differentiated cells was performed by characterizing them by morphology identifying the presence of multipolar cells that presented extended neurites. The presence of neurites

occurred after 3 DIV (Fig. 3.1) and that was the time point selected to start the immunocytochemistry characterization experiments.

Expression of MN markers SM132 (Fig. 3.2) and ChAT (Fig. 3.3) were identified after 3 DIV in differentiated NSC34 cells after their first passage. However, expression of GluA2 subunit of the AMPA receptor was observed after the fifth passage (Fig. 3.4). Based on these results passage 5 was selected as the starting point to conduct the MeHg exposure studies because one of the main objectives of this study was to identify the effects of MeHg on AMPA receptor expression.

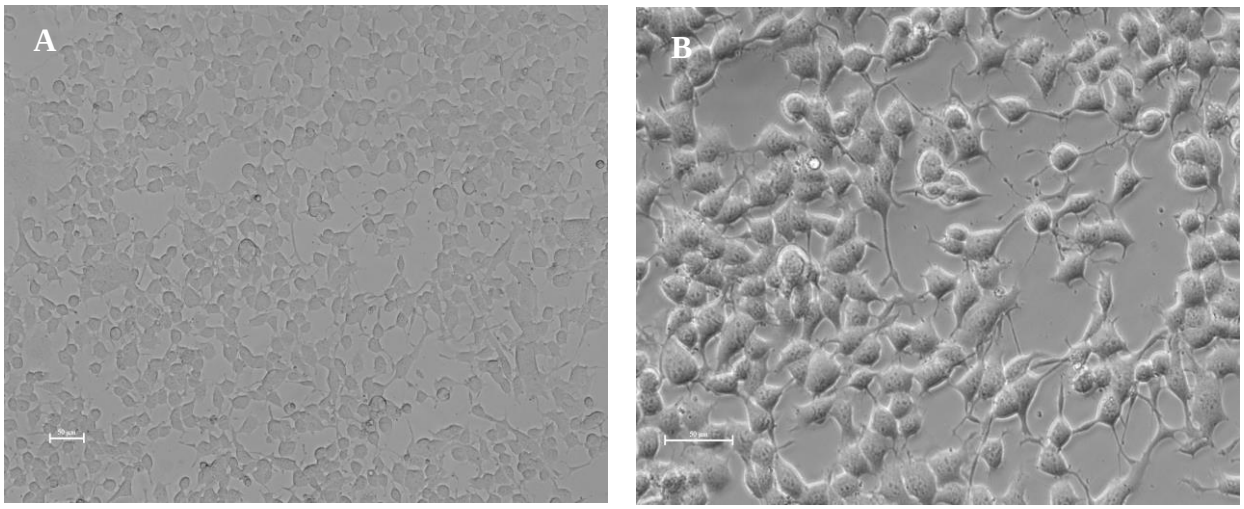

Figure 3.1. Brightfield image of differentiated NSC34 cells on DIV 3. After 3 DIV differentiated NSC34 cells had multipolar shape and neurites. This is not present in undifferentiated NSC34 cells (not shown). Brightfield image of DIV 3 NSC34 cells taken at 10x (A) and 20x magnification (B). Scale bar = 50 µm.

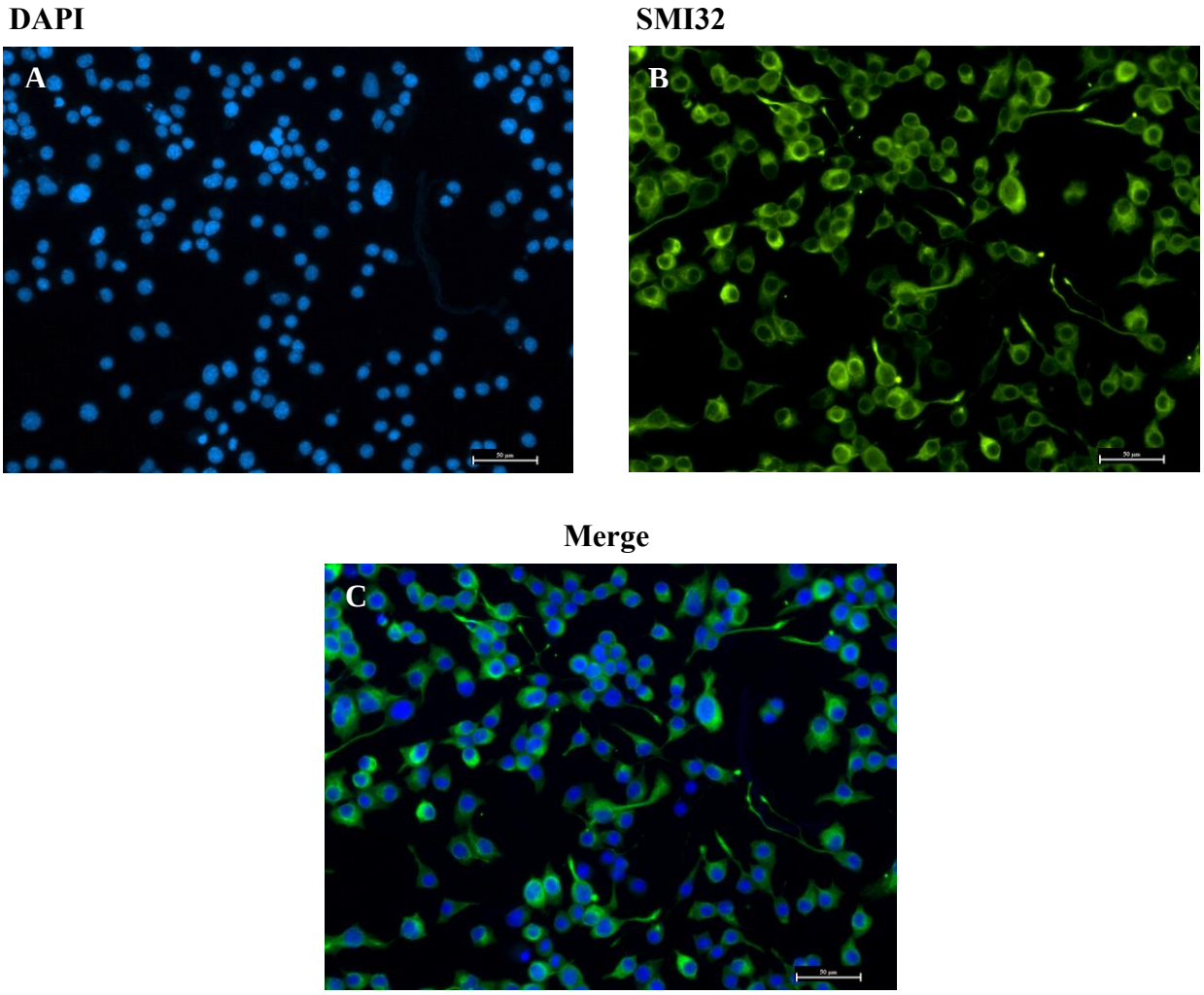

Figure 3.2. Expression of non-phosphorylated neurofilament H (SMI32) is detected in differentiated NSC34 cells after 3 DIV. Differentiated NSC34 cells were fixed after 3 DIV and immunolabeling was performed using rabbit anti SMI32 primary antibody and secondary antibody Alexa Fluor 488. Images were taken at 20x magnification from the same field of cells. Scale bar = 50 µm.

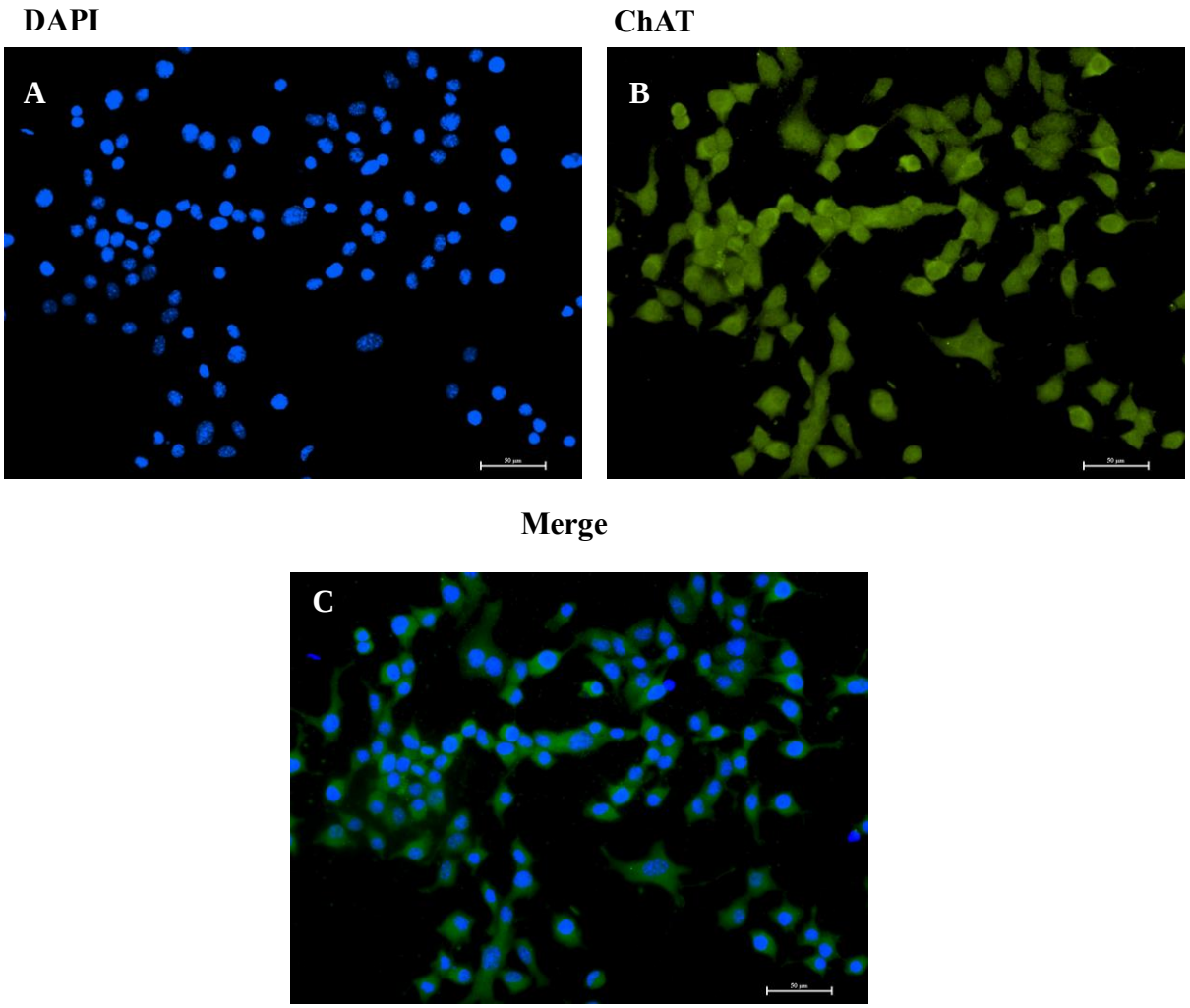

Figure 3.3 Expression of the choline acetyl transferase (ChAT) protein is detected in NSC34 cells after 3 DIV. Differentiated NSC34 cells were fixed after three days *in vitro* and immunolabeling was performed using rabbit anti ChAT primary antibody and secondary antibody FITC. Images were taken at 20x magnification from the same field of cells. Scale bar = 50 µm.

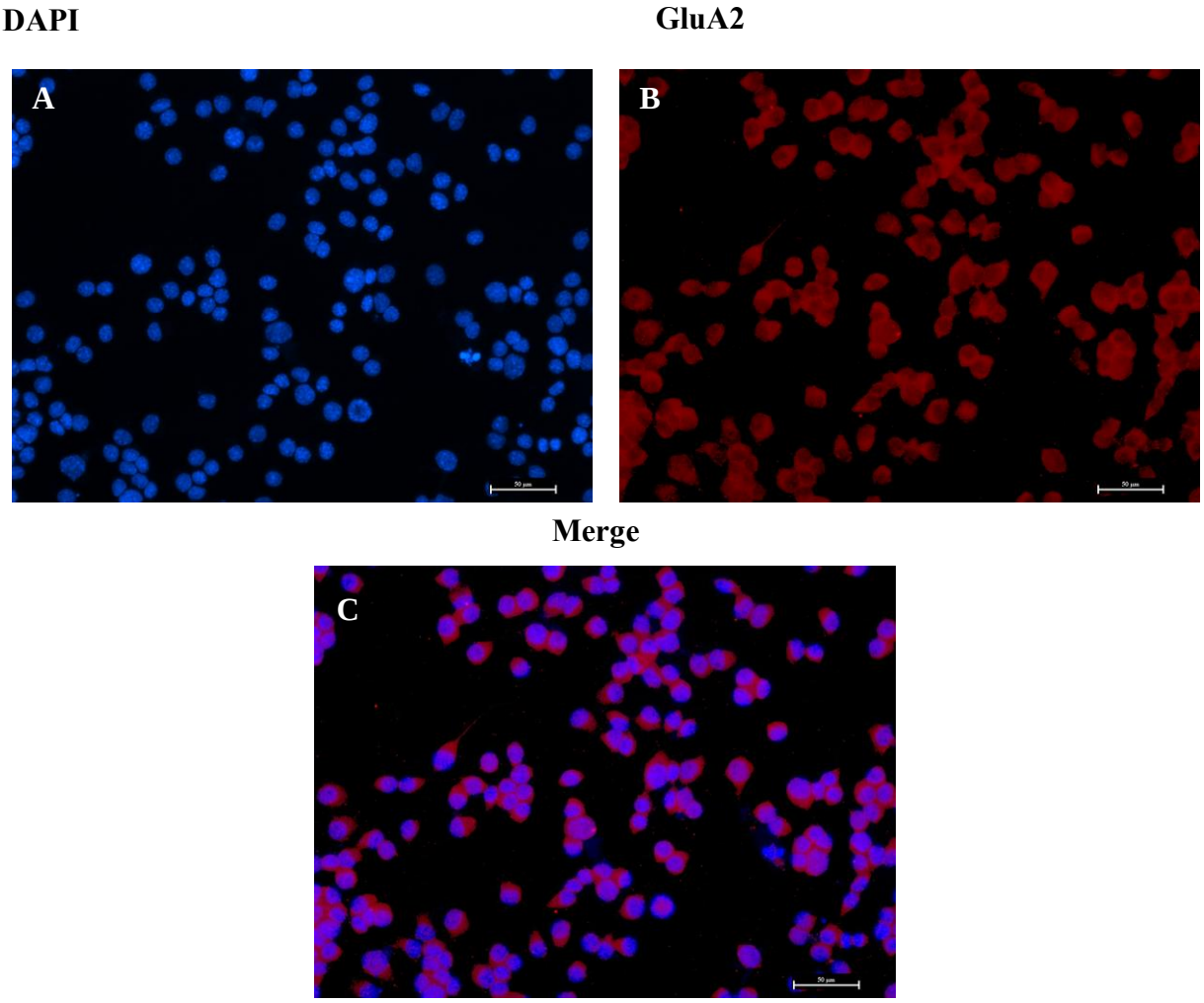

Figure 3.4. Expression of the AMPA receptor GluA2 subunit is detected in NSC34 cells after 3 DIV. Differentiated NSC34 cells were fixed after 3 DIV and immunolabeling was performed using rabbit anti GluA2 primary antibody and secondary antibody Alexa Fluor 594. Images were taken at 20x magnification from the same field of cells. Scale bar = 50 µm.

b. Exposure to low MeHg concentrations lead to a concentration dependent cell death in NSC34 cells

Viability of NSC34 cells was assessed immediately after 24 or 48 hr MeHg exposure using trypan blue cell exclusion assay. After 24 hr MeHg exposure a significant difference between 0 and 1 or 1.5 µM concentrations was measured (Fig. 3.5A). After 48 hr MeHg exposure a concentration dependent reduction was measurable when compared to control (0 µM) or between the different concentrations (Fig. 3.5B). There was a significant difference between 0 µM MeHg compared to 0.5 and 1.5 µM. Also, 0.5 µM was significantly different than 1 and 1.5 µM (Fig. 3.5B). This observation is consistent with what had been observed in a study of MeHg toxicity in NSC34 cells discussed previously (Chapman and Chan, 1999).

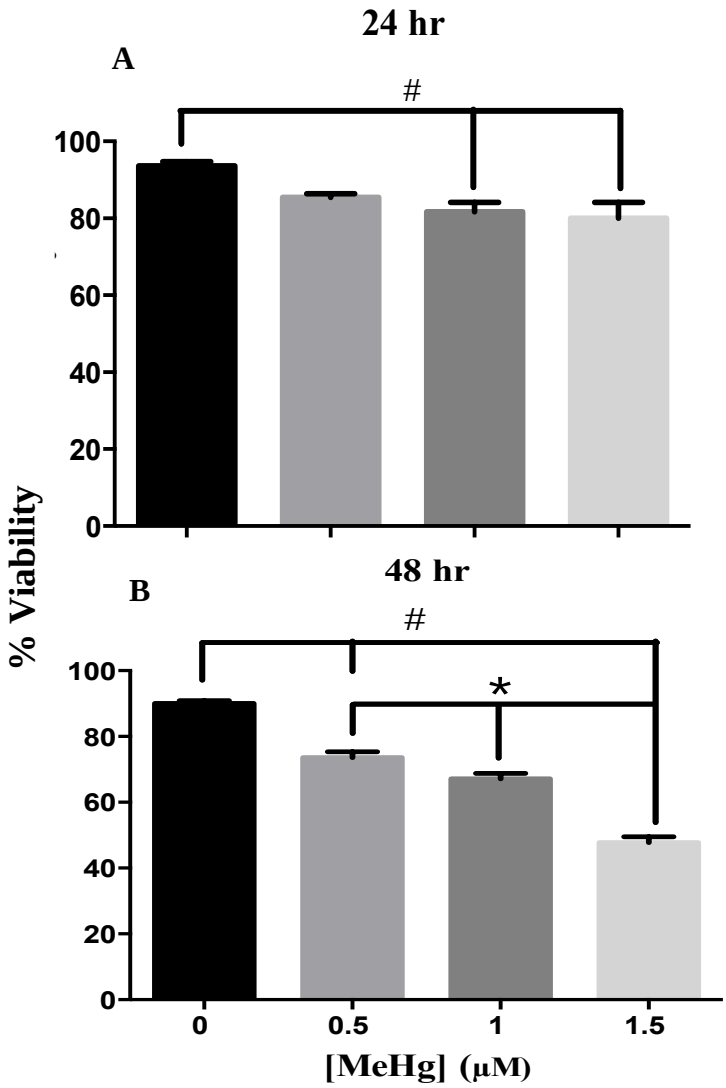

Figure 3.5. MeHg exposure and cell death of NSC34 cells. 24hr MeHg exposure leads to cell death of NSC34 cells at 1 and 1.5 μM concentrations (A). 48 hr MeHg exposure leads to a concentration dependent cell death of NSC34 cells (B). Differentiated DIV 3 NSC34 cells were exposed to MeHg for 24 or 48 hr and cell viability was assessed immediately after. 24 hr MeHg exposure significantly reduced percent viability at 1.0 and 1.5 μM concentrations (A). After 48 hr exposure MeHg led to a concentration dependent decrease of cell viability (B). (#) indicates a significant difference from control (0 μM MeHg). (*) indicates a significant difference between 0.5 μM and 1.0 μM; and 0.5 μM and 1.5 μM MeHg exposure ($p \leq 0.05$). Values are represented as mean ± SEM (n = 3).

c. Exposure to low concentrations of MeHg for 24 or 48 hr alters AMPA receptor expression differentially in NSC34 cells

To identify if low concentrations of MeHg altered gene expression of AMPA receptor subunits qPCR was performed in RNA of differentiated NSC34 cells exposed to MeHg for 24 and 48 hr. The goal of this experiment was to identify if alterations occur at these concentrations before we moved to the human cells. Also, we wanted to know if alterations occur, this could be one possible way by which AMPA receptors could be contributing to MeHg-induced alterations in MNs. This would also be consistent with the results obtained after low dose chronic MeHg exposure in rats (chapter two). After 24 hr MeHg exposure AMPA receptor gene expression is altered in NSC34 cells in a concentration dependent manner (Fig 3.6A). After 48 hr gene expression of all subunits studied are reduced at 0.5 and 1.0 µM MeHg exposures. However, at 1.5 µM MeHg exposure there is an increase in the expression of GluA3 (Fig. 3.6B). Significance of these results has not been assessed because statistical analysis cannot be performed at this point as we have an n = 2.

Taken together these data demonstrates that in NSC34 cells MeHg causes cell death in a concentration dependent manner and that it alters AMPA receptor gene expression at low concentrations. These results support my hypothesis that changes in expression of AMPA receptors occur after MeHg exposure and this could be one of the mechanisms by which these receptors are contributing to alterations in Ca^{2+}_i homeostasis after MeHg exposure. In order to identify if this could be the case in human MNs similar experiments were performed using hiPSC-MNs.

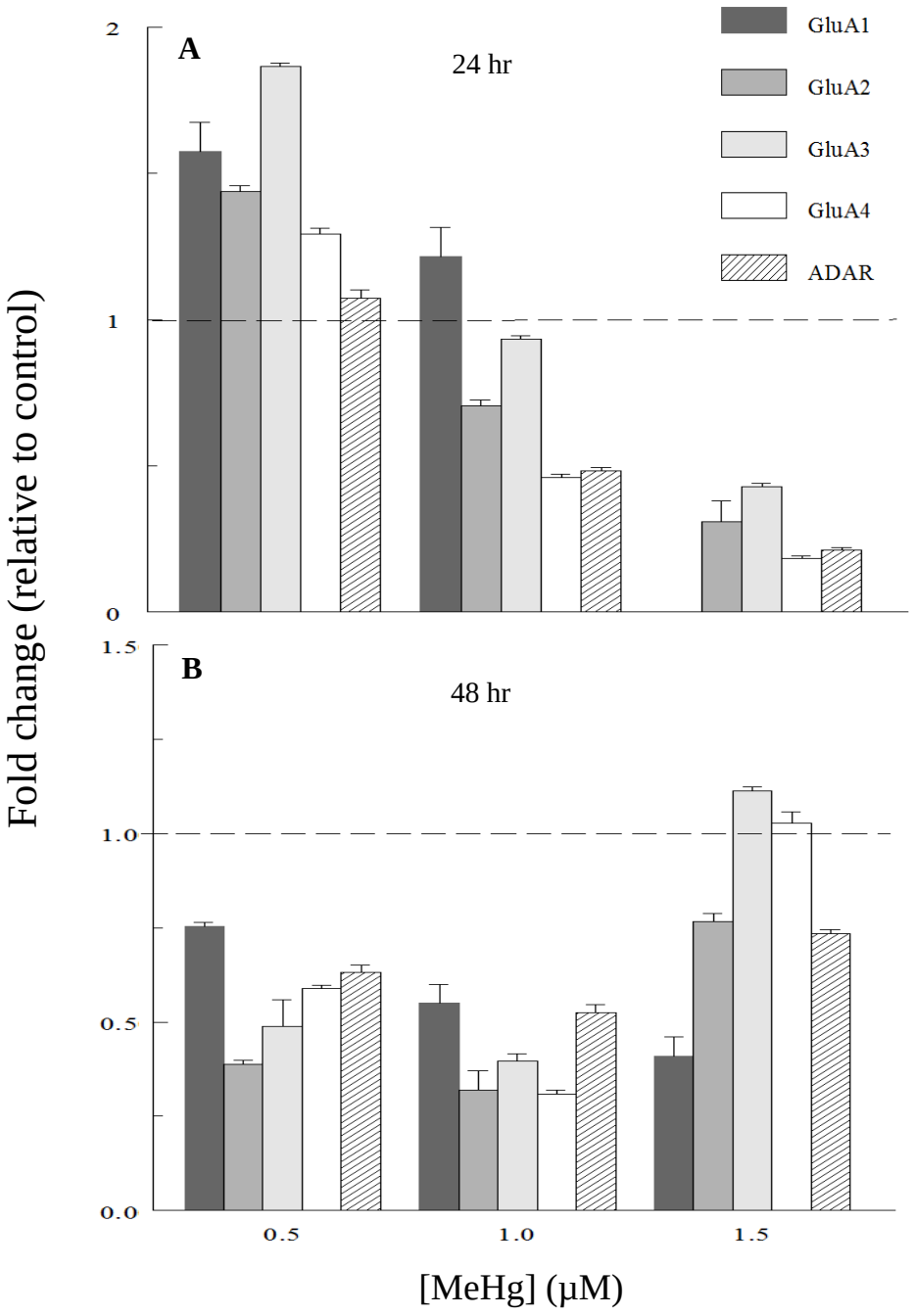

Figure 3.6. Relative expression of the AMPA receptor GluA subunits and ADAR2 in NSC34 cells after MeHg exposure. AMPA receptor GluA 1 – 4 expression in differentiated DIV3 NSC34 cells after 24 (A) or 48 hr (B) exposure to 0.5, 1.0 or 1.5 µM MeHg. Fold change in gene expression was calculated for each gene following the $2^{\Delta\Delta}$Ct method (Livak method). Values are represented as mean ± SEM (n = 2).

d. HiPSC-MNs grow in poly-l-ornitine and laminin coated dishes for up to 14 days *in vitro*

HiPSC-MNs used for this study recently came out to the market. In the supplier's protocol, it is suggested that the cells be cultured with astrocytes to allow them to have a longer lifespan *in vitro*. However, because I wanted to characterize MeHg effects in MNs in isolation I grew them without astrocytes. Thus, optimization of the cell density, by which they could be plated without astrocytes to reduce cell loss, and to obtain single cells to facilitate the cell viability and Ca^{2+} microfluorimetry recordings was performed. The selected cell density to perform my experiments was 1.2×10^5 cells/ml seeded in Poly-l-ornithine and laminin coated glass coverslips. Poly-l-ornithine and laminin were used as the substrates. These are the most commonly used when culturing human neural stem cells (Yang, 2014). After 24 hr *in vitro* hiPSC-MNs start growing neurites (Fig. 3.7A) and after 7 DIV they have differentiated completely and have long neurites and morphology of that of a mature MN (Fig. 3.7B). In a pilot experiment, I was able to keep the hiPSC-MN cultures for up to 14 days *in vitro*. However, for the experiments presented in this chapter only DIV 7 -11 hiPSC-MNs were used.

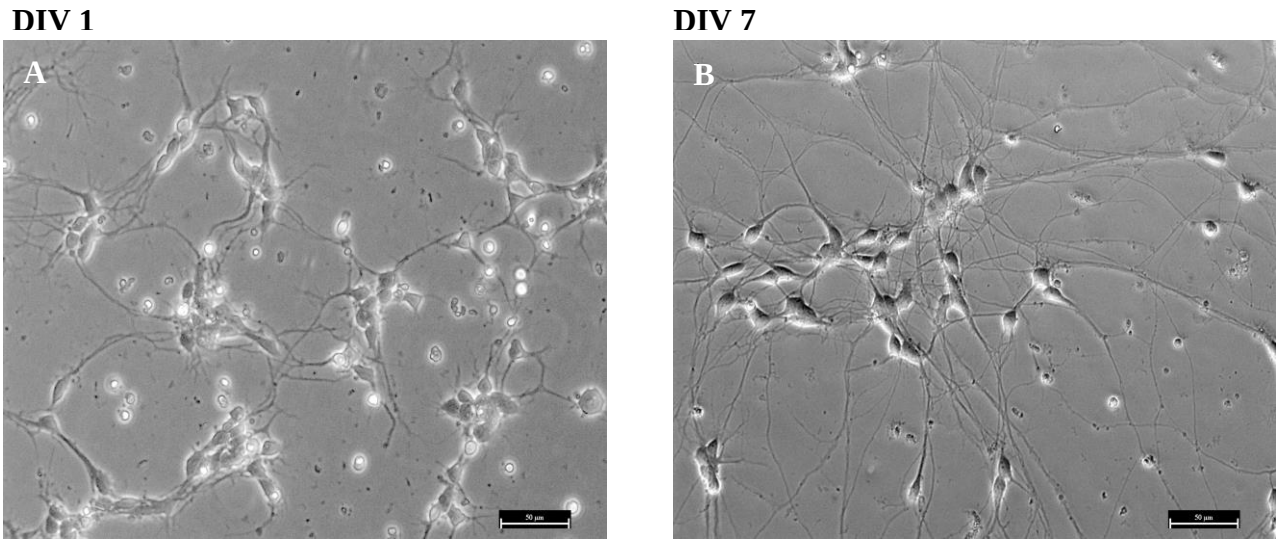

Figure 3.7. Morphology of hiPSC-MNs plated in poly-l-ornithine and laminin coated dishes. HiPSC-MNs present neurites after 1 DIV (A) and these extend and connect with neighboring neurons after at least 5 DIV. Panel (B) shows DIV 7 cell morphology. Long processes and morphological features as differentiated mature MNs can be observed. Micrograph was taken at 20x magnification. Scale bar = 50 µm.

e. HiPSC-MNs express ChAT, NFH, AMPA receptor subunits, and ADAR

Immunocytochemistry experiments were performed to identify the density of α MNs in the hiPSC-MN cell cultures. Alpha MNs can be identified from γ MNs by the abundant expression of a neuronal nuclear protein called NeuN (Friese et al. , 2009). Cells that express ChAT, NFH and NeuN are considered α MNs. The immunofluorescence results demonstrated that most of the cell population in our hiPSC-MN cultures are α MNs (Fig. 3.8). Because the main goal of this study was to identify the role of AMPA receptors in MeHg-induced toxicity, identification of AMPA receptor expression was performed. Immunocytochemistry for the presence of GluA1, the most abundant subunit of the AMPA receptors, and GluA2, the subunit that confers Ca^{2+} permeability to the receptors was made and expression of both was observed after 7 DIV (Fig. 3.9). Expression of the RNA editing enzyme ADAR2 was also identified in cultures from DIV 7 (Fig. 3.10). Based on these results DIV 7 was selected as the day to begin all experiments and MeHg exposures.

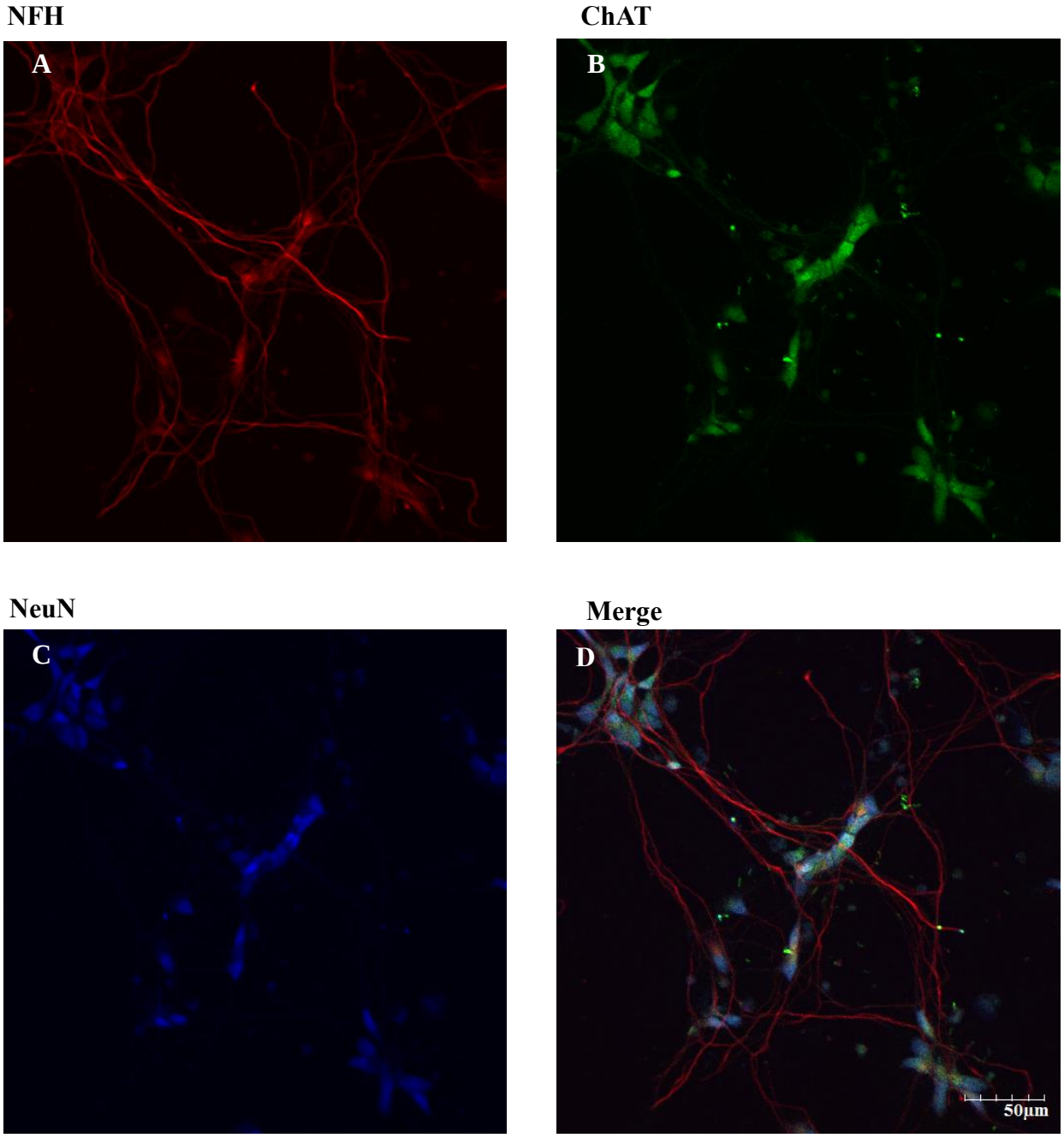

Figure 3.8. Expression of neurofilament H (NFH), choline acetyl transferase (ChAT) and neuronal nuclear protein (NeuN) in hiPSC-MNs after 7 DIV. DIV 7 hiPSC were fixed and immunolabeling was performed using mouse anti-NeuN primary antibody and anti-mouse Alexa Flour 405 (A). Rabbit anti-ChAT primary antibody and goat anti-rabbit Alexa Flour 488 secondary antibody was used (B). Chicken anti-NFH and goat anti-chicken Alexa Flour 594 secondary antibody was used (C). Merged images of NeuN, ChAT, and NFH showed the abundance of α MNs in our hiPSC-MN cultures. Images were taken at 20x magnification with 2x zoom form the same field of cells. Scale bar = 50 µm.

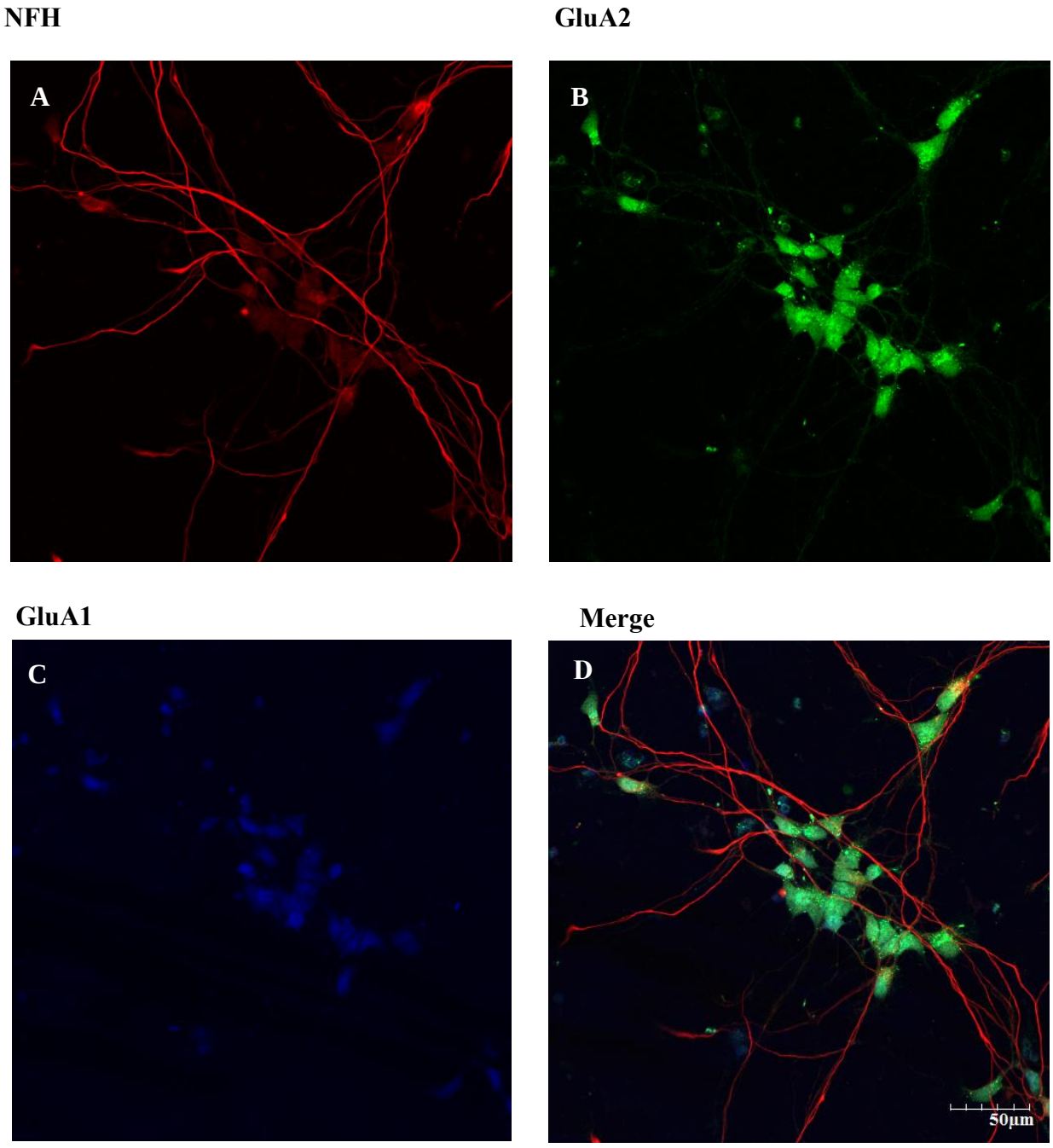

Figure 3.9. Expression of NFH, GluA2 and GluA1 subunit on hiPSC-MNs after 7 DIV. DIV 7 hiPSC were fixed and immunolabeling was performed using chicken anti-NFH primary antibody and goat anti chicken Alexa Flour 594 second antibody (A). Rabbit anti-GluA2 primary antibody conjugated with Alexa Flour 488 secondary antibody was used (B). Rabbit anti-Glua1 and goat anti-rabbit Alexa Flour 405 secondary antibody was used (C). Merged images of NFH, GluA1, and GluA2 showed these subunits in our hiPSC-MN cultures. Images were taken at 20x magnification with 2x zoom form the same field of cells. Scale bar = 50 µm.

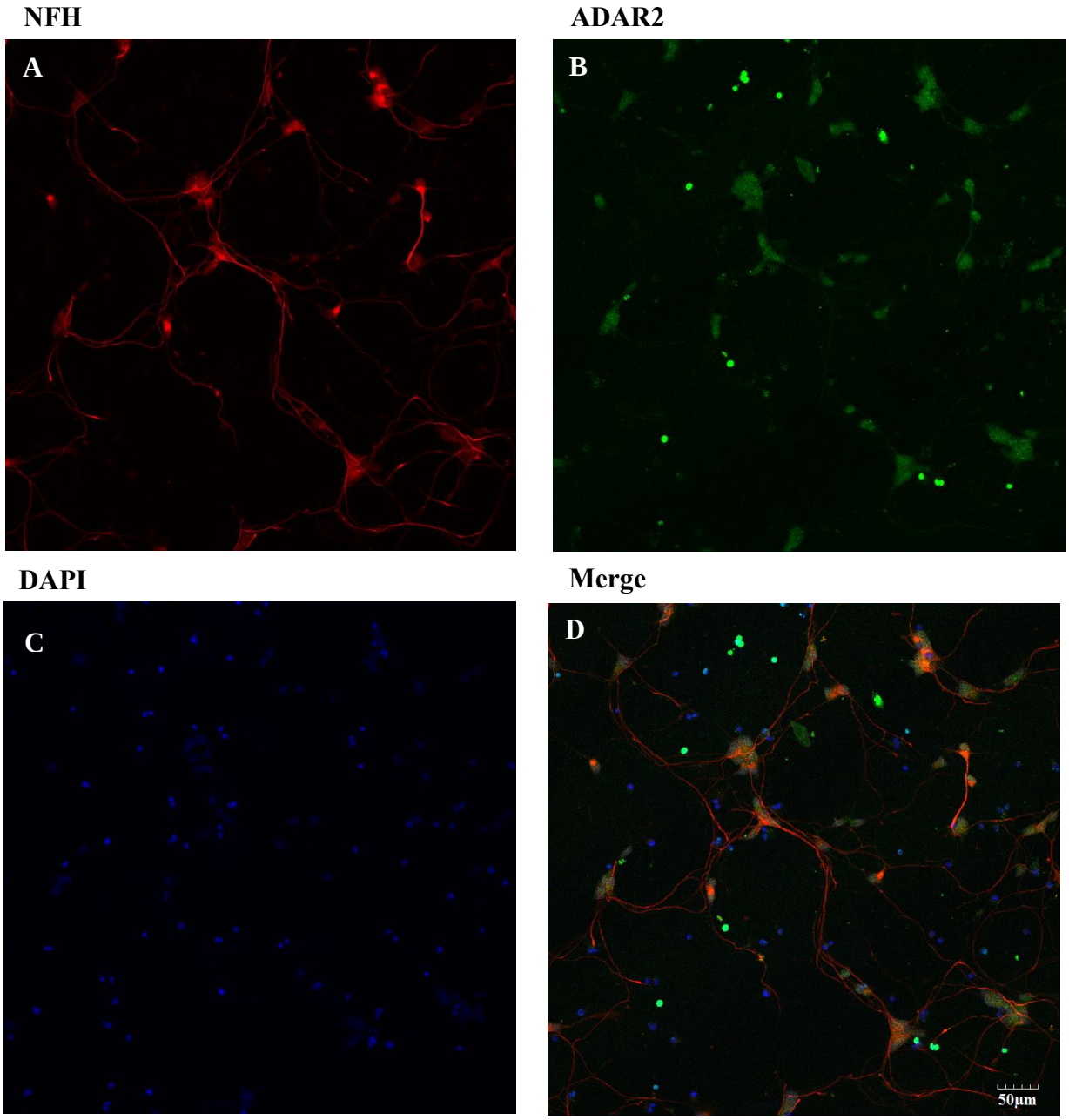

Figure 3.10. Expression of NFH, ADAR2 and DAPI on hiPSC-MNs after 7 DIV. DIV 7 hiPSC-MNs were fixed and immunolabeling was performed using chicken anti-NFH primary antibody and anti-chicken Alexa Flour 595 (A). Rabbit anti-ADAR2 primary antibody and goat anti-rabbit Alexa Flour 488 secondary antibody was used (B). Nuclear DNA stain DAPI is shown in panel (C). Merged image show expression of RNA editing enzyme ADAR2 in hiPSC-MNs. Images were taken at 20x magnification form the same field of cells. Scale bar = 50 µm.

f. Morphological changes on hiPSC-MNs are observed after MeHg exposure

MeHg exposure to 1 µM MeHg for 1.5, 6 or 18 hr leads to fragmentation of neurites in cerebellar granule cells (Castoldi et al. , 2000). After 1 hr exposure significant cell death at that concentration does not occur. Studies using MNs *in vitro* have demonstrated that they are susceptible to MeHg toxicity in a similar way as cerebellar granule cells (Ramanathan and Atchison, 2011). Thus, before selecting the duration of exposure for the experiments of this study it was appropriate to identify structural changes in these cells as these precede cell death (Castoldi et al. , 2000). This allows for identification of an exposure which will be appropriate for performing studies which aim at identifying molecular events that leads to cell death. Fragmentation of neurites was observed after 12 hr exposure to 1 and 1.5 µM MeHg (Fig. 3.11). 24 hr MeHg exposure caused neurite beading and fragmentation in all concentrations (0.5 – 1.5 µM) (Fig. 3.11). The effects appeared to increase as the concentrations of MeHg increased (Fig. 3.11). These results and the significant decrease in gene expression of AMPA receptor subunits observed in this same exposure (data not shown) led to abandon chronic exposures as a paradigm for this study.

Delayed MeHg effects are well known (Rice, 1996) and these have not been identified *in vitro* for human MNs. However, rodent spinal cord MNs accumulate MeHg and cell death occurs as a delayed effect, observed days (~10) after MeHg exposure had stopped (Moller-Madsen, 1990, 1991, Su et al. , 1998). Morphological changes were assessed in hiPSC-MNs 24 hr after a 1 hr exposure to 0.5 – 1.5 µM MeHg (Fig. 3.12). HiPSC-MNs did not show any morphological changes except 24 hr after exposure to 1.5 µM MeHg (Fig. 3.12). These results led to the following questions: what are the delayed effects of MeHg in cell viability of hiPSC-MNs? Can 1 hr MeHg exposure lead to long lasting changes in gene expression of the AMPA receptors or

the RNA editing enzyme ADAR like the ones observed in brainstem of rats (Chapter two) and in NSC34 cells?

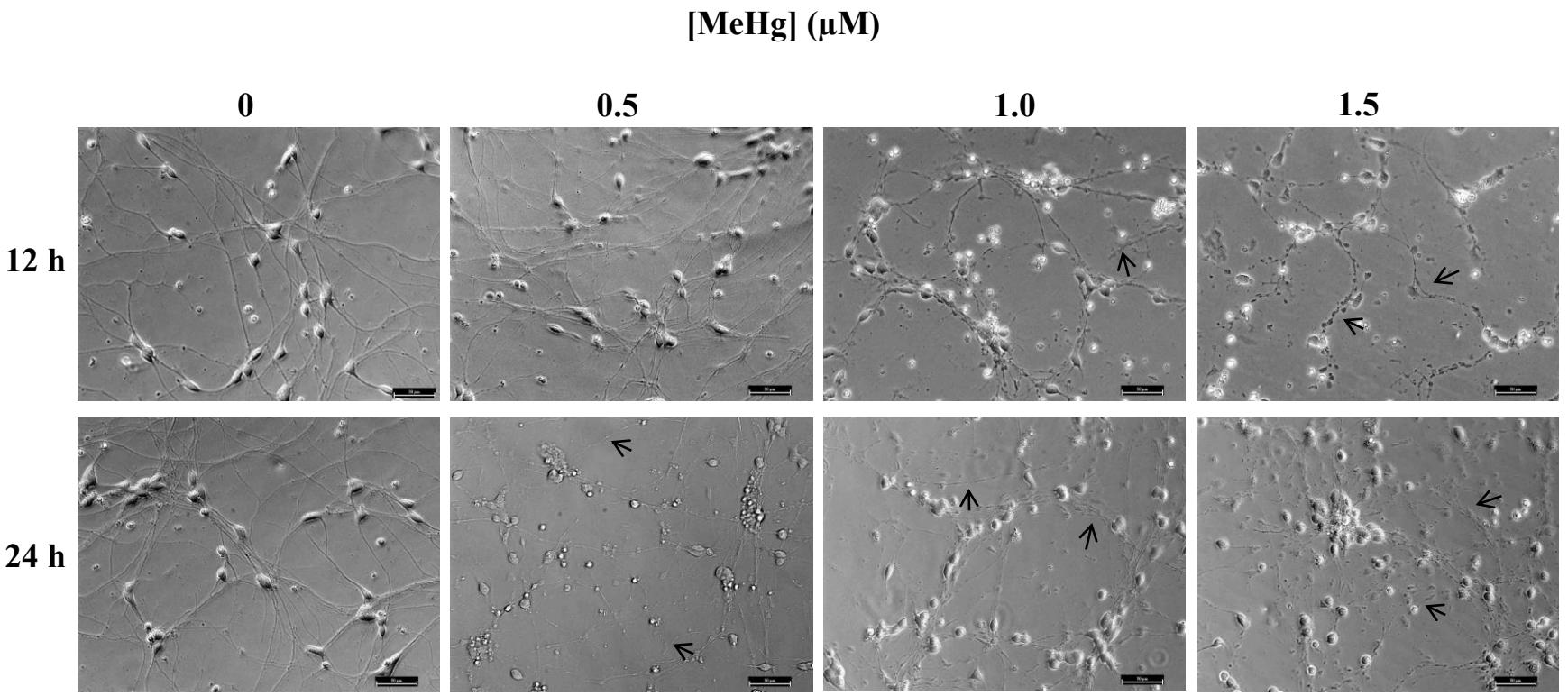

Figure 3.11. Effect of 12 or 24 hr MeHg exposure on hiPSC-MNs morphology assessed immediately after exposure. Micrographs of hiPSC-MNs exposed to MeHg for 12 or 24 hr present alterations in cell morphology (note arrows) in the form of neurite beading and fragmentation. Micrographs are brightfield images of hiPSC-MNs taken in 20x magnification. Scale bar = 50 µM.

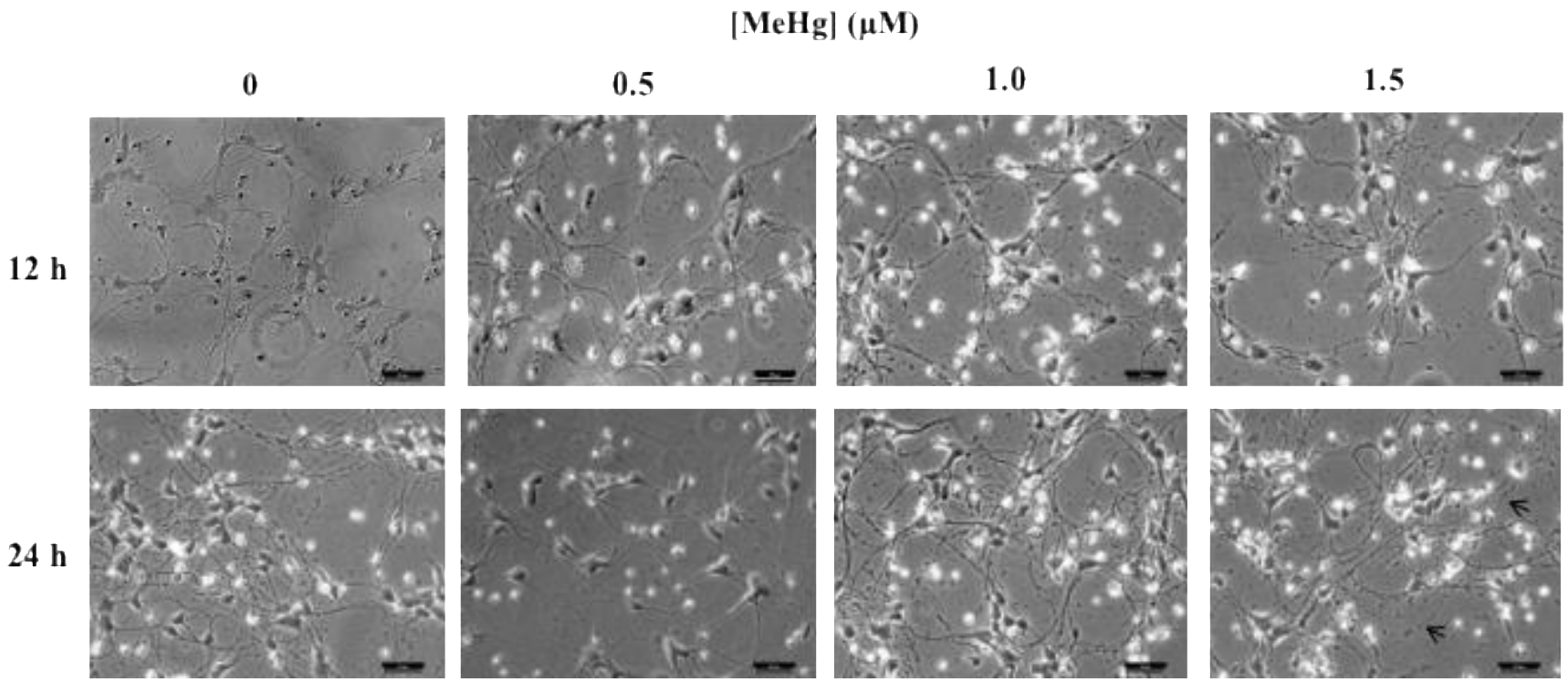

Figure 3.12. Effect of 1 hr MeHg exposure on hiPSC-MNs morphology assessed after 12 and 24 hr. Micrographs of hiPSC-MNs exposed to MeHg for 1 hr and observed after 12 or 24 hr did not present alterations in cell morphology except at 1.5 µM where fragmentation of neurites was observed (note arrows). Micrographs are brightfield images of hiPSC-MNs taken in 20x magnification. Scale bar = 50 µM.

g. Concentration-dependent cell death of hiPSC-MNs occur after 1 hr MeHg exposure

Cell viability was inversely proportional to MeHg concentrations 24 hr post exposure (Fig. 3.13). Effects of 1 hr MeHg exposure were assessed after 24 hr and showed a significant reduction in the percent viability of cells exposed to 1 or 1.5 µM MeHg compared to untreated controls. Exposure to 0.1 µM was significantly different than 1 and 1.5 µM MeHg. Representative micrographs of the cell viability assay show that untreated cells (0 µM MeHg) have long processes connected between each other and the number of live cells labeled by calcein-AM (green) are greater than the dead cells (red) labeled by ethidium homodimer (Fig. 3.13B). Cells exposed to 1.5 µM MeHg had a greater number of dead cells (red) and presented fragmentation and beading of axons (Fig. 3.13C) as observed in the morphological study (Fig. 3.11-12). These results demonstrate that 1 hr MeHg exposure is sufficient to elicit cell death in hiPSC-MNs.

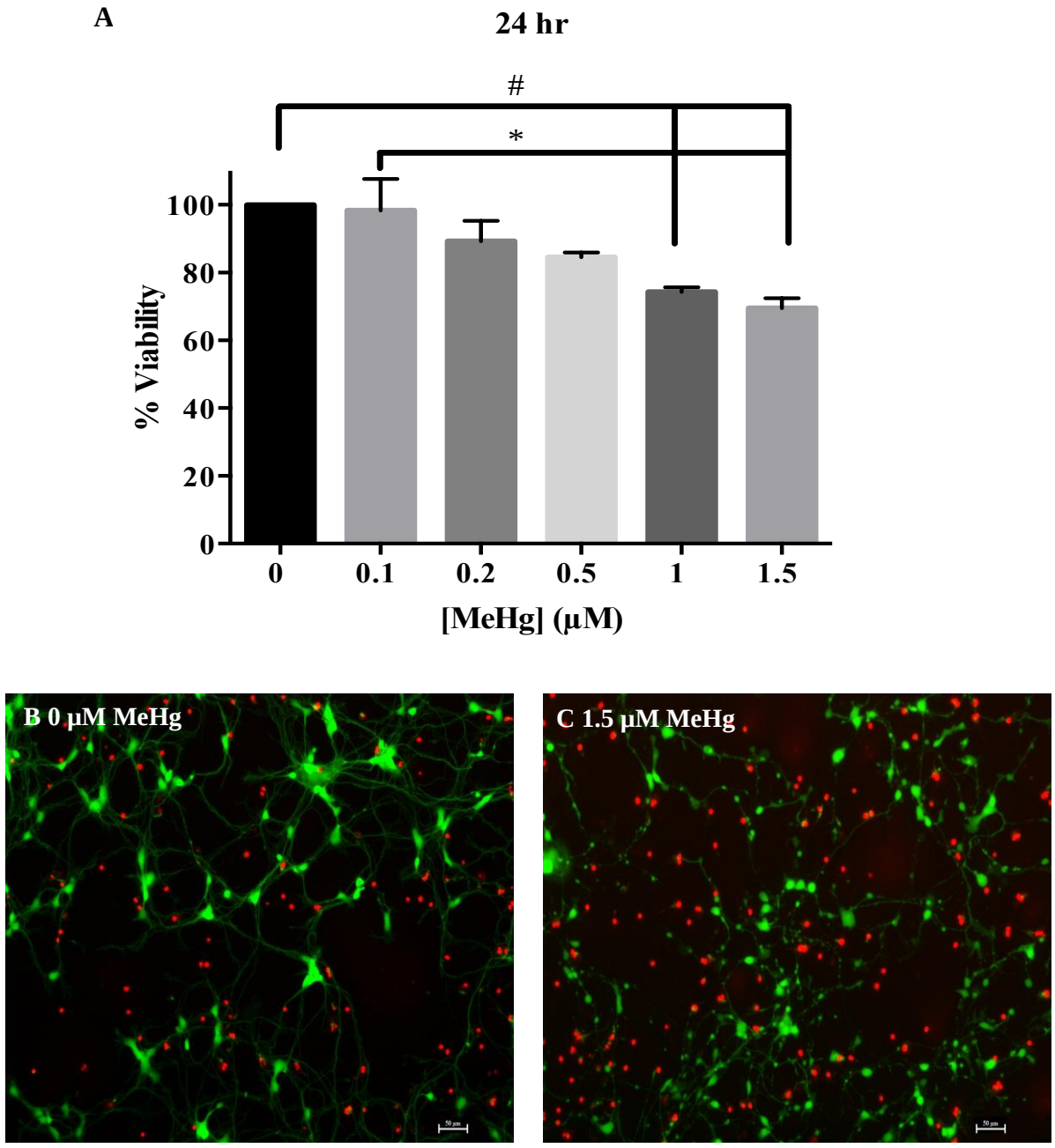

Figure 3.13. Delayed effects of MeHg in cell viability were assessed 24 hr after exposure. Cell viability measured with Calcein-AM/Ethidium homodimer showed a concentration dependent cell death in hiPSC-MNs after exposure to 0.1 - 1.5 µM MeHg for 1 hr and assessed after 24 hr (A). Representative micrograph of 0 µM MeHg (B) and 1.5 µM MeHg exposed hiPSC-MNs (C) after labeling for cell viability using Calcein-AM (green) and Eth-D (red). (#) indicates a significant difference from control (0 µM MeHg). (*) indicates a significant difference between 0.1 µM compared to 1.0 and 1.5 µM MeHg exposure ($p \leq 0.05$). Values are represented as mean ± SEM (n = 3). Scale bar = 50 µM.

h. MeHg elicits a bi-phasic increase in $[Ca^{2+}]_i$ in hiPSC-MNs

MeHg-induced increases in $[Ca^{2+}]_i$ have been identified *in vitro* in spinal cord MNs from mice (Ramanathan and Atchison, 2011). These occur in a bi-phasic manner. To identify if this occurred in a human MN cell model, recordings were performed using hiPSC-MNs. In hiPSC-MNs a similar response as seen in mouse MNs was observed, which is characteristic of MeHg toxicity. A representative tracing of Fura-2 fluorescence ratio $F_{340/380}$ from a hiPSC-MN exposed to 1.5 µM MeHg is shown in Fig. 3.14. The first phase observed is due to the release of Ca^{2+} from intracellular stores and the second phase is due to the influx of Ca^{2+} from extracellular sources (Marty and Atchison, 1997). This occurred in all MeHg exposures (0.1 - 1.5 µM). MeHg induced an increase in Fura-2 fluorescence in a time- and concentration-dependent manner (Fig 3.15). In the 1st phase there is a significant difference between the time-to-onset of cells exposed to 0.1 µM MeHg and all other concentrations (Fig. 3.15A). In the second phase, there was a significant difference between the 0.1 µM and all other concentrations as well as 0.5 µM MeHg compared to all other concentrations (Fig. 3.15B).

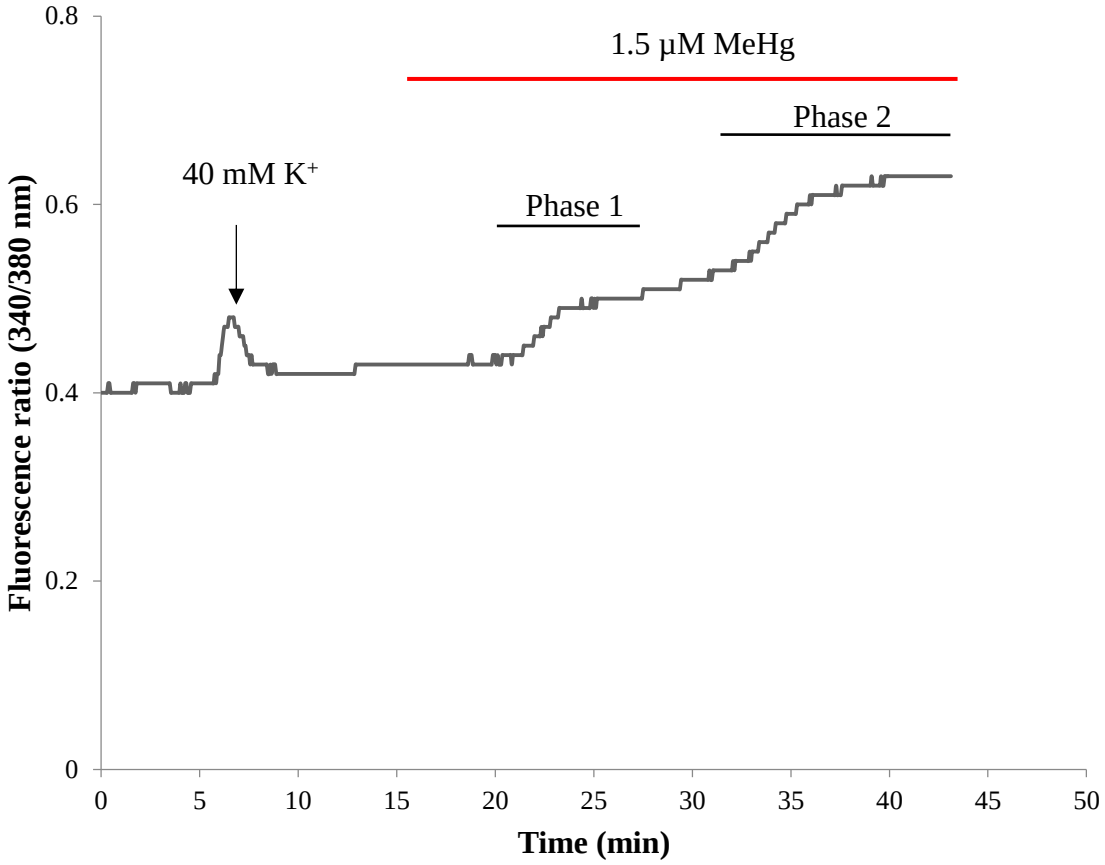

Figure 3.14. Acute MeHg exposure alters $[Ca^{2+}]_i$ homeostasis in hiPSC-MNs in a biphasic manner. A representative tracing of Fura-2 fluorescence ratio $F_{(340/380)}$ from a cell soma of a single hiPSC-MN during exposure to 1.5 µM MeHg.

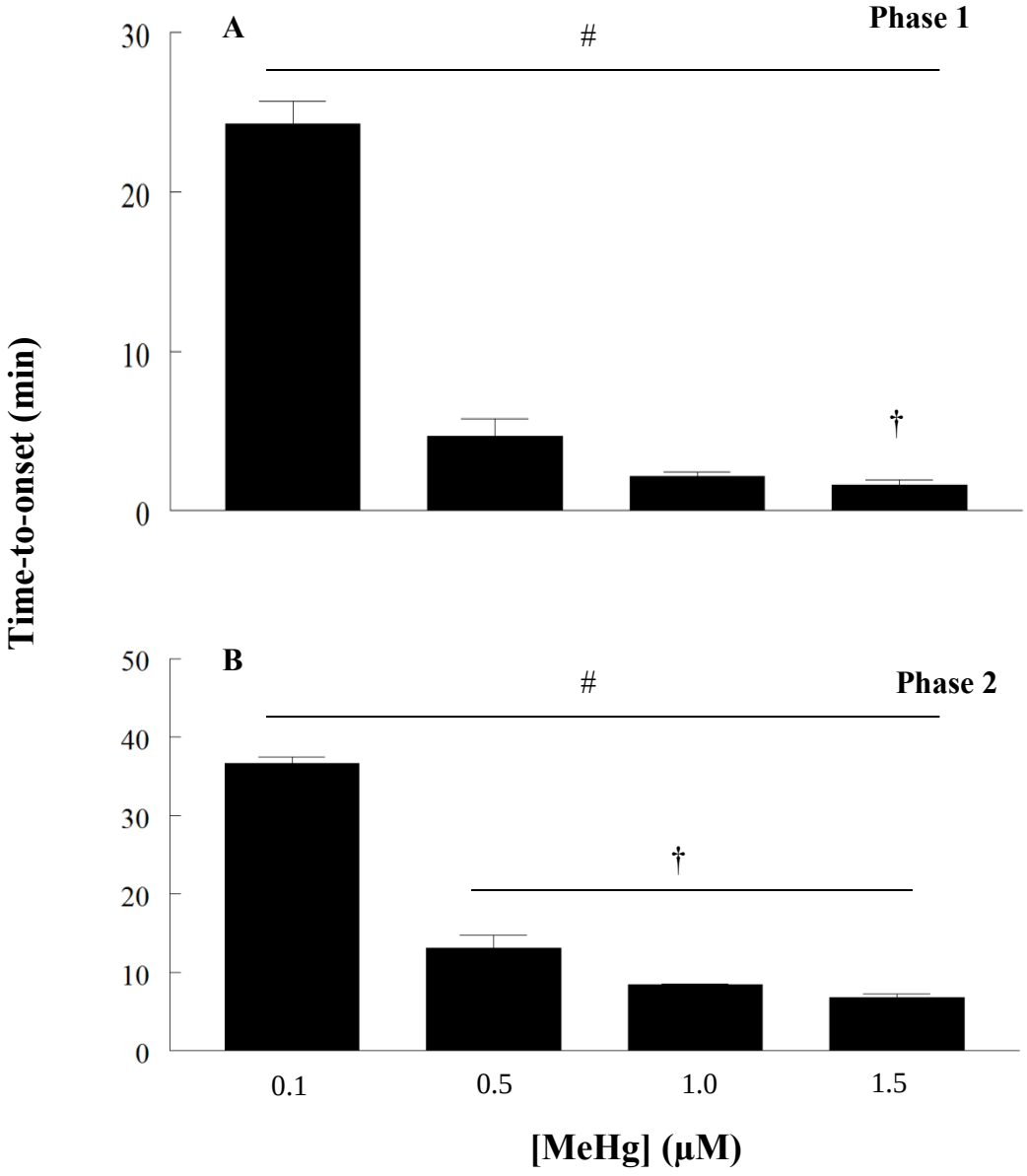

Figure 3.15. Time-to-onset of increase in fura-2 fluorescence during perfusion of hiPSC-MNs with MeHg (0.1 - 1.5 µM) in normal HBS. Untreated hiPSC-MNs maintain a basal fura-2 fluorescence for more than 60 min. (#) indicates significant difference between 0.1 µM versus 0.5 µM, 1 µM and 1.5µM, (†) indicates a significant difference between 0.5 µM versus 1.5 µM. In phase 2, (#) indicates significant difference between 0.1 µM versus 0.5 µM, 1 µM and 1.5 µM, (†) indicates a significant difference between 0.5 µM versus 1.0 µM and 1.5 µM. Values are represented as mean ± SEM ($n \geq 4$). Each n represents the recording of fura-2 fluorescence value from the soma of 6 - 10 hiPSC-MNs per dish.

i. MeHg-induced increases in $[Ca^{2+}]_i$ in hiPSC-MNs are mediated by AMPA receptors

AMPA/KA receptor antagonist CNQX was used in order to identify if AMPA receptors could be playing a role in the observed increases in $[Ca^{2+}]_i$ in hiPSC-MNs. Exposure to 20 µM CNQX led to a delay in the time-to-onset of the first and second phase of Fura-2 fluorescence in all the MeHg exposures (0.1 - 1.5 µM) (Fig. 3.16). Effects were significant in both phases. This was the first indicator that AMPA receptors are contributing to alterations in Ca^{2+} in our MN model. To identify if Ca^{2+} permeable AMPA receptors were indeed contributing to the increases in Ca^{2+}, exposure to the Ca^{2+} permeable AMPA receptor blocker NAS was done. Exposure to 50 µM NAS led to a significant decrease of the second phase of Fura-2 fluoresence in hiPSC-MNs exposed to 1.5 µM MeHg (Fig. 3.17). Exposure to both the blocker and MeHg occurred simultaneously.

To confirm the second phase observed after MeHg exposure was due to the influx of extracellular Ca^{2+} recordings were made with Ca^{2+} free HBS (contains 20 µM EGTA). MeHg used in this experiment was also prepared in the Ca^{2+} free HBS. Exposure to MeHg in Ca^{2+} free HBS led to the presence of a first phase of Fura-2 fluorescence that is characteristic of release of Ca^{2+} from intracellular stores. The absence of the second phase indicates that in hiPSC-MNs the second phase is due to the influx of extracellular Ca^{2+}. A representative tracing of one of our recordings is shown in Figure 3.18. This is similar to what has been observed in primary neuronal cells including mouse MNs after MeHg exposure (Ramanathan and Atchison, 2011).

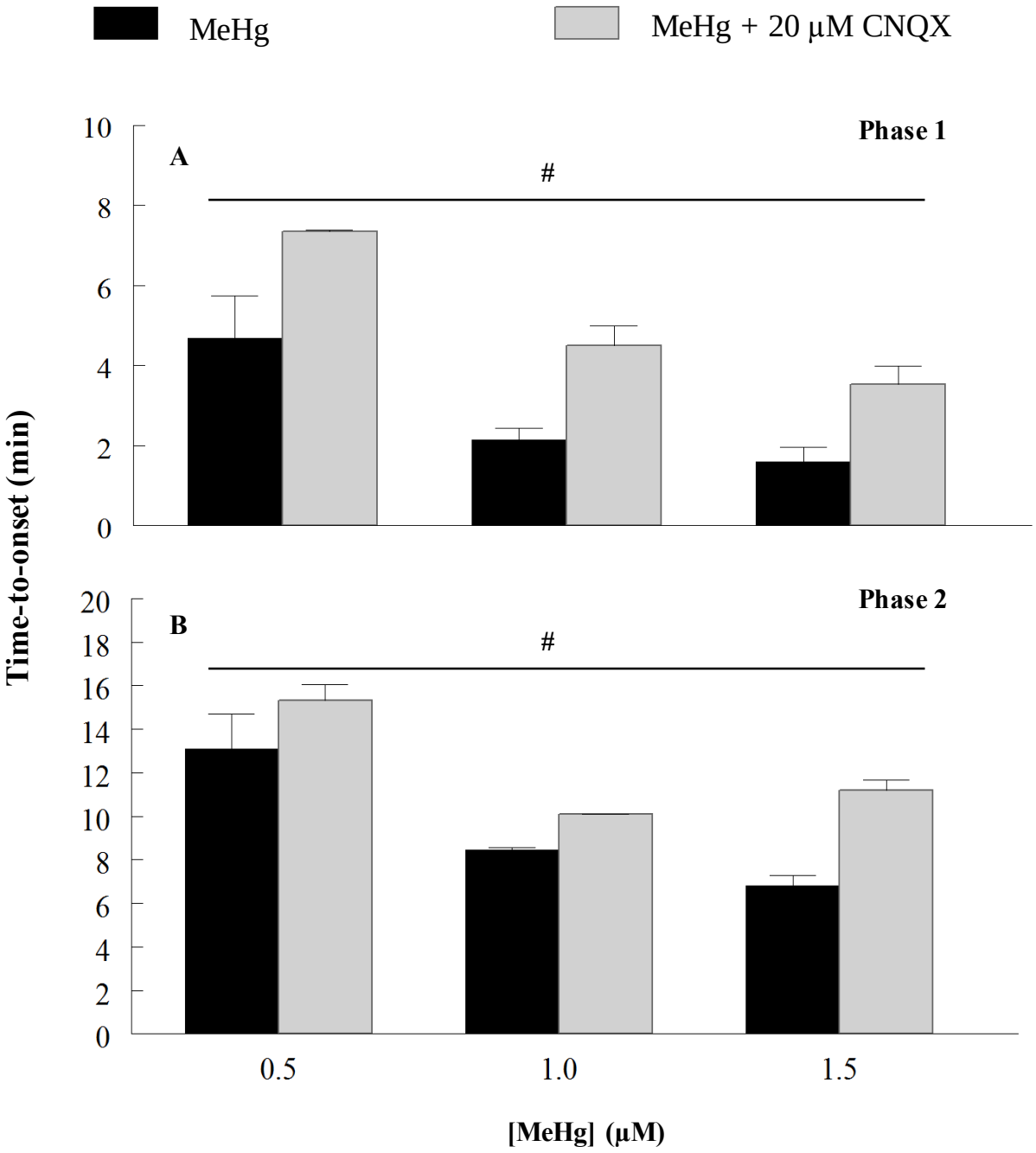

Figure 3.16. Acute MeHg exposure induced increases of Ca^{2+}_i in hiPSC-MN are mediated in part by AMPA/KA receptors. MeHg-induced increase in fluorescence time-to-onset is delayed by exposure to 20 µM CNQX, an AMPA/KA receptor antagonist, showing that this receptor is contributing to MeHg-induced increases in $[Ca^{2+}]_i$ in hiPSC-MNs. (#) indicates significant difference between 0.5 µM versus 1.0 µM and 1.5 µM. Values are represented as mean ± SEM ($n \geq 4$).

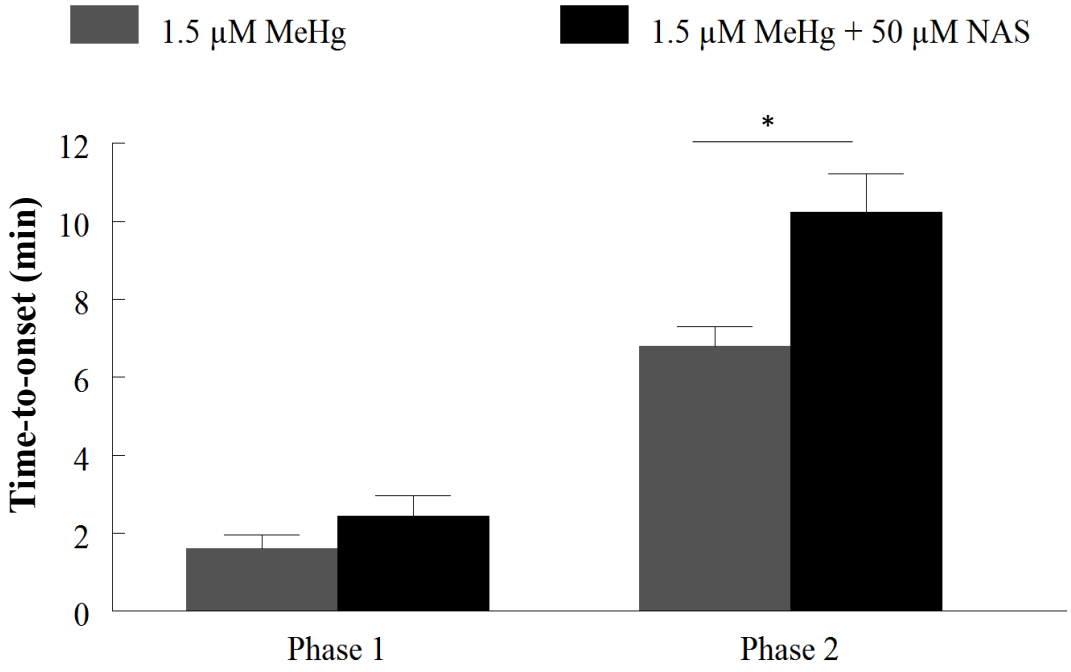

Figure 3.17. Acute MeHg exposure induced increases of Ca^{2+}_i in hiPSC-MNs are mediated in part by Ca^{2+} permeable AMPA receptors. MeHg-induced increase in fluorescence time-to-onset is delayed by exposure to 50 µM NAS, a Ca^{2+} permeable AMPA receptor antagonist, confirming that this receptor is contributing to MeHg-induced increases in $[Ca^{2+}]_i$ in hiPSC-MNs. (*) indicates significant difference between 1.5 µM MeHg alone vs 1.5 µM MeHg + 50 µM NAS. Values are represented as mean ± SEM (n = 3).

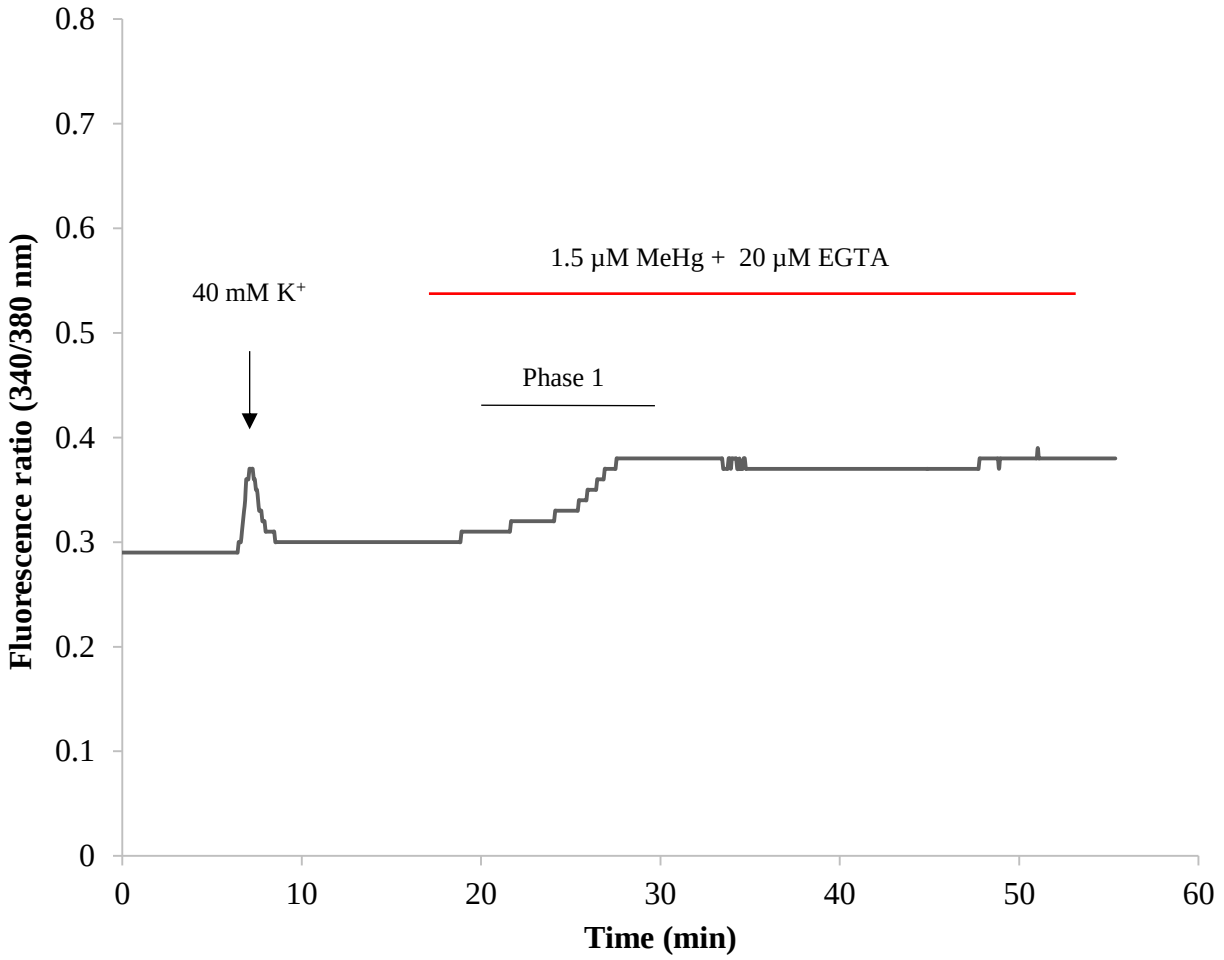

Figure 3.18. Representative tracing of Fura-2 fluorescence ratio $F_{(340/380)}$ from a hiPSC-MN during exposure to 1.5 µM MeHg + 20 µM EGTA. Initial peak represents increase in Ca^{2+} as a result of depolarization of the cell after 1 min exposure to 40 mM KCl. Exposure to 1.5 µM MeHg + 20 µM EGTA containing HBS (Ca^{2+} free HBS) removed the 2nd phase commonly observed with MeHg exposure. This demonstrates that the 2nd phase is dependent on the influx of extracellular Ca^{2+}.

j. Delayed effects of MeHg exposure on gene expression of AMPA receptor GluA subunits and ADAR in hiPSC-MNs

Because alterations in expression of AMPA receptors and the RNA editing enzyme ADAR2 can be one of the mechanisms by which they contribute to increases in Ca^{2+} in MNs identification of possible alterations were investigated. Alterations of AMPA receptor expression in MNs after MeHg exposure have not been previously addressed. Thus, to identify if AMPA receptor expression was affected after exposure to MeHg my approach was to identify changes in gene expression as these could serve as an indicator of what could be occurring at the protein level. Expression of AMPA receptor subunits GluA1 - 4 were performed by quantitative real-time PCR (Fig. 3.19). The results show that MeHg leads to a significant increase in expression of all the GluA subunits and ADAR2 at 0.1 µM concentration. Increase in levels of ADAR2 were observed at all concentrations except 1.5 µM MeHg. All other subunits were decreased. These measurements were performed in RNA isolated 24 hrs after 1 hr MeHg exposure. This was mainly to identify if delayed effects occurred after MeHg exposure.

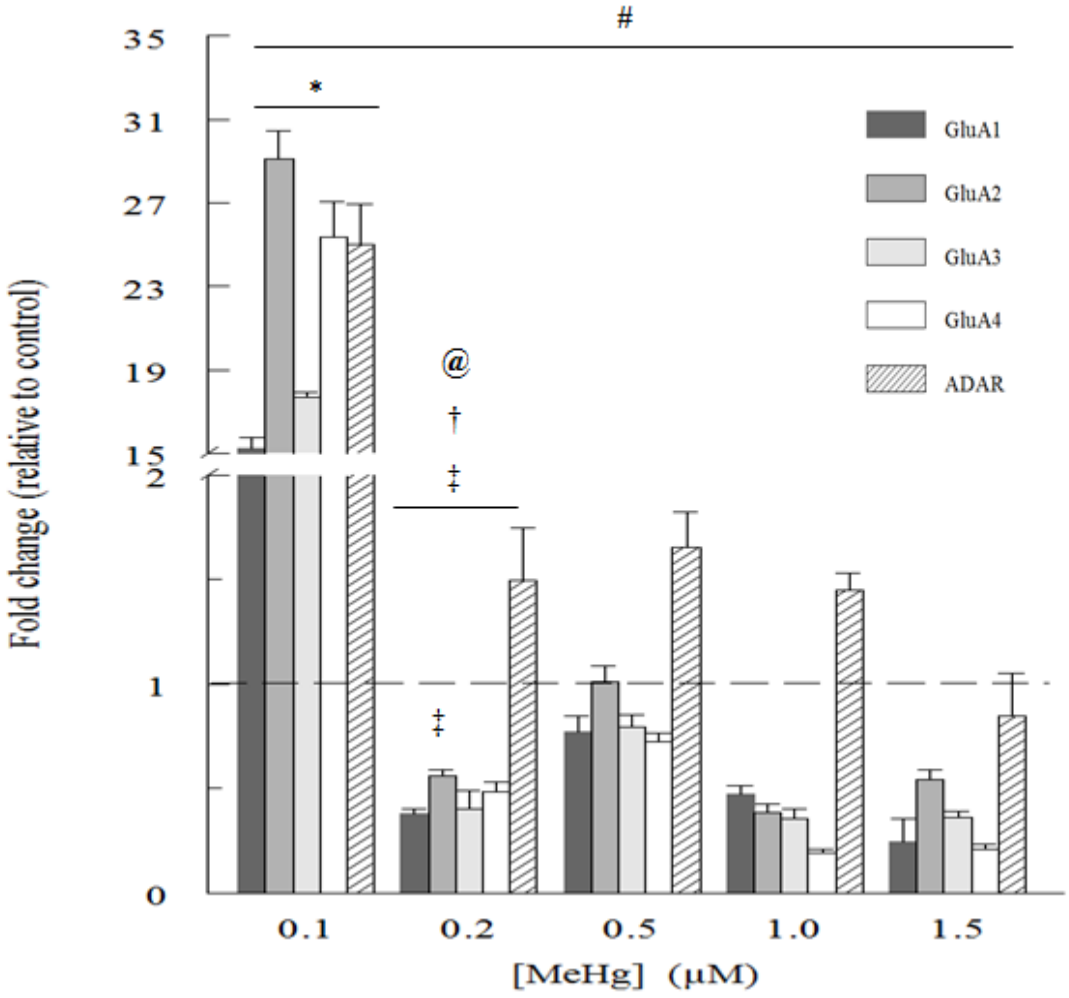

Figure 3.19. Delayed MeHg effects on relative expression of AMPA receptor subunits and ADAR after 1 hr MeHg exposure. AMPA receptor GluA 1- 4 subunit expression in hiPSC after 0.1-1.5 µM MeHg exposure for 1 hr, assessed after 24 hrs of exposure. (*) indicates a significant difference between control and 1.0 µM MeHg exposure ($p \leq 0.05$). (#) indicates a significant difference between 0.1 µM versus 0.2 µM, 0.5 µM, 1 µM, and 1.5 µM of MeHg exposure ($p \leq 0.05$). (‡) indicates a significant difference between GluA1 versus GluA2 and GluA4 ($p \leq 0.05$). (†) indicates a significant difference between GluA2 and GluA3 ($p \leq 0.05$). (@) indicates a significant difference between GluA3 versus GluA4 and ADAR ($p \leq 0.05$). Values are represented as mean ± SEM (n = 3), three replicates per group.

E). Discussion

MeHg toxicity leads to motor dysfunction that has been associated with the degeneration of cerebellar granule cells (Hunter and Russell, 1954). However, evidence has demonstrated that MeHg accumulates and leads to the degeneration of spinal cord MNs, and effects are most pronounced in α MNs. This has been observed in *in vivo* studies (Moller-Madsen, 1990, 1991, Su, Wakabayashi, 1998). Effects of MeHg on MNs have not been characterized, and this could indicate another potential mechanism by which MeHg is leading to motor impairment and ataxia. *In vitro* studies have shown that MeHg leads to increases in Ca^{2+} in mice spinal cord MNs and that these are mediated in part by NMDA and AMPA receptors (Ramanathan and Atchison, 2011). The effects of MeHg on AMPA receptors have not been studied nor the role Ca^{2+} permeable AMPA receptors may play in MeHg induced toxicity in MNs. To identify if these alterations occur in human MNs and if AMPA receptors play a role in them, experiments were performed using hiPSC-MNs. Before performing the experiments in hiPSC-MNs most of the methods were optimized in a neuroblastoma MN cell line, NSC34. HiPSC-MNs are very costly, thus the ability to characterize the effects of MeHg on the NSC34 cell model first allowed me to have a baseline which was used to start out the other *in vitro* experiments.

I began the study by characterizing NSC34 cells to identify if they presented MN characteristics, such as the expression of ChAT and SMI32. The presence of ChAT, SMI32 and the glutamate receptor subunit GluA2 was identified after 3 DIV. In rodent primary MNs MeHg toxicity occurs at very low concentrations (0.1 - 1.5 μM) and during acute (~1 hr) exposure (Ramanathan and Atchison, 2011). In NSC34 cells a similar low concentration was used and the effects seem to be more pronounced after 48 hr. This is consistent with a study performed in NSC34 cells that focused on identifying the toxicity of MeHg and Hg on MNs where it was

identified that MeHg LD_{50} is 1.7 µM. In that study a concentration-dependent cell death occurred after 48 hr of exposure (Chapman and Chan, 1999). That correlates with what has been found in this study. Another important finding is that MeHg seems to cause a concentration dependent effect in the gene expression of AMPA receptors in NSC34 cells. These results support the idea that MeHg effects in MNs may be in part mediated by increased expression of the Ca^{2+} permeable AMPA receptors. This was mainly due to the decrease observed in the RNA editing enzyme ADAR2 and the GluA2 subunit. However, only two samples in triplicate were studied (n =2), thus statistical analysis could not be performed. The results of this first study were used to design the hiPSC-MN experiments.

The cultures of hiPSC-MNs used in our experiments were mostly α MNs (~80%). This was identified after expression of ChAT, NeuN and NFH were present and overlapped in most of the cells. Expression of AMPA receptor GluA1 and GluA2, as well as the RNA editing enzyme ADAR2 was also identified in DIV7 HiPSC-MNs. After characterizing the cells for the presence of these key proteins MeHg experiments were performed. The concentrations selected (0.1 - 1.5 µM) were based on our morphological experiments and originally based on the findings from NSC34 cells and mouse MNs described previously. *In vitro* MeHg exposure ranging from 0.1 µM - 1.5 µM increased $[Ca^{2+}]_i$ in a time-and-concentration dependent manner in hiPSC-MNs. These alterations were mediated in part by Ca^{2+} permeable AMPA receptors, as exposure to 50 µM NAS, a Ca^{2+} permeable AMPA receptor blocker, decreased the time-to-onset in Fura-2 fluorescence 340/380. This was also observed when exposure to AMPA/Kainate receptor antagonist, CNQX, lead to a delay in the time-to-onset in hiPSC-MNs. This can also suggest that Kainate receptors may also be contributing to the observed $[Ca^{2+}]_i$ alterations. Finally, concentration dependent cell death occurs in hiPSC-MNs after MeHg exposure. This was

observed as a delayed effect measured 24 hr after MeHg exposure. At that time fragmentation of neurons was observed at the 1.5 µM MeHg exposure. All the results obtained are consistent with previous findings in cerebellar granule cells and in mouse MNs. However, one difference is the concentrations that led to the observed alterations. In human and mouse MNs low concentrations cause toxicity. This is similar to cerebellar granule cells, the most susceptible neuronal cell to MeHg toxicity. Thus, one question that comes to mind is, what makes these cells less susceptible to MeHg toxicity than cerebellar granule cells at the systemic level?

In conclusion, this study demonstrated that in a human model of MNs (hiPSC-MNs) low concentrations of MeHg lead to 1) MeHg induced increases in $[Ca^{2+}]_i$ in a bi-phasic manner, and these are mediated by AMPA receptors, 2) concentration dependent cell death, 3) neurite fragmentation at 1.5 µM concentration and 4) altered expression of AMPA GluA subunits and ADAR2 RNA editing enzyme. Taken together these results suggest that AMPA receptors are key players in MeHg-induced toxicity in MNs.

CHAPTER FOUR: SUMMARY AND CONCLUSIONS

A) Summary and conclusions

The studies described in this thesis aimed to characterize MeHg mediated effects on AMPA receptors and their role in MeHg-induced Ca^{2+} dysregulation in MNs. MeHg exposure *in vitro* leads to a time- and concentration-dependent increase in $[Ca^{2+}]_i$ in cerebellar granule cells, neuroblastoma cells, and MNs among other cell types (Edwards, Marty, 2005, Hare, McGinnis, 1993, Marty and Atchison, 1997, Ramanathan and Atchison, 2011). MeHg-induced alterations in $[Ca^{2+}]_i$ occur in two distinct kinetic phases. The first phase results from the release of Ca^{2+} from intracellular stores and the second one results from the influx of extracellular Ca^{2+} (Marty and Atchison, 1997). In all cases ligand and voltage gated Ca^{2+} channels (VGCCs) have been identified as key players in these alterations.

These observations led me to design the first set of experiments in which a comparison was made of MeHg effects on ligand and VGCCs. The objective of experiments described in Chapter two was to investigate MeHg effects on gene expression of AMPA, NMDA and VGCC subunits in the cerebellum and brainstem of rats. Comparing the expression of nerve membrane proteins can reveal whether MeHg exposure results in changes in gene expression of nerve membrane proteins for which functional effects occur in brainstem and cerebellum.

In vitro and *in vivo* studies have demonstrated that MeHg alters expression of NMDA receptor subunits (Baraldi, Zanolo, 2002, Liu, Wang, 2009) and this has been identified as possible contributor to MeHg-induced alterations in cognitive functions (Onishchenko et al. , 2007). Also, cell death in the brainstem has been observed after acute MeHg exposure, and this is mediated in part by NMDA receptors, as co-administration of NMDA receptors antagonist MK801 decreased cell death (Miyamoto, Nakanishi, 2001). This has also been observed *in vitro* (Ndountse and Chan, 2008). Taken together these studies suggest that NMDA receptors

contribute to MeHg-induced toxicity in neuronal cell types and that this could be due to the alterations in gene expression that occur. In our study, we observed increases in NR1 and NR2A in the brainstem and NR2C in the cerebellum. This supports the hypothesis that NMDA receptors contribute to MeHg-induced toxicity and should be studied further.

MeHg effects in gene expression levels of VGCCs have not been studied before, and MeHg effects on AMPA receptors is not known. I hypothesized that MeHg effects in gene expression of all the receptors studied were going to be more pronounced in the cerebellum than in brainstem of rats. This mainly due to the known susceptibility of cerebellar granule cells to MeHg toxicity. Since cerebellar granule cell death after MeHg exposure is triggered in part by the alterations in $[Ca^{2+}]_i$ that are mediated by ion channels such as the VGCCs. Although VGCCs contribute to increases in $[Ca^{2+}]_i$ in neuronal cells after MeHg exposure, they are blocked by MeHg irreversibly (Edwards, Marty, 2005, Hajela, Peng, 2003, Hare, McGinnis, 1993, Marty and Atchison, 1997, Peng, Hajela, 2002, Ramanathan and Atchison, 2011). Thus, if these channels are still contributing to MeHg-induced increases in $[Ca^{2+}]_i$ but are also being blocked, it suggests that there could be a compensatory mechanism such as the increase in expression that could be leading to more available channels in the membrane.

Contrary to my hypothesis I found that MeHg effects were more pronounced in brainstem than in cerebellum of rats as significant increases in transcript levels of the channels was noted after almost all levels of exposure. This could indicate that brainstem neuronal populations can compensate for MeHg effects and the cerebellum does not because downregulation in expression of all receptors was predominant in this latter part. A comparative study like this one have not been done before and effects of MeHg on AMPA receptor and VGCC expression has not been identified previously. In summary, the study in chapter two demonstrates that low-dose MeHg

exposure during development alters gene expression levels of ligand and VGCCs and these effects are more pronounced in the brainstem compared to the cerebellum. Further studies that focus on measuring protein levels and perform functional experiments such as electrophysiology would provide additional confirmation to my hypothesis and results.

The study on chapter two could have been strengthened with the addition of several other experiments. Significant alterations in expression of the receptors studied were observed mostly at 30 days of exposure. The addition of time point before (20 – 25 days) and after 30 days could have given us information about how these changes occur. Also, to identify if the changes observed at the gene level correlated with the protein levels would have been a good addition. This could have been done by performing western blot analysis or immunocytochemistry of the proteins studied. If specific changes were to be identified in specific regions of the brainstem, then *in situ* hybridization would have been the best approach. Another approach that could be performed is to isolate the RNA from MNs and cerebellar granule cells from tissue of exposed rats by using laser capture micro dissection. That would allow identification of gene expression changes specifically in the cells of interest.

Experiments described in chapter three demonstrated that acute MeHg exposure leads to cell death of hiPSC-MNs, increases in $[Ca^{2+}]_i$ in a bi-phasic manner, and alterations in gene expression of AMPA receptor subunits and the RNA editing enzyme ADAR2. The most important finding of that chapter was that MeHg-induced alterations in hiPSC-MNs are mediated by Ca^{2+} permeable AMPA receptors.

The importance of those findings are the applications they can have to study gene x environment interaction relationship between MeHg and ALS. MeHg accelerated the onset of ALS like symptoms in a mouse model with a genetic predisposition to the disease (SOD1G93A)

(Johnson, Yuan, 2011). This suggested a possible gene x environment interaction. This has been suggested previously in other studies due to the similarities between the mechanism of toxicity of MeHg and the mechanism observed in ALS patients (Johnson, Yuan, 2011, Praline, Guennoca, 2007, Roos, Vesterberg, 2006, Sutedja, Veldink, 2009) (Table. 4.1). Thus, to demonstrate that hiPSC-MNs are indeed susceptible to MeHg toxicity and that the alterations in Ca^{2+} are mediated by AMPA receptors solidifies that hypothesis further.

Table 4.1. Comparison of mechanisms underlying toxicity in ALS and MeHg.

Mechanisms of toxicity	
Amyotrophic Lateral Sclerosis (ALS)	**Methylmercury (MeHg)**
Increase in glutamate release (Cleveland, Rothstein, 2001)	Increase in glutamate release (Yuan, Atchison, 2007)
Increase in $[Ca^{2+}]_i$ (Cleveland, Rothstein, 2001)	Increase in $[Ca^{2+}]_i$ (Ramanathan, Atchison, 2011, Limke, Heidemann, 2004)
Mitochondrial damage (Cleveland, Rothstein, 2001)	Mitochondrial damage (Limke, Atchison 2002)
Increase in ROS (Cleveland, Rothstein, 2001)	Increase in ROS (Aschner, Syversen, et al., 2007)
Impaired function of astrocyte transporter EAAT2 (Cleveland, Rothstein, 2001)	Impaired function of astrocyte transporter EAAT2 (Aschner, Yao, et al., 2000)

a. Relevance of dissertation results to amyotrophic lateral sclerosis

ALS is a chronic motor neuron disease characterized by the degeneration of α and γ MNs from the motor cortex and spinal cord (Cleveland, Rothstein, 2001). Degeneration of these MNs leads to muscle weakness, atrophy and spasticity. The disease occurs mostly in adults over 50-60 years old. However, there are reported cases in young adults (Haley, 2003). After diagnosis, the patient's survival time is approximately five years, and in most cases, death is due to respiratory failure (Cleveland, Rothstein, 2001). Currently there is no effective treatment for the disease and the only FDA-approved treatment (Riluzole), only prolongs the life of the patient by approximately three months (Bellingham, 2011).

ALS affects more than 30,000 Americans and it is estimated that 5,600 people are diagnosed each year. Familial form of ALS (FALS) occurs through dominant inheritance mutations, including several mutations in superoxide dismutase 1 (*SOD1*) (Swarup and Julien, 2011). Sporadic ALS (SALS) is not inherited, however approximately 10% of cases express mutations in SOD1 (Pasinelli and Brown, 2006, Swarup and Julien, 2011). In both forms of ALS the mechanism of disease and the phenotypic changes are indistinguishable. Mechanisms of pathogenesis in ALS include increased protein aggregation, increased formation of reactive oxygen species, impairment of the astrocytic excitatory amino acid transporter 2 (EAAT2), increased glutamate in the synapse (glutamate excitotoxicity), over activation of the glutamate AMPAR, Ca^{2+} dysregulation and mitochondrial dysfunction (Pasinelli and Brown, 2006). Almost all of these mechanisms have been identified using rodent models, especially the mouse expressing the mutant SOD1-G93A (which has an amino acid substitution of glycine to alanine at residue 93), a mutation that leads to a toxic gain of function (Gurney, 1994). SOD1 is a Cu/Zn^{2+} superoxide dismutase that is ubiquitously expressed in all cells. Mutations in SOD1

comprise 20% of all FALS mutations and 2-3% of all ALS cases (Swarup and Julien, 2011). However, the causative factor for SALS and the progression of FALS by which overexpression of SOD1-G93A leads to motor neuron cell death is still not known. For 90% of ALS cases there is no identifiable cause or genetic bases. It is believed that gene x environment interactions could be contributing to the development of the disease (Morahan, Yu, Trent, et al., 2007, Migliore, Coppede, 2009). However, human epidemiological studies have not unequivocally identified a particular environmental causative agent for ALS, except for the Chamorro natives of Guam for which an excitatory amino acid found in the food was causative (Armon, 2003). Although there is this gap in ALS research, environmental toxicants are still considered possible contributors to the development of ALS. Environmental toxicants such as lead and mercury are some of the most commonly identified as candidates for gene x environment interaction due to their prevalence in the environment, mechanism of toxicity and several reported case studies (Johnson, Yuan, 2011, Praline, Guennoca, 2007, Roos, Vesterberg, 2006, Sutedja, Veldink, 2009).

The study that demonstrated a possible gene x environment correlation of MeHg in the onset of ALS used the SOD1-G93A mouse model. In these mice exposure to low dose MeHg led to an early onset of ALS phenotype measured as motor dysfunction in the rotorod performance test (Johnson, Yuan, 2011). This study also showed that MeHg exposure leads to increases in $[Ca^{2+}]_i$ in brainstem MNs that were mediated in part by AMPA receptors. The results presented in chapter three demonstrate that low dose MeHg exposure leads to a concentration dependent cell death, increases in $[Ca^{2+}]_i$ that are mediated by AMPA receptors and alterations in the AMPA receptor expression in human MNs. Thus, if this is the case in normal humans MNs, in a population that has a predisposition to ALS due to mutations, degeneration of these cells may

occur faster when exposed to MeHg. This should be the goal of future studies. *In vitro* experiments should be performed using hiPSC-MNs derived from ALS patients or ones that are made with techniques such as CRISPR Cas9 that present the SOD1G93A or a different ALS mutation. Using these cells effects of MeHg should be characterized and identification of cell death, alterations in $[Ca^{2+}]_i$ and the role of AMPA receptors should be addressed to identify if the mechanism of cell death occurs in a similar way as it has been observed in normal hiPSC-MNs exposed to MeHg. The results from those studies would give a better idea of the contribution of MeHg to the development of ALS and its potential identification as a gene x environment contributor to the development of this disease. However, to identify if that is the case effects have to be identified at the systemic level. One way this could be done *in vitro* is by using co-cultures of hiPSC-MNs and astrocytes or myotubes. Based on the results from this dissertation and the information in the literature I believe that MeHg effects in MNs can have an additive effect in ALS predisposed populations and this could have been the case in the mouse study performed using the SOD1-G93A mouse model.

In this dissertation, I have demonstrated that acute or chronic MeHg exposure alters gene expression of AMPA receptors and their RNA editing enzyme ADAR2 using three different models, suggesting that these alterations occur and can be contributing to MeHg toxicity. I also demonstrated **for the first time** that in a human model of MNs MeHg disrupts $[Ca^{2+}]_i$ in a bi-phasic manner and that AMPA receptors are contributing to these alterations.

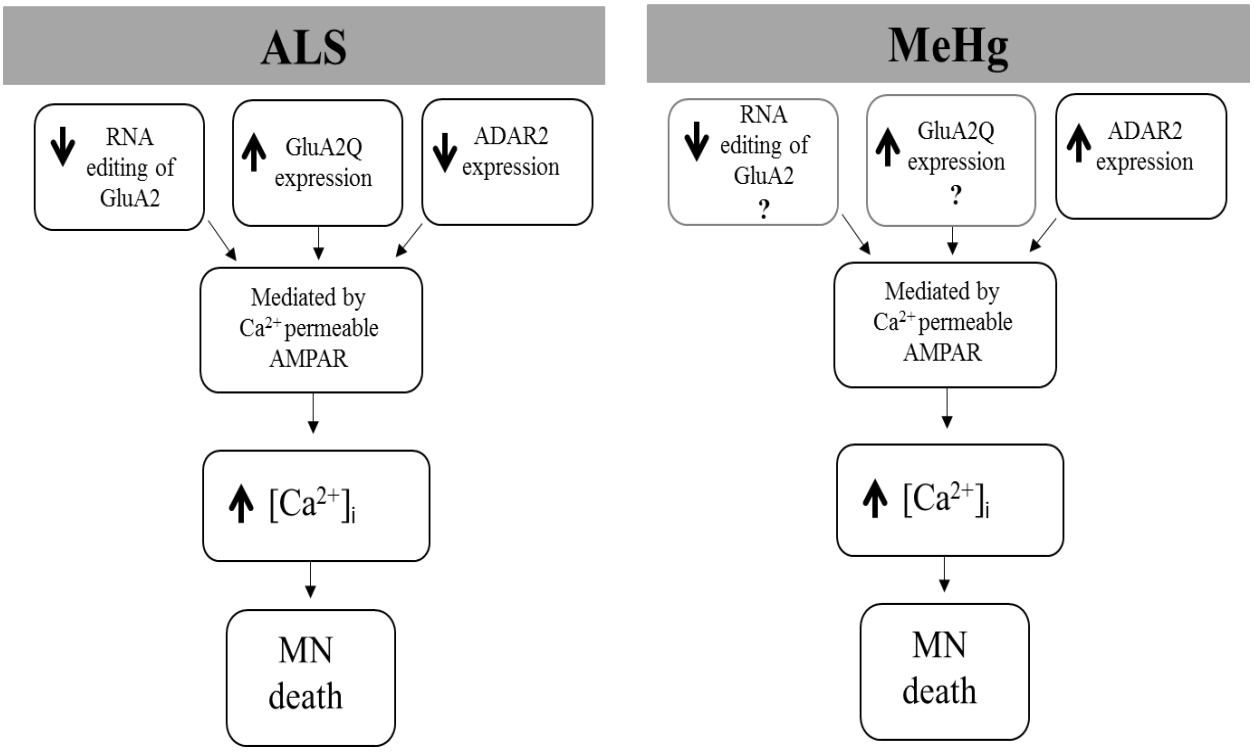

Figure 4.1. Role of AMPAR in ALS and MeHg toxicity on MNs. In ALS, AMPAR contribute to the alterations in intracellular Ca^{2+} observed in MNs (Kwak, Kawahara, 2005, Kwak, 2010). This effect is in part due to the decrease in RNA editing of the GluA2 subunit (Kwak, Kawahara, 2005, Takuma, 1999), which results in the unedited form of GluA2 (GluA2Q) containing receptors in MNs. This is one of the mechanisms that contribute to MN cell death in ALS (Cleveland, Rothstein, 2001). MeHg-induced Ca^{2+} dysregulation in MNs is also mediated in part by Ca^{2+} permeable AMPAR. This was observed in a mouse model of ALS (Johnson, Yuan, 2011), in primary MNs from mouse (Ramanathan and Atchison, 2011), and here in chapter three using hiPSC-MNs. The work from chapter three of this dissertation shows for the first time that in human MNs there is a decrease in all the GluA subunits after 0.2- 1.5 µM MeHg and an increase in ADAR mRNA levels. Also, that MeHg increases intracellular Ca^{2+} through Ca^{2+} permeable AMPAR and that low concentrations of MeHg (0.1 – 1.5 µM) lead to cell death of this cell type *in vitro*. These results suggest a similar mechanism of toxicity of MeHg on human MNs compared to ALS contributing to the hypothesis that if there is a genetic predisposition to the disease (ALS), exposure to MeHg can have an additive effect and accelerate MN cell death. This should be the focus of future studies.

APPENDIX

BRIDGE TO NEUROSCIENCE WORKSHOP: AN EFFECTIVE EDUCATIONAL TOOL TO INTRODUCE PRINCIPLES OF NEUROSCIENCE AND REINFORCE PARTICIPATION OF HISPANIC STUDENTS IN NEUROSCIENCE-RELATED RESEARCH

Alexandra Colón-Rodríguez,[1,2#] Chelsea T. Tiernan,[3] Eileen S. Rodríguez-Tapia,[4] & William D. Atchison[1,2]

[1]Comparative Medicine and Integrative Biology Program, College of Veterinary Medicine, Michigan State University, East Lansing, Michigan, United States of America

[2]Department of Pharmacology and Toxicology, College of Veterinary Medicine, Michigan State University, East Lansing, Michigan, United States of America

[3]Department of Translational Science & Molecular Medicine, College of Human Medicine, Michigan State University, Grand Rapids, Michigan, United States of America

[4]Neuroscience Program, College of Natural Science, Michigan State University, East Lansing, Michigan, United States of America

*Corresponding author
E-mail: atchiso1@msu.edu (WDA)

[#]Current address: University of California Davis Genome and Biomedical Sciences Facility, 451 Health Sciences Dr., Room 4617A, Davis, CA 95616. United States

A) Abstract

Neuroscience as a discipline is rarely covered in educational institutions in Puerto Rico. In an effort to overcome this deficit we developed the Bridge to Neuroscience Workshop (BNW), a full-day hands-on workshop in neuroscience education. BNW was conceived as an auxiliary component of a parent recruitment program called Bridge to the PhD in Neuroscience Program (BPNP). The objectives of BNW are to identify promising students for BPNP, and to increase awareness of neuroscience as a discipline and a career option. BNW introduces basic concepts in neuroscience using a variety of educational techniques, including mini-lectures, interactive discussions, case studies, experimentation, and a sheep brain dissection. Since its inception in 2011 BNW has undergone a series of transformations that continue to improve upon an already successful and influential educational program for underrepresented minorities. As of Fall 2016, we have presented 21 workshops, impacting 200 high school and 424 undergraduate students. BNW has been offered at University of Puerto Rico (UPR)-Arecibo, UPR-Cayey, UPR-Humacao, Pontificia Universidad Católica de Ponce, and Universidad Interamericana de Puerto Rico-Arecibo. A pre-and post evaluation was given to evaluate material comprehension and thus measure effectiveness of our one-day interactive workshop. Our results suggest that both high school and undergraduate students have little prior knowledge of neuroscience, and that participation in BNW improves not only understanding, but also enthusiasm for the discipline. Currently, our assessment has only been able to evaluate short-term effects (e.g. comprehension and learning). Therefore, our current focus is developing methods capable of determining how participation in BNW impacts future academic and career decisions.

B) Introduction

The lack of ethnic diversity in neuroscience is a persistent problem. Most minority groups, including Hispanics, are underrepresented at all levels of higher education academic pipeline as compared to their corresponding representation in the U.S. population. In 2013 the National Science Foundation reported a total of 795 doctorate recipients in the field of neuroscience corresponding to US citizens and permanent residents. Hispanics comprised only 7.8% of degree recipients, but encompass 17.1% of the U.S. population (US Census, 2014). This discrepancy becomes more pronounced at the level of tenured and tenure-track faculty. Among the top 100 U.S. biological science departments, Hispanics account for only 4.3%, 2.6%, and 1.8% of assistant, associate, and full professors, respectively (Nelson , 2010). This lack of ethnic diversity is of significant consequence. As a scientific community, we are losing critical talent and diverse perspectives that enhance creativity and innovation in scientific endeavors. If not remedied, underrepresentation of minorities could contribute to the loss of our country's global technical and intellectual leadership.

One strategy to tackle the underrepresentation of minorities in neuroscience is community outreach and science education targeting specific minority populations during the formative stages of their academic scholarship. The University of Puerto Rico (UPR) public collegiate system is an ideal population of Hispanic students from which to recruit future neuroscientists. UPR consists of 10 sub-graduate campuses located throughout the Commonwealth of Puerto Rico, a U.S. territory in the northeastern Caribbean. Between 2009 and 2013, UPR became the 2nd leading university to award doctoral degrees to Hispanic recipients (Flegener , 2013). Despite this achievement, exposure to neuroscience at the collegiate level in the UPR system remains low. A search of UPR curricular offering through the official UPR webpage reveals that only 2

of the 9 campuses that grant bachelor of science degrees offer a course specifically in neuroscience: UPR-Cayey and UPR-Rio Piedras. UPR-Rio Piedras has a National Institute of Health Enhancing Neuroscience Diversity through Undergraduate Research Education Experiences (NIH-ENDURE) program since 2011 which provides research opportunities in neuroscience to students in their institution. Outside of the UPR system, there are 2 private institutions with a neuroscience course as part of their bachelor of science curriculum: University of Turabo and Pontifical Catholic University of Puerto Rico. In 2015 the Central University of Bayamon established a Bachelor's Degree in Neuroscience, making it the first and only undergraduate institution in Puerto Rico with an academic program specializing in neuroscience. More recently, 2016, NeuroBoricuas was launched as a program that provides workshops in neuroscience related topics to K-12 and the community in general.

The extent to which neuroscience-related courses are offered in K-12 educational curricula in Puerto Rico may also contribute to the scarcity of Hispanic representation in the neurosciences. The public K-12 Science Program in Puerto Rico focuses on the scientific method and understanding the rationale for this process of investigation. The program classifies the sciences into four domains: life, physical, terrestrial, and spatial. Core concepts from each domain are first introduced at the elementary level, and then expanded upon at the intermediate and high school levels. Although it is plausible that specific science courses cover concepts in neuroscience, these topics would most likely be introduced superficially at the high school level. Students attending a subset of public magnet schools for science and mathematics have the highest likelihood of exposure to the neurosciences. These institutions offer more advanced science disciplines, such as organic and inorganic chemistry, genetics, microbiology, biochemistry, human anatomy and physiology. Therefore, although these schools still do not offer a specific

course for neuroscience, basic concept in neuroscience are undoubtedly introduced (Author's Note: This information was obtained from the official public policy about the organization and curricular offering for the Science Program in elementary, intermediate and superior levels of public schools in Puerto Rico) (RicoDpEdP, 2014).

Taken together this information suggests that neuroscience as a discipline is rarely covered in educational institutions in Puerto Rico. In an effort to overcome this omission, we developed the Bridge to Neuroscience Workshop (BNW), a full-day hands-on workshop in neuroscience education. The BNW was conceived as an auxiliary component of a parent recruitment program called Bridge to the PhD in Neuroscience Program (BPNP). BPNP was developed by Dr. William D. Atchison at Michigan State University in 2010 after 12 years of collaboration with the UPR-Cayey. BPNP is a 4-year program spanning the final two years of undergraduate studies and the first two years of graduate studies. BPNP aims to provide professional development, neuroscience related research experience, increased awareness of neuroscience as a prospective discipline, and facilitate top-down student-directed mentorship.

As a supplement to BPNP, BNW was designed to identify promising students for BPNP, and to increase awareness of neuroscience as a discipline and a viable career option. BNW, in collaboration with BPNP, has helped identify and recruit promising students since its inception in 2011. The purpose of this article is to (1) provide educators and students with access to the BNW educational materials to continue neuroscience education; and (2) provide evidence demonstrating the effectiveness of BNW as a tool to engage high school and undergraduate students in neuroscience education and reinforce student participation in neuroscience-related research. As such, we first describe the components of BNW including educational materials and activities. Secondly, we evaluate previous participants' performance on pre- and post-

evaluations, discuss participant feedback, and report participants' subsequent research-related activities.

Bridge to Neuroscience Workshop

BNW was designed by nine graduate students at Michigan State University, under the direction of Dr. William D. Atchison. These graduate students wrote a grant to obtain funding for workshop materials and travel expenses, designed lecture and activity materials, and wrote the accompanying workbook. Additionally, most of these graduate students traveled to Puerto Rico on at least one occasion to lead the workshop.

Content description

BNW is comprised of: a) a written entrance evaluation given upon arrival to assess students' prior knowledge of neuroscience; b) the workshop, which includes 4 sessions: 1) "Getting to Know Your Nervous System", 2) "Your Nervous System at Work", 3) "Common Diseases of the Nervous System", and 4) "Sheep Brain Dissection"; and c) an exit evaluation given to assess comprehension of material discussed throughout the day.

Entrance and Exit Evaluation

The entrance and exit evaluations are described in the methods section below.

Workshop Session 1: getting to Know Your Nervous System

The workshop begins with a session entitled "Getting to Know Your Nervous System", in which basic concepts of the central nervous system are taught through mini-lectures and interactive activities. First, a "Matching Activity" uses comparative neurobiology to discuss gross anatomical features of the brain. Students correlate anatomical features with function to identify the brains of eight different animals. Next students model the basic structure of a neuron

in the “Giant Rope Neuron” activity. Then students utilize their working model to perform action potentials and synaptic transmission. In the final activity of the first session, students explore basic electrophysiology associated with action potentials using the SpikerBox (Marzullo & Gage, 2012), a device that allows students to visualize and listen to action potentials firing from the leg of a cockroach.

Workshop Session 2: Your Nervous System at Work

The second session, “Your Nervous System at Work”, is an experiment-driven exploration of the sensory, motor, and autonomic systems, which expands upon the concepts introduced during Session 1. Students learn how to formulate testable hypotheses, design experiments, make observations, and report results. “Tasting With Your Nose” examines the hypothesis that sensory systems integrate to produce particular perceptual experiences, in this case taste. “Reaction Time” investigates how the central nervous system assimilates sensory input to regulate movement. Finally, “Experimentation with Blood Pressure”, gives students an opportunity to formulate their own unique hypotheses, and design experiments to test how specific environmental factors (e.g. caffeinated drinks, exercise, relaxation, etc.) modulate blood pressure.

Workshop Session 3: Common Diseases of the Nervous System

The third session includes a mini lecture and case studies for the identification of “Common Diseases of the Nervous System”. In this session students learn about the symptoms, mechanism of pathogenesis, pathology, diagnosis and treatment of Parkinson’s disease, Alzheimer’s disease, Amyotrophic Lateral Sclerosis and stroke. The session starts with a brief lecture on the symptoms and pathology of each neurological disease, once finished the students are assigned a case study (1 per group of 5 students) and charged with identifying the neurological disease. A

closing discussion explains mechanisms of pathogenesis and available treatments for each disease.

Workshop Session 4: Sheep Brain Dissection

The final session of the workshop is the "Sheep Brain Dissection". The sheep brain dissection is an opportunity for students to explore a real brain. Participants are able to identify the structures of the brain discussed throughout the day and also perform dissections in order to identify internal structures.

Educational materials

In addition to workshop discussions and activities, a workbook is used throughout the workshop sessions to supplement oral lessons and engage the students. This booklet contains a summary of all the topics covered in the workshop, including organization of the nervous system, structure and function of neurons, generation and propagation of action potentials, synaptic transmission, sensation, movement, autonomic function, and diseases of the nervous system. There are descriptive figures, thought-provoking questions, and space available for data collection and observational notes associated with each activity or experiment.

Importantly, the workbook is written in English and Spanish to facilitate the understanding of material for students who are not fluent in English. BNW is conducted entirely in English in order to give students an opportunity to practice using the language in an academic setting. However, because most of the material is novel and challenging, without the aid of the Spanish workbook, attendee's comprehension and ultimately their engagement in the workshop may have been hindered. At the end of the day, workshop attendees are encouraged to take their workbook home as an educational resource.

C) Methods

General Description

From the years of 2011 to 2016 a total of 21 workshops have been conducted at five different sub-graduate institutions in Puerto Rico. The five institutions that have served as hosts for BNW are: University of Puerto Rico at Cayey (UPR-Cayey) and University of Puerto Rico at Arecibo (UPR-Arecibo), University of Puerto Rico at Humacao (UPR-Humacao), Pontifical Catholic University of Puerto Rico in Ponce and Universidad Interamericana de Puerto Rico in Arecibo (Fig. A.1). The workshops were conducted Saturday, Sunday or Monday (normal school day) from 9:00 am to 5:00 pm.

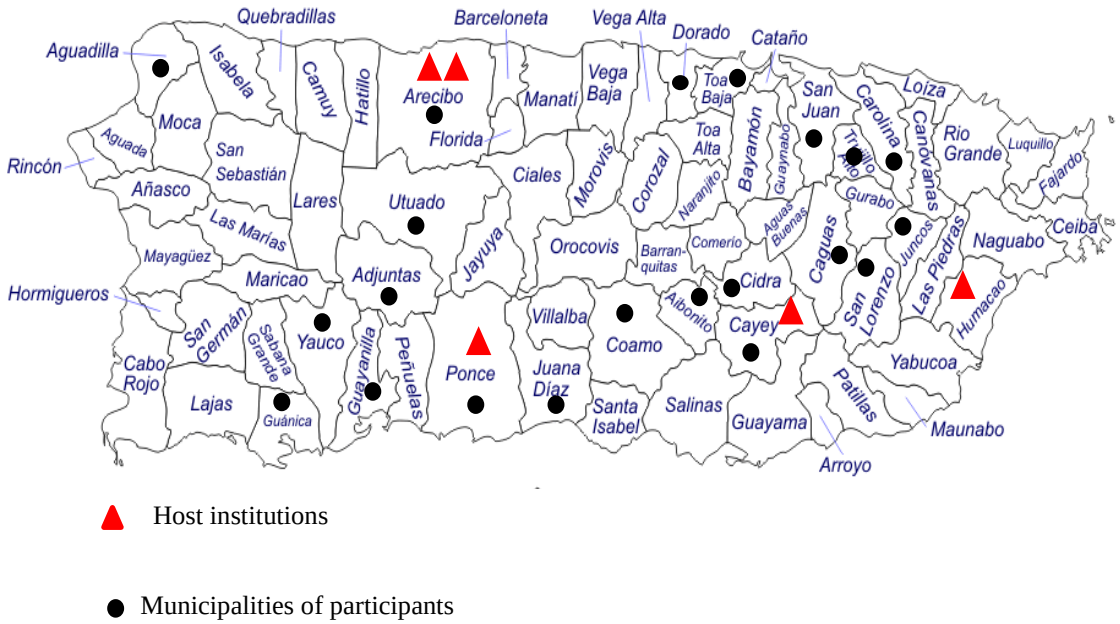

Figure A.1. Map of Puerto Rico indicating the municipalities of BNW participating institutions. The municipalities of Arecibo, Cayey, Humacao and Ponce have hosted the 21 previously conducted workshops. The undergraduate institutions that served as hosts are; the University of Puerto Rico-Arecibo, Universidad Interamericana de Puerto Rico-Arecibo, University of Puerto Rico-Cayey, University of Puerto Rico-Humacao, and the Pontificia Universidad Católica de Ponce. High schools from 12 different municipalities have participated in the workshops.

Participants and Volunteers

BNW participants included both high school and undergraduate students. High school participants were recruited by contacting science teachers employed at local schools surrounding host institutions and by word of mouth. Undergraduate participants were recruited primarily from the host institutions, through our website (www.bridgetoneuroscienceworkshop.com) and Facebook page (Bridge to the PhD in Neuroscience). However, announcements were also made at neighboring collegiate institutions to encourage additional undergraduate participation. Recruited students were required to submit a signed parental authorization form through the program email prior to participation. High school science teachers from invited schools were strongly encouraged to participate by providing a certification of workshop completion and a monetary compensation.

Each workshop accommodated up to 30 students, and the same workshop was conducted for high school or undergraduate students, however high school and undergraduate student populations were never mixed. Participants were divided into small laboratory groups of 4-5 students. Embedded within each laboratory group was an undergraduate Puerto Rican student who had either previously attended BNW as a participant, or was currently enrolled in the parent BPNP. These advanced undergraduate students ensured that workshop participants understood the material being presented and assisted participants with BNW activities and experiments. Workshops were led by 3-4 graduate students recruited from the Michigan State University Neuroscience Program, the Department of Pharmacology & Toxicology, and the Comparative Medicine & Integrative Biology Program. These graduate students introduced the sessions with mini-lectures, demonstrated activities, and facilitated group discussions.

Feedback from participants

Evaluations

All participants were given 15 minutes to complete a short evaluation at the beginning (pre-test) and at the end (post-test) of the workshop. The tests consisted of 11 multiple choice and short answer questions addressing recall and comprehension of the discussed material. The following core concepts were assessed: unique structure and function of brain and neurons, generation and conduction of electrical signals, synaptic transmission, perception and integration of sensory stimuli, and role of autonomic nervous system in the control of fight-or-flight response. Evaluations were scored blinded to student ID as well as to the pre- and post-test score. Differences in the mean percentage of correct, incorrect, and incomplete responses between pre- and post-tests within high school and undergraduate students were compared and statistical significance was determined using two-way analysis of variance (ANOVA). When the omnibus test met the criterion for significance Sidak's post-hoc test was used to make all possible comparisons. All tests were two-tailed, and the criterion for significance was set at $p < 0.05$. GraphPad Prism 6 software (GraphPad software, Inc.) was used for all statistical tests.

Feedback Form

Feedback forms were administered at the end of the workshop to gauge interest and seek recommendations. These forms were purposefully short and open-ended, asking participants to describe two things that they liked from the workshop and one thing that they would change ("Two Stars and a Wish"). Feedback and pre- and post-test evaluation responses were anonymous; no personal information was gathered from any participant in any of the conducted workshops.

D) Results

In order to identify students' knowledge and understanding of neuroscience prior to the workshop and after the workshop an entrance (pre-test) and exit evaluation (post-test) was given. The evaluations had the same questions in order for us to make a direct comparison of the understanding of the neuroscience concepts taught, before and after the workshop. Evaluations were given in all 21 workshops and the responses from 129 high school and 303 undergraduate students are presented in Fig A.2-3.

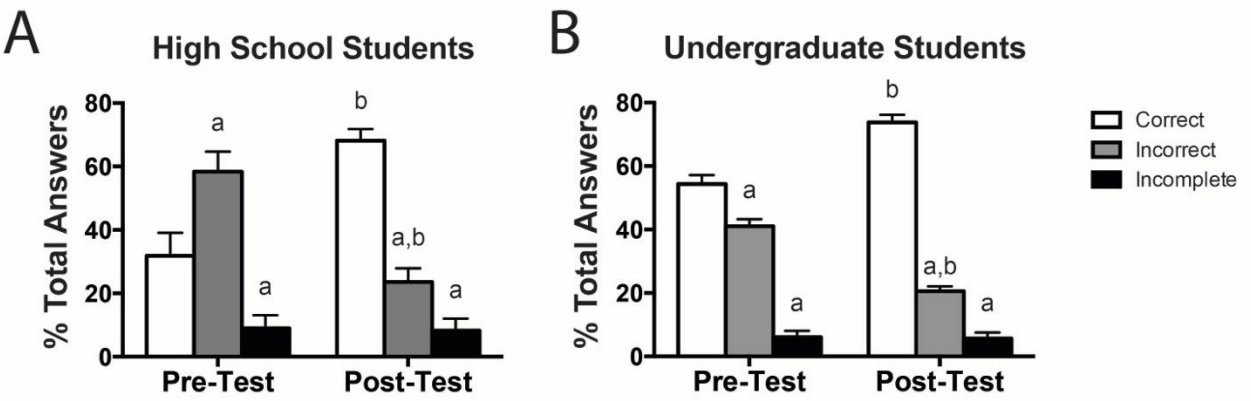

Figure A.2. Uneven distribution of knowledge about neuroscience between undergraduate and high school students prior to BNW. (A) High school students had a significantly higher mean percentage of incorrect answers. After the BNW correctly answered questions increased significantly for High school (A) and undergraduate students (B). Incomplete answers did not differ significantly between the pre- and post-test for either high school (A) or undergraduate students (B). The error bars represent the standard error of the mean (SEM) of an N = 129 high school and N = 303 undergraduate students.

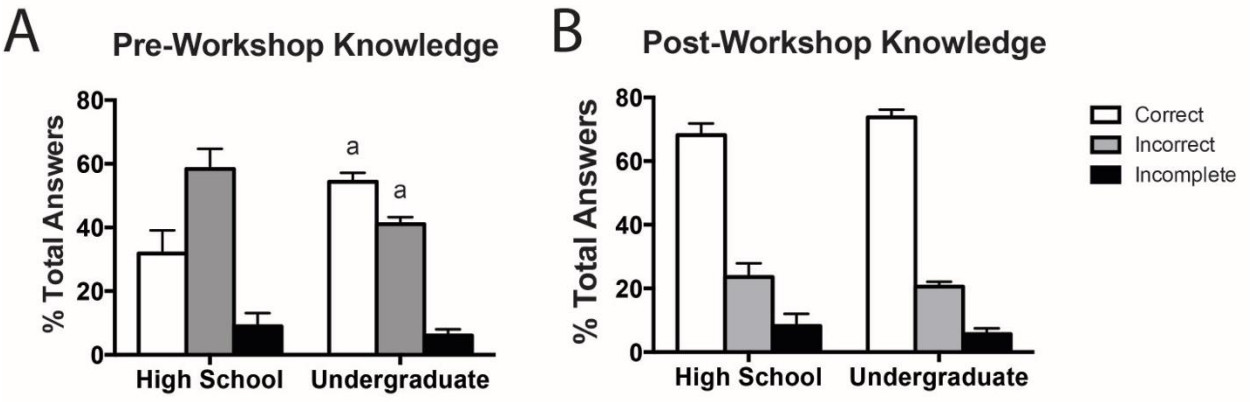

Figure A.3. Completion of BNW increased percentage of correct answers for both high school and undergraduate students. Prior to BNW high school students had a greater number of incorrect answers compared to undergraduate students (A). Completion of BNW significantly increased mean percentage of correct answers in both high school and undergraduate students (B). The distribution of correct answers in high school and undergraduate students was not different after completion of BNW (B). The error bars represent the standard error of the mean (SEM) of an N = 129 high school and N = 303 undergraduate students.

Pre- and Post-test evaluations

High school participants answered significantly more questions incorrectly (58.4 ± 6.3%) than correctly (31.8 ± 7.2%; p=0.003) on the pre-test, and left 9.0 ± 4.1% of pre-test questions incomplete (Fig. A.2A). Conversely, undergraduate participant's answered 54.4 ± 2.8% of the total questions correctly and 41.0 ± 2.2% incorrect (p=0.0001), leaving 6.0 ± 2.0% incomplete (Fig. A.2B).

Post-test responses were used to assess participants' comprehension of material discussed during the workshop. After attending BNW, the mean percentage of correctly answered questions increased from 31.8 ± 7.2% (pre-test) to 68.2 ± 3.7% (post-test) for high school students ($p<0.0001$; Fig. A.2A), and from 54.4 ± 2.8% (pre-test) to 73.8 ± 2.4% (post-test) for undergraduate students ($p<0.0001$; Fig. A.2B). Accordingly, the mean percentage of incorrectly answered questions on the post-test decreased from 58.4 ± 6.3% (pre-test) to 23.6 ± 4.3% (post-test) for high school students (p=0.0001; Fig. A.2A) and from 41.0 ± 2.2% (pre-test) to 20.6 ± 1.5% (post-test) for undergraduate students ($p<0.0001$; Fig. A.2B). The mean percentage of incomplete answers did not differ significantly between the pre- and post-tests for either high school (8.9 ± 4.1% (pre-test) vs. 8.2 ± 3.8% (post-test); $p>0.05$) or undergraduate students (6.0 ± 2.0% (pre-test) vs. 5.6 ± 1.9% (post-test); $p>0.05$).

High school and undergraduate participant performance on pre- and post-test evaluations

Comparison of high school and undergraduate participant pre-test performance revealed significant differences in prior knowledge between these cohorts (Fig. A.3A). Undergraduate students scored significantly more questions correctly on the pre-test (54.3 ± 2.8%) as compared to high school students (31.8 ± 7.2%; p=0.0002). As such, the mean percentage of incorrect answers on the pre-test was significantly higher for high school students (58.4 ± 6.3%) than

undergraduate students (41.0 ± 2.2%; p=0.005). There was no difference in the mean percentage of incomplete pre-test responses between high school (8.9 ± 4.1%) and undergraduate students (6.0 ± 2.0%; p>0.05).

Post-test high school and undergraduate performance was very similar (Fig. A.3B). There was no significantly difference between the cohorts for the mean percentage of correct answers (68.2 ± 3.7% (high school) vs. 73.8 ± 2.4% (undergraduate); p>0.05), incorrect answers (23.6 ± 4.2% (high school) vs. 20.6 ± 1.5% (undergraduate); p>0.05), or incomplete answers (8.2 ± 3.8% (high school) vs. 5.6 ± 1.9% (undergraduate); p>0.05).

A representation of one pre- and post-test answer is shown in Fig. A.4. This question aimed to address understanding of the unique structure and function of neurons by asking the student to draw a model of a neuron including structures used for sending and receiving information. In the pre-test evaluation, the student had only a vague interpretation of a neuron. The student's response during the post-test evaluation illustrates a much more comprehensive understanding of the structure and function of a neuron.

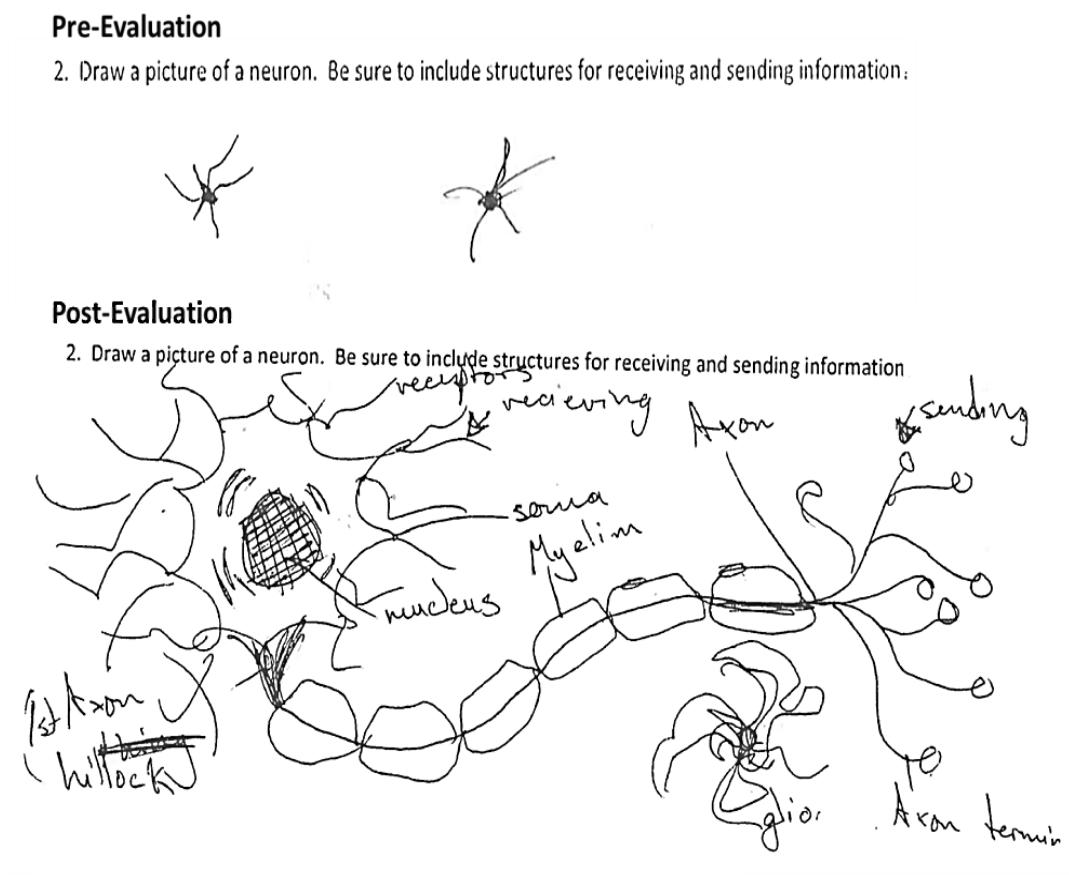

Figure A.4. Representative response of a BNW participant. These drawings are the answer of a BNW participant to a question addressing understanding of the unique structure and function of neurons concept. The question is as follow: *Draw a picture of the neuron. Make sure to include structures for receiving and sending information.*

Feedback Form Results

Our feedback form, "Two Stars and a Wish", asked participants to describe two aspects of the workshop they enjoyed or found interesting, and one thing they would have changed. Responses from 336 students are summarized in Table A.1. Participants enjoyed the hands-on experiments and activities (18%), liked the lecture topics (12%) and the interactive nature of the workshop (12%). Recommended changes included the suggestion to divide the workshop and have shorter lectures (14%), add more case studies for the "Common Diseases of the Nervous System" activity (11%), and implementing follow-up workshops (10%). Importantly, 21% of attendees indicated they would not change anything about the workshop. These responses and suggestions are being taken into consideration as we continue to modify the content for future workshops.

Table A.1. Most common two stars and a wish response from 336 students.

Two Stars and a Wish	Comment from students	%
Two things they liked from BNW	Enjoyed the experiments & activities	18.3
	Like the lecture topics	12.8
	Llike the interactive, dynamic nature of the workshop	12.1
	Explanations were easy to understand/ Well organized	10.1
	Loved the dissection of the brain	9.8
	Like the neurological disease lecture and case studies	7
	Like the enthusiasm and energy of the presenters, knowledge of presenters	6.3
	Like the giant rope neuron activity	4.6
	Thought there was a good distribution of time and the workshop was well organized	1.9
	Like the jelly bean activity	1.7
One thing they would change	Would not change anything	21.2
	Divide the workshop and have shorter lectures	13.6
	Add more case studies of neurological diseases	11.2
	Increase the number of workshops, a whole series of workshops instead of only one day	10.4
	Add more hands on activities	10
	Use brains from different species for the brain dissection activity	5.2
	Would like to see a real human brain	3.2
	Change the language to Spanish	2.8
	Talk about the summer opportunities at Michigan State University	2.4
	Allow more more time for participants to perform the brain dissection	2

BNW Participant Impact

Twenty-one workshops have been implemented during 12 different weekends between the years of 2011-2015. In that time, 200 high school students from 35 different schools and 424 undergraduate students from more than 10 different institutions have attended BNW (Table A.2). In addition, 20 high school teachers participated with their respective schools. Summary of participants is shown in Table A.2.

Our effort has contributed to the recruitment of 64 students into the parent BPNP Summer Program including the 5 undergraduate students enrolled in BPNP post-baccalaureate program, and the 23 students currently in graduate school at MSU and elsewhere.

Table A.2. Schools and undergraduate institutions participating in BNW from 2011-2015.

Year	Date	Host institution	Teacher attendees	High school (HS) or undergraduate (U) attendees	Total participants
2011	24-Sep	UPR-Cayey	5	HS	25
	25-Sep	UPR-Cayey	5	HS	25
2012	18-Feb	UPR-Cayey	4	HS	25
	19-Feb	UPR-Cayey	1	HS	25
	20-Feb	UPR-Cayey	0	U	25
	Fall	UPR-Arecibo	0	U	20
	Fall	UPR-Arecibo	0	U	20
2013	27-Apr	UPR-Cayey	0	U	25
	28-Apr	UPR-Arecibo	0	U	25
	21-Sep	UPR-Cayey	0	U	25
	22-Sep	UPR-Cayey	0	U	25
2014	13-Dec	UPR-Cayey	0	U	14
	14-Dec	UPR-Cayey	1	11 HS/ 11 U	23
2015	28-Feb	UPR-Humacao	2	HS	30
	28-Feb	UPR-Humacao	0	HS	32
	1-Mar	UPR-Humacao	0	U	25
	1-Mar	UPR-Humacao	0	1 HS/ 27 U	28
	10-Apr	Pontificia Universidad Católica de Ponce	0	U	19
	10-Apr	Pontificia Universidad Católica de Ponce	0	U	23
	11-Apr	Pontificia Universidad Católica de Ponce	2	13 HS/ 9 U	22
	11-Apr	Pontificia Universidad Católica de Ponce	0	5 HS/ 16 U	21
	9-May	Universidad Interamericana de Arecibo	0	U	22
	9-May	Universidad Interamericana de Arecibo	0	8 HS/ 12 U	20
	11-May	UPR-Arecibo	0	U	25
	21-Nov	Pontificia Universidad Católica de Ponce	0	U	31
	22-Nov	UPR-Cayey	0	U	25
Totals:	21 workshops	5 undergraduate host institutions	20	200 HS/ 424 U	624 total participants

E) Discussion

The lack of diversity in the neurosciences is well documented (Weekes, 2012), and poses a significant hindrance to the innovation of our research, the progress of our field, and the societal impact of our discoveries. Collectively, the neuroscience community is responsible for developing engaging solutions to encourage the participation of underrepresented minorities in the neurosciences, and science in general. With this in mind, we developed BNW. Our results demonstrate that a one-day, hands-on workshop is an effective tool for increasing awareness of neuroscience as a discipline and potential career option. Seventeen of BNW participants have continued on to graduate school where they are pursuing degrees in neuroscience-related fields. In addition to documenting the impact of BNW, we have detailed the structure of our workshop and provided open access to all of the educational materials used for BNW so that other educators and outreach coordinators may build upon our ideas to continue diversifying the sciences.

Results of the pre- and post-evaluations revealed that completion of BNW improves comprehension of neuroscience in both high school and undergraduate students. Prior to attending the workshop, most participants had only superficial exposure to core neuroscience concepts. BNW successfully improved comprehension of many basic facets of the neurosciences, as determined by improved performance on post-evaluation scores as compared to pre-evaluation scores. The observation that a one-day interactive workshop enriched participants' comprehension of neuroscience principles is remarkable, and demonstrates that BNW is an effective learning tool. However, one limitation to the present analysis is the truncated timeline for evaluating learning. At present, we do not have the resources or infrastructure necessary to track BNW participants longitudinally, and thus we are only able to

assess comprehension immediately after completion of the workshop. In the future, we aim to develop a longitudinal survey evaluating the long-term impact of BNW on learning retention and also participant career trajectories.

Participant feedback demonstrated that the workshop topics, hands-on experiments and presenter enthusiasm are the most well received aspects of the workshop, and motivate participant engagement and learning. Although the majority of students enjoyed the topics and overall workshop design, one major suggestion was to restructure the first session, "Getting to Know Your Nervous System". Initially, the first session was primarily lecture-based and had four short experiments spaced between lecture topics. Based on information gathered from the feedback forms, we were able to identify specific modifications to improve to the workshop, including the addition of breaks in between the lecture and session 1 experiments, as well as added time for the brain dissection. We added three 5 min breaks in session 1, and shortened the peripheral nervous system part in session 2 allowing more time for the brain dissection activity.

The active learning, experiment-based approach of BNW is one of its most notable strengths. The activities and experiments used in BNW (included in supplemental material) request participants to immediately reflect upon concepts discussed in the mini-lectures, and use that information to solve problems and answer questions. Active learning and the associated intrinsic motivation are well-established educational methods for improving retention (Lucariello, 2016, Michael, 2006). An example of one interactive activity used in BNW is the Giant Rope Neuron, which asks participants to model a neuron, highlighting the main compartments and functions, using rope, plastic rings, ping-pong balls, and other small household objects. To successfully complete this activity, participants need to use what they just learned about neurons to create a working model and correctly explain the models' components

and functions. The design of application activities, such as the aforementioned, has also been performed by other groups to reinforce comprehension of the concepts by students especially in pre-collegiate academic levels (Marzullo & Gage, 2012, Romero-Calderon, et, al., 2012). In addition, activities in BNW invite students to practice the scientific process. Some of the activities are designed with the purpose of making students think about a problem, construct a hypothesis, design a method to test that hypothesis, collect observations, make conclusions, and report those to the rest of the group. These types of activities greatly inspire the inquisitive nature of students and have been used by others to engage them in the scientific process while improving their critical thinking and effective communication skills (Hammond, et. al., 2010). It has also been found that scientist classroom visits have a great impact in students attitude towards science (US Census, 2014).

An additional key characteristic of BNW is the organization of our instructional teams, which relies on top-down student-directed mentorship. Essentially, graduate student instructors lead the workshops, senior undergraduate students moderate small groups of workshop attendees, and the participants themselves collaborate to learn from one another. This type of infrastructure has numerous educational, training and recruitment benefits both between and within each tier.

At the foundation of our model, workshop attendees are organized into small laboratory groups in an effort to promote an inclusive, peer-learning environment. BNW requires these student groups to utilize concepts introduced during the mini-lectures to cooperatively solve problems proposed during the activities. For example, during the first workshop session, students learn about basic structural features of a neuron and how those features impart function. Immediately thereafter, they are given a variety of household objects, such as bowls, ropes, and

small plastic balls, to model a neuron. Only by interacting with and learning from one another can the students successfully complete this task. Although the workshop facilitators guide them, the students generate the final product. This instructional design gives participants ownership of the knowledge they acquire without potential intimidators, such as language barriers or inexperience.

The middle tier of our leadership design is composed of senior undergraduate students embedded within each attendee laboratory group. These senior undergraduates are enlisted from the BPNP to assist the graduate student instructors. Their primary responsibility is to ensure the participants comprehend material being discussed and engage in workshop activities. For many of these senior undergraduates, assisting with BNW is their first teaching experience. In this sense, the workshop is a unique training opportunity for BPNP undergraduates to begin developing verbal pedagogical skills. However, these BPNP undergraduates serve an addition critical role as mentors to the BNW attendees. Because these senior undergraduates share a similar ethnic and educational background with most of the BNW participants, they exemplify the first attainable phase of training to become a neuroscientist.

At the top, graduate students gain valuable experience designing and implementing neuroscience-related educational activities at both the high school and collegiate level. Considering the paucity of comprehensive teaching opportunities in most graduate programs, BNW is an invaluable training opportunity for those graduate students seeking alternative careers in education and community outreach. Additionally, these graduate students serve as role models to both the BPNP senior undergraduates and the BNW student participants.

One reason proposed to explain the lack of ethnic diversity in science is the low number of minorities among faculty ranks. Undergraduate students of color are less likely to enter a

university that employs a low number of faculty of color (Fitzakerley, et al., 2013). Furthermore, minority students are less likely to pursue careers within scientific disciplines if they lack appropriate mentors and role models (Nelson, 2010). However, this results in a conundrum; until minority students are exposed to mentors from similar ethnic backgrounds, we will never comprehensively diversify scientific disciplines. BNW, together with BPNP, represents one attempt to break this cycle. At each workshop, attendees witness students, not unlike themselves, successfully engaging in scientific scholarship and research. With each year, our programs recruit additional minority students, and with each year, these students advance to more senior positions.

BNW has been very successful in teaching basic concepts of neuroscience and encouraging students to pursue careers in science and research. In this line, 64 of the students that participated in BNW have been recruited to participate in the BPNP summer program. Participation in the BPNP summer program provides each student direct research experience in neuroscience related fields including; neurotoxicology, neuropharmacology, neurophysiology, behavioral neuroscience, and psychology. More than twenty of these students have continued to pursue graduate degrees in neuroscience related areas. This proves that BNW efforts have been successful at retaining and guiding Hispanic students towards a career in neuroscience by introducing them to this exciting field and by exposing them to new opportunities in the area of research in neuroscience.

F) Future Directions

BNW as an outreach activity will continue in Puerto Rico with the overall goal of reaching a greater population of students. This will be achieved by bringing BNW to new institutions located closer to a population of students unable to attend previously conducted

workshops due to transportation issues. BNW will also be conducted in the contiguous United States starting in the fall of 2017. Two workshops will be conducted during each weekend visit to host institutions. One workshop will be conducted on Saturday and one on Sunday. Each visit will allow for the conduction of a workshop for 30 students. We aim to increase our impact by increasing our exposure not only in Puerto Rico but now implementing the workshops in the mainland U.S.

G) Acknowledgements

We thank the current and former MSU graduate students who contributed to the design and implementation of BNW: Drs. Chelsea Hutch, Bradley Hammond, Halie Kerver, Brenda-Marrero-Rosado and Samuel Pappas, as well as Carla Dams. We also thank our partner institution UPR-Cayey, specifically the Research Initiative for Scientific Enhancement Program (RISE). We are greatly indebted to the RISE director Dr. Robert Ross for his assistance with logistics and recruitment of attendees in Cayey. We thank the UPR-Arecibo, UPR-Humacao, Pontificia Universidad Católica de Puerto Rico in Ponce and the Universidad Interamericana de Puerto Rico at Arecibo for their efforts in organization and recruitment of participants. Lastly, we acknowledge the contributions of the graduate student presenters, undergraduate UPR student volunteers who assisted the workshop laboratory groups, and the many BNW participants who have helped make this endeavor a tremendous success.

Finally, we are very grateful for the funding provided by the College of Natural Science, the Neuroscience Program and the Comparative Medicine and Integrative Biology Program at Michigan State University to support the submission of this manuscript.

Author Contributions

Designed activities: ACR, ESRT, CTT, WDA

Performed evaluations: ACR, ESRT, CTT, WDA

Analyzed the data: ACR, ESRT, CTT

Wrote the paper: ACR, ESRT, CTT, WDA

REFERENCES

REFERENCES

Al-saleem T. Levels of mercury and pathological changes in patients with organomercury poisoning. Bull World Health Organ. 1976;53 Suppl:99-104.

Andersen C, Ledet-Jensen J, Ørntoft T. Normalization of real-time quantitative RT-PCR data: a model based variance estimation approach to identify genes suited for normalization - applied to bladder- and colon-cancer data-sets. Cancer Res. 2004:5245-50.

Aranda PS, LaJoie DM, Jorcyk CL. Bleach gel: a simple agarose gel for analyzing RNA quality. Electrophoresis. 2012;33:366-9.

Armon C. Western Pacific ALS/PDC and flying foxes: What's next? Neurology. 2003;61:291–29.

Arvidson B. Inorganic mercury is transported from muscular nerve terminals to spinal and brainstem motoneurons. Muscle Nerve. 1992;15:1089-94.

Aschner M, Eberle NB, Goderie S, Kimelberg HK. Methylmercury uptake in rat primary astrocyte cultures: the role of the neutral amino acid transport system. Brain Res. 1990;521:221-8.

Aschner M, Syversen T, Souza DO, Rocha JB, Farina M. Involvement of glutamate and reactive oxygen species in methylmercury neurotoxicity. Braz J Med Biol Res. 2007;40:285-91.

Aschner M, Yao C, Allen J, Tan K. Methylmercury alters glutamate transport in astrocytes. Neurochem Int. 2000;37:199-206.

Ashe K. Elevated mercury concentrations in humans of Madre de Dios, Peru. PLoS One. 2012;7:1-6.

Atchison WD. Is chemical neurotransmission altered specifically during methylmercury-induced cerebellar dysfunction? Trends Pharmacol Sci. 2005;26:549-57.

Atchison WD, Narahashi T. Methylmercury-induced depression of neuromuscular transmission in the rat. Neurotoxicology. 1982;3:37-50.

Babetto E, Mangolini A, Rizzardini M, M L, Conforti L, Rusmini P, et al. Tetracycline-regulated gene expression in the NSC34-tTA cell line for investigation of motor neuron diseases. Mol Brain Res. 2005;140:63-72.

Bakir F, Damluji SF, Amin-Zaki L, Murtadha M, Khalidi A, al-Rawi NY, et al. Methylmercury poisoning in Iraq. Science. 1973;181:230-41.

Baraldi M, Zanoli P, Tascedda F, Blom JM, Brunello N. Cognitive deficits and changes in gene expression of NMDA receptors after prenatal methylmercury exposure. Environ Health Perspect. 2002;110:855-58.

Bear MF, Connors BW, Paradiso MA. Neuroscience: Exploring the Brain. 3rd ed. Philadelphia: Lipppincott Williams and Wilkins; 2006.

Bellingham MC. A review of the neural mechanisms of action and clinical efficiency of riluzole in treating amyotrophic lateral sclerosis: what have we learned in the last decade? CNS Neurosci Ther. 2011;17:4-31.

Bettler B, Mulle C. Review: neurotransmitter receptors. II. AMPA and kainate receptors. Neuropharmacology. 1995;34:123-39.

Bleakman D, Lodge D. Neuropharmacology of AMPA and kainate receptors. Neuropharmacology. 1998;37:1187-204.

Boron WF, Boulpaep EL. Medical Physiology. 2 ed. Philadelphia, PA: Saunders; 2009.

Brookes N. In vitro evidence for the role of glutamate in the CNS toxicity of mercury. Toxicology. 1992;76:245-56.

Burke RE. Motor unit types: functional specializations in motor control. Trends Neurosci. 1980;3:255-8.

Burke RE, Levine DN, Tsairis P, Zajac FE, III. Physiological types and histochemical profiles in motor units of the cat gastrocnemius. J Physiol (Lond). 1973;234:723-48.

Cashman NR, Durham HD, Blusztajn JK, Oda K, Tabira T, Shaw IT, et al. Neuroblastoma x spinal cord (NSC) hybrid cell lines resemble developing motor neurons. Dev Dyn. 1992;194:209-21.

Castoldi A, Barni S, Turin I, Gandini C, Manzo L. Early acute necrosis, delayed apoptosis and cytoskeletal breakdown in cultured cerebellar granule neurons exposed to methylmercury. J Neurosci Res. 2000;59:775-87.

Catterall WA. Voltage-gated calcium channels. Cold Spring Harb Perspect Biol. 2011;3:a003947.

Census US. U.S. Census Bureau: State and Country Quick Facts. http://quickfacts.census.gov/qfd/states/00000.htm2014.

Chapman LA, Chan HM. Inorganic mercury pre-exposures protects against methyl mercury toxicity in NSC-34 (neuron x spinal cord hybrid) cells. Toxicology. 1999;132:167-78.

Clarkson TW. Environmental contaminants in the food chain. Am J Clin Nutr. 1995;61:682S-6S.

Clarkson TW, Magos L. The toxicology of mercury and its chemical compounds. Crit Rev Toxicol. 2006;36:609-62.

Cleveland DW, Rothstein JD. From Charcot to Lou Gehrig: deciphering selective motor neuron death in ALS. Nat. Rev. Neurosci. 2001;2:806–19.

Dietrich MO, Mantese CE, Anjos GD, Souza DO, Farina M. Motor impairment induced by oral exposure to methylmercury in adult mice. Environ Toxicol Pharmacol. 2005;19:169-75.

Edwards JR, Marty MS, Atchison WD. Comparative sensitivity of rat cerebellar neurons to dysregulation of divalent cation homeostasis and cytotoxicity caused by methylmercury. *Toxicol Appl Pharmacol*. 2005;208:222-32.

Eggett C, Crosier S, Manning P, Cookson M, Menzies F, McNeil C, et al. Development and characterization of a glutamate-sensitive motor neurone cell line. J Neurochem. 2000;74:1895-902.

Ekino S, Susa M, Ninomiya T, Imamura K, Kitamura T. Minamata disease revisited: an update on the acute and chronic manifestations of methyl mercury poisoning. J Neurol Sci. 2007;262:131-44.

Eto K. Pathology of Minamata disease. Toxicol Pathol. 1997;25:614-23.

Eto K, Tokunaga H, Nagashima K, Takeuchi T. An autopsy case of Minamata disease (methylmercury poisoning)- pathological viewpoints of peripheral nerves. Toxicol Pathol. 2002;30:714-22.

Fiegener M. Doctorate recipients from U.S. universities: 2013 digest. Survey of Earned Doctorates. http://www.nsf.gov/statistics/sed/2013/data-tables.cfm: National Science Foundation; 2015.

Fitzakerley J, Michlin M, Paton J, Dubinsky J. Neuroscientists' classroom visits positively impact student attitudes. PLoS ONE. 2013;8:e84035 - e.

Fraser B. Peru's gold rush raises health fears. Nature. 2016;534:162.

Friese A, Kaltschmidt J, Ladle D, Sigrist M, Jessell T, Arber S. Gamma and alpha motor neurons distinguished by expresion of transcription factor Err3. Proc Nat Acad Sci, USA. 2009;106:13588-93.

Fukada K, Zhang F, Vien A, Cashman N, Zhu H. Mitochondrial proteomic analysis of a cell line model of familial amyotrophic lateral sclerosis. Mol Cell Proteomics. 2004;3:1211-24.

Gao Y, Ding Y, Shi R, Tian Y. Effects of methylmercury on postnatal neurobehavioral development in mice. Neurotoxicol Teratol. 2008;30:462-7.

Gardner E. Peru battles the golden curse of Madre de Dios. Nature. 2012;486:306-7.

Gomes C, Escrevente C, Costa J. Mutant superoxide dismutase 1 overexpression in NSC34 cells: Effect of trehalose on aggregation, TDP-43 localization and levels of co-expressed glycoproteins. Neurosci Lett. 2010;475:145-9.

Greger, I. H., Khatri, L. & Ziff, E. B. RNA editing at arg607 controls AMPA receptor exit from the endoplasmic reticulum. Neuron. 2002;34:759–72.

Greger, I. H., Khatri, L., Kong, X. & Ziff, E. B. AMPA receptor tetramerization is mediated by Q/R editing. Neuron. 2003;40:763–74.

Grosskreutz J, Van Den Bosch L, Keller BU. Calcium dysregulation in amyotrophic lateral sclerosis. Cell Calcium. 2010;47:165-74.

Grynkiewicz G, Poenie M, Tsien RY. A new generation of Ca^{2+} indicators with greatly improved fluorescence properties. J Biol Chem. 1985;260:3440-50.

Gurney ME. et al. Motor neuron degeneration in mice that express a human Cu, Zn superoxide dismutase mutation. Science. 1994;264:1772–1775.

Hajela R, Peng S, Atchison W. Comparative effects of methylmercury and Hg^{2+} on human neuronal N- and R-type high-voltage activated calcium channels transiently expressed in human embryonic kidney 293 cells. J Pharmacol Exp Ther. 2003;306:1129-36.

Haley, RW. Excess incidence of ALS in young Gulf War veterans. Neurology. 2003;61:750–6.

Hammond C, Karlin D, Thimonier J. Creative research science experiences for high school students. PLoS Biol. 2010;8:9 - 11.

Hare MF, McGinnis KM, Atchison WD. Methylmercury increases intracellular concentrations of Ca^{++} and heavy metals in NG108-15 cells. J Pharmacol Exp Ther. 1993;266:1626-35.

Hemendinger R, Armstrong III E, Persinski R, Todd J, Mougeot J, Volvovitz F, et al. Huperzine A provides neuroprotection against several cell death inducers using in vitro model systems of motor neuron cell death. Neurotox Res. 2008;13:49-62.

Henley J, Wilkinson K. Synaptic AMPA receptor composition in development, plasticity and disease. Nat Rev Neurosci. 2016:337-50.

Herden CJ, Pardo NE, Hajela RK, Yuan Y, Atchison WD. Differential effects of methylmercury on gamma-aminobutyric acid type A receptor currents in rat cerebellar granule and cerebral cortical neurons in culture. J Pharmacol Exp Ther. 2008;324:517-28.

Higuchi Mea. RNA editing of AMPA receptor subunits GluR-B: A base-paired intron-exon structure determines position and efficiency. Cell. 1993;75:1361-70.

Horowitz HM, Jacob DJ, Amos HM, Streets DG, Sunderland EM. Historical mercury releases from commercial products: global environmental implications. Environ Sci & Tech. 2014;48:10242-50.

Huh KH, Wenthold RJ. Turnover analysis of glutamate receptors identifies a rapidly degraded pool of the n-methyl-d-aspartate receptor subunit, NR1, in cultured cerebellar granulle cells. J Biol Chem. 1999;274(1):151-7.

Hunter D, Russell D. Focal cerebral and cerebellar atrophy in a human subject due to organic mercury compounds. J Neurol Neurosurg Psychiat. 1954;1954:235-41.

Ince P, Stout N, Shaw P, Slade J, Hunziker W, Heizmann CW, et al. Parvalbumin and calbindin D-28k in the human motor system and in motor neuron disease. Neuropathol Appl Neurobiol. 1993;19:291-9.

Johnson FO, Yuan Y, Hajela RK, Chitrakar A, Parsell DM, Atchison WD. Exposure to an environmental neurotoxicant hastens the onset of amyotrophic lateral sclerosis-like phenotype in human Cu2+/Zn2+ superoxide dismutase 1 G93A mice: glutamate-mediated excitotoxicity. J Pharmacol Exp Ther. 2011;338:518-27.

Juang M. Depression of frog muscle contraction by methylmercuric chloride and mercuric chloride. Toxicol Appl Pharmacol. 1976;35:183-5.

Juang M, Yonemura K. Increase spontaneous transmitter release from presynaptic nerve terminal by methylmercuric chloride. Nature. 1975;256:211-3.

Kanning KC, Kaplan A, Henderson CE. Motor neuron diversity in development and disease. Annu Rev Neurosci. 2010;33:409-40.

Kawahara Y, Ito K, Sun H, Kanazawa I, Kwak S. Low editing efficiency of GluR2 mRNA is associated with a low relative abundance of ADAR2 mRNA in white matter of normal human brain. Eur J Neurosci. 2003;18:23-33.

Kawahara Y, Kwak S, Sun H, Ito K, Hashida H, Aizawa H, et al. Human spinal motoneurons express low relative abundance of GluR2 mRNA: an implication for excitotoxicity in ALS. J Neurochem. 2003;85:680-9.

Kwak, S. & Kawahara, Y. Deficient RNA editing of GluR2 and neuronal death in amyotropic lateral sclerosis. J. Mol. Med. (Berl). 2005;83:110–20.

Kwak S, Hideyama T, Yamashita T, Aizawa H. AMPA receptor-mediated neuronal death in sporadic ALS. Neuropathology. 2010;30:182-8.

Limke TL, Atchison WD. Acute exposure to methylmercury opens the mitochondrial permeability transition pore in rat cerebellar granule cells. Toxicol. Appl. Pharmacol. 2002;178: 52–61.

Limke T, Heidemann S, Atchison W. Disruption of intraneuronal divalent cation regulation by methylmercury: are specific targets involved in altered neuronal development and cytotoxicity in methylmercury poisoning? Neurotoxicology. 2004a;25:741-60.

Limke T, Otero-Montañez J, Atchison W. Evidence for interactions between intracellular calcium stores during methylmercury-induced intracellular calcium dysregulation in rat cerebellar granule neurons. *J Pharmacol Exp Ther*. 2003;304:949-58.

Limke TL, Atchison WD. Application of single-cell microfluorimetry to neurotoxicology assays. Curr Protoc Toxicol. 2009;42:12.15:12.5.1-.5.3.

Limke TL, Bearss JJ, Atchison WD. Acute exposure to methylmercury causes Ca^{2+} dysregulation and neuronal death in rat cerebellar granule cells through an M3 muscarinic receptor-linked pathway. Toxicol Sci. 2004;80:60-8.

Limke TL, Heidemann SR, Atchison WD. Disruption of intraneuronal divalent cation regulation by methylmercury: are specific targets involved in altered neuronal development and cytotoxicity in methylmercury poisoning? Neurotoxicology. 2004;25:741-60.

Liu W, Wang X, Zhang R, Zhou Y. Effects of postnatal exposure to methylmercury on spatial learning and memory and brain NMDA receptor mRNA expression in rats. Toxicol Lett. 2009;188:230-5.

Livak KJ, Schmittgen TD. Analysis of relative gene expression data using real-time quantitative PCR and the 2(-Delta Delta C(T)) Method. Methods. 2001;25:402-8.

Lu J, Duan W, Guo Y, Jiang H, Li Z, Huang J, et al. Mitochondrial dysfunction in human TDP-43 transfected NSC34 cell lines and the protective effect of dimethoxy curcumin. Brain Res Bull. 2012;89:185-90.

Lucariello J, Nastasi B, Anderman E, Dwyer C, Ormiston H, Skiba R. Science supports education: The behavioral research base for psychology's top 20 principles for enhancing teaching and learning. Mind, Brain and Education. 2016;10:55 - 67.

Mahajan SS, Thai KH, Chen K, Ziff E. Exposure of neurons to excitotoxic levels of glutamate induces cleavage of the RNA editing enzyme, adenosine deaminase acting on RNA 2, and loss of GLUR2 editing. Neurosci. 2011;189:305-15.

Maier O, Böhm J, Dahm M, Brück S, Beyer C, Johann S. Differentiated NSC-34 motorneuron-like cells as experimental model for cholinergic neurodegeneration. Neurochem Int. 2013;62:1029-38.

Marty MS, Atchison WD. Pathways mediating Ca^{2+} entry in rat cerebellar granule cells following *in vitro* exposure to methyl mercury. Toxicol Appl Pharmacol. 1997;147:319-30.

Marzullo T, Gage G. The SpikerBox: A low cost, open-source bioamplifier for increasing public participation in neuroscience inquiry. PLoS ONE. 2012;7.

McAlpine D, Araki S. Minamata disease: an unusual neurological disorder caused by contaminated fish. Lancet. 1958;2:629-31.

Michael J. Where's the evidence that active learning works? . Advances in Physiology Education. 2006;30:159 - 67.

Migliore L, Coppedè F. Genetics, environmental factors and the emerging role of epigenetics in neurodegenerative diseases. Mutat. Res. 2009;667:82–97.

Miyamoto K, Nakanishi H, Moriguchi S, Fukuyama N, Eto K, Wakamiya J, et al. Involvement of enhanced sensitivity of N-methyl-D-aspartate receptors in vulnerability of developing cortical neurons to methylmercury neurotoxicity. Brain Res. 2001;901:252-8.

Møller-Madsen B. Localization of mercury in CNS of the rat. II. Intraperitoneal injection of methylmercuric chloride (CH_3HgCl) and mercuric chloride ($HgCl_2$). Toxicol Appl Pharmacol. 1990;103:303-23.

Møller-Madsen B. Localization of mercury in CNS of the rat. III. Oral administration of methylmercuric chloride (CH_3HgCl). Fundam Appl Toxicol. 1991;16:172-87.

Montgomery KS, Mackey J, Thuett K, Ginestra S, Bizon JL, Abbott LC. Chronic, low-dose prenatal exposure to methylmercury impairs motor and mnemonic function in adult C57/B6 mice. Behav Brain Res. 2008;191:55-61.

Morahan, JM, Yu B, Trent RJ, Pamphlett R. Genetic susceptibility to environmental toxicants in ALS. Am. J. Med. Genet. B. Neuropsychiatr. Genet. 2007;144B:885–90.

Mutkus L, Aschner JL, Syversen T, Aschner M. Methylmercury alters the in vitro uptake of glutamate in GLAST- and GLT-1-transfected mutant CHO-K1 cells. Biol Trace Elem Res. 2005;107:231-45.

Muyderman H, Hutson PG, Matusica D, Rogers ML, Rush RA. The human G93A-superoxide dismutase-1 mutation, mitochondrial glutathione and apoptotic cell death. Neurochem Res. 2009;34:1847-56.

Ndountse L, Chan H. Methylmercury increases N-methyl-D-aspartate receptors on human SH-SY 5Y neuroblastoma cells leading to neurotoxicity. Toxicology. 2008a;249:251-5.

Ndountse LT, Chan HM. Methylmercury increases N-methyl-D-aspartate receptors on human SH-SY 5Y neuroblastoma cells leading to neurotoxicity. Toxicology. 2008b;249:251-5.

Nelson D, Brammer C, Rhoads H. A national analysis of minorities in science and engineering faculties at research universities. Oklahoma Universiy Diversity in Science Association. 2010;2:1.

Onishchenko N, Tamm C, Vahter M, Hokfelt T, Johnson JA, Johnson DA, et al. Developmental exposure to methylmercury alters learning and induces depression-like behavior in male mice. Toxicol Sci. 2007;97:428-37.

Palecek J, Lips MB, Keller BU. Calcium dynamics and buffering in motoneurones of the mouse spinal cord. J Physiol (Lond). 1999;520:485-502.

Pamphlett R, Waley P. Motor neuron uptake of low dose inorganic mercury. J Neurol Sci. 1996;135:63-7.

Paoletti P, Bellone C, Zhou Q. NMDA receptor subunit diversity: impact on receptor properties, synaptic plasticity and disease. Nat Rev Neurosci. 2013;14:383-400.

Pardo N, Hajela R, Atchison W. Acethylcholine release at neuromuscular junction of adult tottering mice is controlled by N-(Cav2.2) and R-type(Cav2.3) but not L-type(Cav1.2) Ca2+ channels. J Pharmacol Exp Ther. 2006;319:1009-20.

Pasinelli P, Brown RH. Molecular biology of amyotrophic lateral sclerosis: insights from genetics. Nat Rev Neurosci. 2006:7:710-23.

Peng SQ, Hajela RK, Atchison WD. Effects of methylmercury on human neuronal L-type calcium channels transiently expressed in human embryonic kidney cells (HEK-293). J Pharmacol Exp Ther. 2002;302:424-32.

Porter S, Umbach P. College major choice: An analysis of person–environment fit. Res High Edu. 2006;47.4:429 - 49.

Praline J, Guennoc AM, Limousin N, Hallak H, de Toffol B, Corcia P. ALS and mercury intoxication: a relationship? Clin Neurol Neurosurg. 2007;109:880-3.

Raimondi A, Mangolini A, Rizzardini M, Tartari S, Massari S, Bendotti C, et al. Cell culture models to investigate the selective vulnerability of motorneuronal mitochondria to familial ALS-linked G93ASOD1. Eur J Neurosci. 2006;24:387-99.

Ramanathan G, Atchison WD. Ca2+ entry pathways in mouse spinal motor neurons in culture following in vitro exposure to methylmercury. Neurotoxicology. 2011;32:742-50.

Rice D. Evidence for delayed neurotoxicity produced by methylmercury. Neurotoxicology. 1996;17:583-96.

Rico DdEdP. Política pública sobre la organización y la oferta curricular del programa de ciencias para los niveles elemental, intermedio y superior de las escuelas públicas de Puerto Rico. In: Rico DdEdP, editor. Departamento de Education Del Estado Libre Asociado de Puero Rico, Carta circular2014.

Røed A, Herlofson BB. Inhibitory effects of $HgCl_2$ on excitation-secretion coupling at the motor nerve terminal and excitation-contraction coupling in the muscle cell. Cell Mol Neurobiol. 1994;14:623-36.

Romero-Calderon R, O'Hare E, Suthana N, Scott-Van Zeeland A, Rizk-Jackson A, Attar A, et al. Project brainstorm: Using neuroscience to connect college students with local schools. PLoS Biol. 2012;10:2 - 5.

Roos PM, Vesterberg O, Nordberg M. Metals in motor neuron diseases. Exp Biol Med (Maywood). 2006;231:1481–7.

Rustam H, Von Burg R, Amin-Zaki L, El Hassani S. Evidence for a neuromuscular disorder in methylmercury poisoning. Arch Environ Health. 1975;30:190-5.

Sathasivam S, AJ G, Shaw P. Characterization of the caspase cascade in a cell culture model of SOD1-related familial amyotrophic lateral sclerosis: expression, activation and therapeutic effects of inhibition. Neuropathol Appl Neurobiol. 2005;31:467-85.

Shafer TJ, Atchison WD. Methylmercury blocks N- and L-type Ca^{++} channels in nerve growth factor-differentiated pheochromocytoma (PC12) cells. J Pharmacol Exp Ther. 1991;258:149-57.

Shafer TJ, Contreras ML, Atchison WD. Characterization of interactions of methylmercury with Ca^{2+} channels in synaptosomes and pheochromocytoma cells: radiotracer flux and binding studies. Mol Pharmacol. 1990;38:102-13.

Sirois JE, Atchison WD. Methylmercury affects multiple subtypes of calcium channels in rat cerebellar granule cells. Toxicol Appl Pharmacol. 2000;167:1-11.

Spalloni A, Nutini M, Longone P. Role of N-methyl-D-aspartate receptors complex in amyotrophic lateral sclerosis. Biochim Biophys Acta. 2012;1832:312-22.

Su M, Wakabayashi K, Kakita A, Ikuta F, Takahashi H. Selective involvement of large motor neurons in the spinal cord of rats treated with methylmercury. J Neurol Sci. 1998;156:12- 7.

Suda I, Hirayama K. Degradation of methyl and ethyl mercury into inorganic mercury by hydroxyl radical produced from rat liver microsomes. Arch Toxicol. 1992;66:398-402.

Suda I, Totoki S, Uchida T, Takahashi H. Degradation of methyl and ethyl mercury into inorganic mercury by various phagocytic cells. Arch Toxicol. 1992;66:40-4.

Sutedja NA, Veldink JH, Fischer K, Kromhout H, Heederik D, Huisman MHB, et al. Exposure to chemicals and metals and risk of amyotrophic lateral sclerosis: A systematic review. Amyotroph Lateral Scler. 2009;10:302-9.

Swarup V, Julien, JP. ALS pathogenesis: recent insights from genetics and mouse models. Prog. Neuropsychopharmacol. Biol. Psychiatry. 2011;35:363–9.

Takeuchi T, Morikawa N, Matsumoto H, Shiraishi Y. A pathological study of Minamata disease in Japan. Acta Neuropathol. 1962;2:40-57.

Takuma, H., Kwak, S., Yoshizawa, T. & Kanazawa, I. Reduction of GluR2 RNA editing, a molecular change that increases calcium influx through AMPA receptors, selective in the spinal ventral gray of patients with amyotrophic lateral sclerosis. Ann. Neurol. 1999;46:806–15.

Umbach J, Gundersen C. Mercuric ions are potent non competitive antagonists of human brain kainate receptors expressed in xenopus oocytes. Mol Pharmacol. 1989;36:582-8.

Vahter M, Mottet NK, Friberg L, Lind B, Shen DD, Burbacher T. Speciation of mercury in the primate blood and brain following long-term exposure to methyl mercury. Toxicol Appl Pharmacol. 1994;124:221-9.

Vandenberghe W, Robberecht W, Brorson JR. AMPA receptor calcium permeability, GluR2 expression, and selective motoneuron vulnerability. J Neurosci. 2000;20:123-32.

Wade L. Gold's dark side. Science. 2013;341:1448-9.

Weekes N. Diversity in neuroscience. We know the problem. Are we really still debating the solutions? 2012; 11(1):a52 – 54.

Xu B, Xu Z, Deng Y, Liu W, Yang H, Wei YG. MK-801 protects against intracellular Ca(2+) overloading and improves N-methyl-D-aspartate receptor expression in cerebral cortex of methylmercury-poisoned rats. J Mol Neurosci. 2013;49:162-71.

Yip RK, Riley DA. Effects of methylmercury on the motor and sensory innervation of the rat extensor digitorum longus muscle. *Environ Res*. 1987;43:85-96.

Yuan Y, Atchison WD. Methylmercury induces a spontaneous, transient slow inward chloride current in Purkinje cells of rat cerebellar slices. J Pharmacol Exp Ther. 2005;313:751-64.

Yuan Y, Atchison WD. Methylmercury differentially affects $GABA_A$ receptor-mediated spontaneous IPSCs in Purkinje and granule cells of rat cerebellar slices. J Physiol (Lond). 2003;550:191-204.

Yuan Y, Atchison WD. Methylmercury-induced increase of intracellular Ca2+ increases spontaneous synaptic current frequency in rat cerebellar slices. Molecular Pharmacology. 2007;71:1109-21.

Yuan Y, Otero-Montanez JK, Yao A, Herden CJ, Sirois JE, Atchison WD. Inwardly rectifying and voltage-gated outward potassium channels exhibit low sensitivity to methylmercury. Neurotoxicology. 2005;26:439-54.